Treatment of Periodontal Disease Via Modulation of Innate Host Response

by

Mostafa Salah Shehabeldin

BDS, Cairo University, 2010

MSc, University of Pittsburgh, 2016

Submitted to the Graduate Faculty of the

School of Dental Medicine in partial fulfillment

of the requirements for the degree of

Doctor of Philosophy

University of Pittsburgh

2021

UNIVERSITY OF PITTSBURGH

SCHOOL OF DENTAL MEDICINE

This dissertation was presented

by

Mostafa Salah Shehabeldin

It was defended on

April 9, 2021

and approved by

Dobrawa Napierala, Associate Professor, Department of Oral and Craniofacial Sciences

Giuseppe Intini, Associate Professor, Department of Periodontics and Preventive Dentistry

Sarah Gaffen, Professor, Division of Rheumatology and Clinical Immunology

Dissertation Director: Charles Sfeir, Associate Professor, Department Periodontics and Preventive Dentistry

Development of Local Sustained Delivery Strategies for Treatment of Periodontitis

Mostafa Salah Shehabeldin, BDS, MSc

University of Pittsburgh, 2021

Periodontal disease (PD) is a chronic inflammatory disease characterized by progressive destruction of tooth supporting structures and microbial dysbiosis. The destructive inflammatory process underlying PD is mediated by components of both the innate and acquired immune systems including immune cells, cytokines, chemokines and lipid mediators. Macrophages and T-helper 17 (Th17) cells are key cellular mediators of the innate and acquired host responses in the periodontal environment, respectively. In many tissues including the periodontium, macrophages are the prototypic phagocytes of the innate immune response. These plastic cells can assume distinct phenotypic subsets to perform a wide array of functions ranging from host defense against invading pathogens to clearance of dead cells and promotion of tissue repair. Similarly, periodontal Th17 cells can exhibit both homeostatic and pathogenic subsets. Homeostatic Th17 cells are essential for immune surveillance and host defense by regulating neutrophils expansion and recruitment at oral barrier sites. Conversely, pathogenic Th17 cells arise in response to oral microbial challenge and drive inflammatory damage in PD via overproduction of their major cytokine IL-17A. In this study, we tested the therapeutic efficacy of modulating macrophages response or IL-17A activity in PD using two polymer based sustained delivery systems. To target macrophages, the chemokine CCL2 was encapsulated in PLGA microspheres and locally delivered at different stages of murine PD severity followed by analysis of bone levels, gene expression profile, osteoclastic activity, periodontal ligament organization and periodontal microbial load and

composition. Using Sc-RNA sequencing technology, we also assessed murine periodontal macrophages gene expression profile and characterized their phenotypic subsets. We also tested the protective effect of local sustained delivery of IL-17A antibodies in murine periodontitis by assessing the changes in bone levels, osteoclastic activity and inflammatory markers. The overall aim of this study was to highlight the clinical translation potential of targeting cellular and non-cellular components of the innate and acquired immune response to treat PD.

Table of Contents

List of Tables

List of Figures

No table of figures entries found.

Preface

I would like to thank every one who helped to complete the work of this dissertation. I would like to thank Dr. Charles Sfeir who took a chance on me when he agreed to be my mentor seven years ago. Working with Dr. Sfeir has been a life changing experience that enabled me to mature as a person, to develop as a scientist and to relentlessly pursue my goals without giving up. I am also very grateful to Dr. Samer Zaky for his friendship, endless support and sincere guidance since the first day I met him at the CCR. The work of this thesis would have never been possible without the technical support provided by Dr. Jin Gao, Yejin Ki and Rong Chong. I am also very glad to have had a chance to collaborate with Dr. Cinthia Pacheco and Dr. Katia Maltos.

I would also like to thank all my PhD committee members Dr. Dobrawa Napierala, Dr. Sarah Gaffen and Dr. Giuseppe Intini. I have learned and benefited significantly from their feedback and comments. I am also very grateful for their flexibility and willingness to work with me on my graduation timeline.

Special thanks to the Department of Oral and Craniofacial Sciences former and current chairs Dr. Mark Mooney and Dr. Elia Beniash. I am also thankful to all members of the Center for Craniofacial regeneration.

Finally, I would like to dedicate this dissertation to my mother Safaa, my father Salah and my brother Mahmoud. Their unconditional love, selflessness and sacrifice have been an inspiration and a driving force behind every success I have achieved. No words can express how forever grateful I am for everything they have done for me.

1.0 Introduction

The periodontium is a unique tissue that invests and supports the tooth and consists of hard (alveolar bone and cementum) and soft (gingiva and periodontal ligament) tissues. Microbial challenge in the periodontium elicits a host inflammatory response that is reversible at its early stage known as gingivitis, and then becomes irreversible when alveolar bone loss starts at its later stage referred as periodontitis. Both gingivitis and periodontitis fall under one entity known as periodontal disease (PD). PD is one of the most common oral diseases, affecting about 47% of adults aged 30 years or older in the United States (Eke et al. 2015a). PD is considered as one of the leading causes of tooth and alveolar bone loss (Ong 1998), and has been implicated in a number of systemic conditions (Cullinan and Seymour 2013; Preshaw et al. 2012). Progressive inflammatory bone loss is a hallmark of periodontitis, and is associated with infection and destruction of other components of the periodontium. Although periodontal pathogens produce toxic agents that can damage the periodontium, the majority of tissue damage in periodontitis is self-inflicted by the host inflammatory response to those pathogens. This host response is mediated by components of the innate and acquired immune systems.

Owing to its inability to self-resolve, chronic periodontal inflammation requires therapeutic intervention to halt disease progression. Over the past decades, the major focus of periodontal therapy has been to reduce the load of inflammation inducing pathogens by both mechanical and chemical means. Although widely accepted, this approach does not always yield consistent and predictable therapeutic outcomes, and in some patients may fail to halt disease progression even in the absence of microbial plaque accumulation. For this reason, periodontal host modulatory

approaches have been investigated in recent years. These approaches have the potential to improve treatment outcomes of periodontitis when used as an adjunct for microbial debridement. This is especially true for patients who fail to respond to standard microbial debridement protocols due to genetic or environmental factors.

In the sections below, we will review the structural changes in the periodontium while it transitions from health to disease. Next, we will discuss the pathogenesis of periodontal disease with an emphasis on the role of host-microbe interaction in disease initiation and progression. Furthermore, we will shed the light on the shortcomings of current periodontal treatment protocols and highlight the potential benefit of host modulatory therapies. Finally, we will provide an overview of the most common animal models for periodontal disease and underline the potential application of PD as a model for other chronic destructive bone diseases.

1.1 The Periodontium: From Health to Disease

The periodontium consists of structures that support the tooth including gingiva, cementum, periodontal ligament and alveolar bone. Each of those structures possess distinct structural characteristics that allow for the maintenance of periodontal health. Periodontal microbial challenge disturbs the integrity of periodontal structures and undermines periodontal homeostasis leading to a transition from a healthy to a diseased periodontium.

The gingiva forms the outermost soft tissue component of the periodontium and is composed of epithelium and connective tissue. The gingival epithelium is subdivided into three

compartments: the **oral**, **sulcular** and **junctional epithelia**. Of all three epithelial compartments, the **junctional epithelium (JE)** exhibits unique characteristics that allow it to play a crucial role in maintaining periodontal homeostasis. The JE is composed of undifferentiated stratified squamous epithelium that is thickest at the base of the gingival sulcus, and tapers in thickness as it descends along the root surface. The JE forms a collar following the tooth cemento-enamel junction, where its tooth-facing layer forms the epithelial attachment consisting of a basal lamina like structure that adheres to the tooth by means of hemidesmosomes. This firm attachment enables the JE to seal off deeper periodontal tissues from the oral environment and prevent pathogenic bacteria from colonizing subgingival tooth surface. In addition to its the firm attachment to tooth surface, the JE can hinder bacterial colonization by exhibiting other unique features (Pöllänen et al. 2003). First, the JE cells undergo rapid turnover, thus are able to repair the tissue damaged by microbial insult efficiently. Second, JE cells have fewer desmosomes resulting in the creation of wider fluid-filled intercellular spaces containing polymorphonuclear phagocytes and monocytes that are able to pass into the gingival sulcus. Third, JE cells have been reported to perform endocytic activity similar to macrophages (Cho and Garant 2000). All these features make the stability of JE a key factor in the maintenance of a healthy periodontium.

The periodontal ligament (PDL) is another soft tissue component of the periodontium. PDL is made of a thin layer of specialized connective tissue interposed between the root cementum and alveolar bone as a continuation of the gingival connective tissue. PDL is composed of cellular and non-cellular elements, where the **principal fibers** form the major non-cellular element of the PDL (Nanci and Bosshardt 2006). The principal fibers of PDL constitute mainly of collagen type I (Huang et al. 1991), and their terminal ends, referred as Sharpey's fibers, calcify as they insert

into the cementum and alveolar bone. The cellular elements of the PDL are composed of connective tissue cells (fibroblasts, osteoblasts and cementoblasts), immune cells (neutrophils, macrophages, lymphocytes and mast cells), and epithelial rest cells (epithelial rests of Malassez). The cellular and non-cellular components of the PDL enable it to perform its physical, formative, nutritional and sensory functions. In this respect, the PDL supports the tooth in its socket, maintains the gingiva in proper relationship to teeth, transmits occlusal load to bone, participates in the remodeling of bone and cementum in response to external load and contains blood vessels and nerve fibers that provide nutrition and sensation to the periodontal apparatus (Nanci and Bosshardt 2006).

The cementum is where the PDL fibers attach on the root surface. The cementum is an avascular hard connective that is present in two varieties: acellular and cellular cementum (Diekwisch 2001). The acellular cementum is found on the cervical half to two third of the root where most of the principal PDL fibers insert forming Sharpey's fibers, which make a significant proportion of the organic constituents of acellular cementum. The cellular cementum is present on the apical half to one third of the root and is characterized by presence of cells trapped in lacunae (cementocytes), randomly organized collagen fibers, less mineralization and a smaller proportion of Sharpey's fibers than acellular cementum.

The alveolar bone is the part of the alveolar process in the maxilla and mandible that forms the inner wall of the tooth socket. The alveolar bone is made of compact bone that is continuous with the outer compact socket wall at the alveolar crest with a layer of trabecular/cancellous bone in between. The alveolar bone is also referred as "bundle bone" since it is the site of PDL fibers

insertion. Bundle bone also contains intrinsic collagen fiber bundles that run parallel to the socket wall. Owing to its intimate relationship to the tooth and PDL, the alveolar bone responds to physiological masticatory forces applied to the tooth by undergoing continuous remodeling. This remodeling process is accentuated the most during orthodontic tooth movement where bone lost in response to pressure on the PDL is replaced by an equivalent amount of bone at the site of tension (Verna et al. 1999).

We described above the characteristic features of the soft and hard tissue components of the periodontium during health. In PD, infection and subsequent periodontal inflammatory response disturb the structural integrity of the periodontal apparatus and compromise its ability to maintain periodontal health. For instance, the integrity of the JE and its ability to act as a barrier can be compromised by certain disease associated periodontal pathogens such as porphyromonas gingivalis (Katz et al. 2002). The invasion and expansion of those pathogens into the periodontal sulcus elicits an inflammatory response and collagen fibers destruction in the connective tissue underlying the JE. This results in apical migration of JE cells along the root surface and deepening of the gingival sulcus. This apical migration stops once the JE cells reach a level of intact connective tissue where they can reestablish the epithelial attachment to the root surface (Pitaru et al. 1989). Furthermore, the invasion of periodontal pathogens into the connective tissue of the gingiva and PDL induces immune cells expansion and chemotaxis and the secretion of pro-inflammatory cytokines (e.g. IL-6, TNF-a, IL-1 β), chemokines (e.g. CXCL12) and proteases (e.g. MMP-8, MMP-9) in an attempt to wall-off pathogens invasion. Those pro-inflammatory mediators induce the uncoupling of bone formation from bone resorption resulting in net bone loss, which marks the transition from gingivitis to periodontitis (Graves et al. 2011). The mechanism of

uncoupled bone remodeling is driven by an imbalance between the receptor activator of nuclear factor kappa-B ligand (RANKL) and its decoy receptor Osteoprotegrin (Boyce and Xing) in favor of RANKL overproduction (Boyce and Xing 2008). The pro-inflammatory cytokines secreted in the inflamed periodontal connective tissue stimulate osteoblasts, bone marrow stromal cells and PDL fibroblasts to secrete RANKL that binds to its receptor RANK on osteoclasts precursors inducing their differentiation, maturation and inflammatory bone loss (Graves et al. 2011). In addition, cementum resorption has been reported in periodontally diseased teeth (Beertsen et al. 2001). The Resorptive defects of root surface cementum act as a reservoir for periodontal pathogens and have been correlated with the severity of periodontal destruction (Mahajan et al. 2017). Finally, the proteases secreted by immune cells in the inflamed periodontium destroy PDL collagen fibers, resulting in further collapse of the periodontal attachment and deepening of the sulcus (Kurgan and Kantarci 2018). Collectively, the transition from periodontal health to disease is associated with pathological changes in both soft and hard tissue components of the periodontium.

1.2 Periodontal Microbial Dysbiosis

It is well established that the dental plaque biofilm is the major etiologic factor in the initiation of PD (Lindhe et al. 1975; Lovegrove 2004). Initially, the dental plaque biofilm is mainly composed of commensal (non-disease causing) microbiota. As the plaque accumulates at the gingival margin, the increase in commensal microbial biomass provokes a breakdown of host-microbe homeostasis. In its early stage, this homeostatic breakdown triggers a reversible inflammatory response that is limited to the gingiva called gingivitis (Murakami et al. 2018). If

the plaque biofilm is left undisturbed for a longer duration, the inflammatory response becomes chronic and advances to deeper subgingival tissues. This creates a periodontal environment that is conducive to the emergence of **keystone pathogens** (species that remodel the microbial community to promote disease), and **pathobionts** (commensal species that can cause disease when host microbe homeostasis is disturbed). Both microbial entities thrive on the nutrients derived from the inflammatory exudates in the chronically inflamed subgingival environment (Lamont et al. 2018), and the lower redox potential typical of an aged plaque (Loesche and Grossman 2001). All these ecological changes promote the diversity of the periodontal microbiota with more pathogenic gram-negative species dominating the microbial community (Marsh 1994). This inflammation-mediated change in the relative abundance of individual members of the periodontal microbiota is termed **dysbiosis** (Darveau et al. 2012). Dysbiosis exacerbates the already deregulated immune homeostasis resulting in an uncontrolled inflammatory response capable of inducing periodontal hard and soft tissue damage (Darveau et al. 2012). Furthermore, the periodontal tissue breakdown products (e.g. degraded proteins and hemin) are used as nutrients by the proteolytic gram-negative bacteria in the dysbiotic microbiota, thus sustaining microbial imbalance (Hajishengallis 2014). This results in a self-reinforcing vicious cycle where uncontrolled inflammation and dysbiosis are fueling each other (Hajishengallis 2015).

1.3 Role of the Host Response

As alluded to above, the mutually beneficial interaction between dysbiotic microbiota and uncontrolled host response is the major mechanism underlying soft and hard tissue destruction in PD. This host response includes components of the innate and acquired immune systems and is

mediated by a wide array of inflammatory mediators including cytokines (e.g. IL-6, TNF-α, IL-17A) and chemokines (e.g. CXCL12) (Graves et al. 2011). The main function of those cytokines and chemokines is to limit periodontal infection by activation and recruitment of phagocytic and other defense cells (Parameswaran and Patial 2010; Scheller et al. 2011). However, those mediators can also indirectly induce tissue destruction by stimulating osteoclastic differentiation and proteolytic enzymes activity, thus promoting periodontal tissue damage, disease progression and dysbiosis (Cochran 2008). Although periodontal pathogens can cause direct tissue destruction by their release of proteolytic enzymes (e.g. collagenase, fibrinolysin) and cytotoxic byproducts (e.g. H_2S), the majority of tissue damage is the net result of an overactive inflammatory response driven by microbial dysbiosis (Cekici et al. 2014b).

A number of inflammatory cells are involved in the destructive periodontal inflammatory response. Among those, macrophages and T-helper 17 (Th17) cells stand out as crucial determinants of PD pathogenesis and fate. Macrophages comprise 6% of all immune cells in periodontal soft tissue biopsies of chronic periodontitis patients (Carcuac and Berglundh 2014). Moreover, the total number of macrophages was found to be higher in the gingival tissues obtained from periodontitis lesions compared to healthy tissues in both humans and mice (Gemmell et al. 2001; Yu et al. 2016). Similarly, Th17 cells were abundant and their signature cytokine IL-17A was highly expressed in human chronic periodontitis lesions (Lester et al. 2007; Ohyama et al. 2009). Furthermore, the severity of human periodontitis has been correlated with an increased expression of IL-17A (Dutzan et al. 2012; Johnson et al. 2004). Thus, the significant presence of macrophages and Th17 cells in the inflamed periodontium support their pivotal contribution to the host response underlying PD.

In addition to the destructive aspect of the periodontal inflammatory response, this response has also a constructive aspect that maintains periodontal immune homeostasis in health, and drives inflammation resolution following plaque removal (Serhan and Savill 2005). However, if plaque is allowed to build up for an extended duration in a susceptible host, the inflammation resolution process becomes impaired leading to the cascade of events resulting in inflammatory damage and dysbiosis. Accordingly, periodontitis has been recently redefined as a disease that stems from a failure to resolve an inflammatory response that has gone beyond the control of the endogenous resolution pathways (Van Dyke and Sima 2020). This notion is supported by reports showing that exogenous induction of inflammation resolution by administering a pro-resolving lipid mediator (RvE1) can reverse inflammatory bone loss and dysbiosis in animal models of periodontitis (Hasturk et al. 2007; Lee et al. 2016b). Along the same lines, one study suggested that the induction of a pro-resolving/M2 macrophages phenotype by oral administration of the PPAR-γ agonist Rosiglitazone inhibits periodontal bone loss and promotes bone repair in mice with experimental periodontitis (Viniegra et al. 2018). Similarly, another study showed that local administration of a pro-resolution glycoprotein called developmental endothelial locus 1 (Del-1) inhibited IL-17A secretion and bone loss in murine periodontitis (Eskan et al. 2012). Collectively, those reports indicate that inflammation resolution mediators exhibit their bone loss protective effects by targeting both innate (macrophages) and adaptive (Th17/IL-17A) inflammatory pathways. Thus, extrinsic induction of inflammation resolution during the course of PD has the potential to reverse microbial subversion of the host response and halt periodontal destruction.

1.4 Current Periodontal Therapeutic Strategies

Current treatment modalities for PD focus on reducing microbial load in the periodontium by periodic debridement of dental plaque using mechanical (scaling and root planning) and chemical (antiseptics and antibiotics) means (Sanz et al. 2015; Teles and Teles 2009). In patients with advanced disease and deep periodontal pockets, it is often difficult to achieve optimum plaque debridement and resolution of clinical signs of inflammation without gaining adequate access to the root surface. For those patients, a surgical approach termed open flap debridement is often prescribed. This surgical approach is occasionally combined with guide tissue regenerative procedures and has been shown to result in reduction of periodontal pocket depth to some extent (Heitz-Mayfield et al. 2002; Needleman et al. 2001). Moreover, adjunctive systemic antibiotic prescription has been employed in patients that continue to have active disease despite strict plaque control measures (Walker et al. 1993). Although some improvement in clinical parameters of PD has been reported with adjunctive systemic antibiotics (Haffajee et al. 2003), their use should be weighed against the benefits in light of the growing global concern of antibiotic resistance (Ventola 2015; Walters and Lai 2015). For this reason, local antimicrobial agents (e.g. Arestin, PerioChip) have also been investigated as adjuncts for PD treatment (Paquette et al. 2008). In this respect, local adjunctive antimicrobials have been reported to improve clinical parameters of PD especially in sites of recurrent disease and when used in sustained release formulations (Matesanz-Pérez et al. 2013; Van Dyke et al. 2002).

1.5 Periodontal Host Modulatory Therapies

The concept of modulating destructive host response as a therapeutic strategy is relatively new in the field of periodontics. This concept has been widely studied in other chronic inflammatory conditions of bone such as rheumatoid arthritis (Guo et al. 2018). Over the past decades, our understanding of PD pathogenesis has evolved from considering it as merely a microbial plaque induced disease to a multifactorial condition in which the host response to microbial insult is instrumental in disease initiation and progression (Bartold and Van Dyke 2013). This fairly recent understanding of PD pathogenesis has propelled the quest for local adjunctive host-modulatory therapies aiming at enhancing the outcomes of current plaque control/debridement protocols. The overall goal of periodontal host modulatory therapies is to restore the host-microbe homeostasis by dampening down the factors that drive destructive inflammation, thus tipping the balance in favor of a constructive healing response.

Sub-antimicrobial Dose Doxycycline (Periostat) is one of the most studied host modulatory agents that is FDA approved for PD treatment. Periostat is prescribed systemically in a small dose of 20 mg twice daily over a period ranging from 3-9 months. At this dose, Periostat exhibits an inhibitory effect on matrix metalloproteinases secreted by immune cells in the inflamed periodontium rather than an antimicrobial effect (Peterson 2004). When used in conjunction with mechanical plaque debridement, Periostat resulted in significant improvement in clinical parameters of PD (Caton 1999). Other systemic host modulatory agents have also shown promise for ameliorating periodontal status such as bisphosphonates and non-steroidal anti-inflammatory drugs (NSAIDs) (Bhavsar et al. 2016; Faizuddin et al. 2012). The mechanism of action of these drugs relies on the inhibition of osteoclastic activity by direct targeting of osteoclasts or by

interfering with the upstream pro-inflammatory pathways supporting their function. Although some clinical benefits can be achieved by the aforementioned systemic periodontal host modulatory therapies, their use may be limited by the undesirable adverse effects associated with their route of administration (e.g. gastrointestinal disorders, osteonecrosis of jaw and increased bleeding tendency).

More recently, the evolution in genomic sequencing, cell tracing and animal genetic modification techniques has advanced our understanding of the specific molecular and cellular factors involved in PD pathogenesis. This evolution also resulted in the emergence of new local periodontal therapeutic approaches that target specific immunologic pathways contributing to destructive periodontal inflammation.

One promising local periodontal immunomodulatory approach is based on activating intrinsic inflammation resolution pathways by local delivery of a class of lipid mediators derived from omega-3 polyunsaturated fatty acids (PUFAs) called resolvins (Serhan et al. 2008). Resolvins drive inflammation resolution by suppressing pro-inflammatory cytokines production, inhibiting neutrophils recruitment, and inducing macrophages phagocytosis of apoptotic neutrophils (efferocytosis). RevE1, a member of the resolvins family, has been shown to abrogate RANKL induced differentiation of pre-osteoclasts and increase OPG secretion by osteoblasts in vitro (Gao et al. 2013; Herrera et al. 2008). Along the same lines, several preclinical studies have indicated that RvE1 local treatment can abrogate periodontal breakdown, promote periodontal repair and reverse periodontal microbial dysbiosis in animal models of PD (Hasturk et al. 2006; Lee et al. 2016a).

Another emerging host modulatory strategy for PD relies on harnessing the body's natural immuno-regulatory mechanisms to resolve local inflammation in the periodontal environment. This approach leverages sustained drug release technologies to locally deliver immune-modulatory peptides in the periodontium. Those peptides (e.g. cytokines, chemokines) are able to recruit or induce specific regulatory immune cells that promote the resolution of periodontal inflammation. In this regard, local sustained release of the T-regulatory cells (Tregs) recruiting chemokine CCL22 into the periodontal tissues was reported to inhibit alveolar bone loss in mouse and canine models of periodontitis (Glowacki et al. 2013). Tregs are known for their ability to secrete anti-inflammatory and pro-reparative cytokines, such as IL-4, IL-10 and TGF-β, and to inhibit osteoclastogenesis (Kim et al. 2007). Similarly, another report indicated that induction of pro-resolving/M2-like macrophages by local sustained delivery of the chemokine CCL2 suppresses inflammatory osteolysis in murine models of PD (Zhuang et al. 2018). Similar to Tregs, M2-like macrophages are well established producers of an array of anti-inflammatory cytokines (IL-10, IL-1ra) and tissue repair mediators (Arg-1, Retnla) (Bosurgi et al. 2017; Evans and Fox 2007; Kitazawa et al. 1994; Novak and Koh 2013).

1.6 Preclinical Models of Periodontal Disease

Animal models have been extensively used in osteoimmunology research to understand the mechanisms driving inflammatory bone loss in periodontal and other skeletal diseases. In particular, PD animal models have been a powerful tool for elucidating periodontal inflammatory pathways, testing new therapies and understanding the link between oral and systemic

inflammation. An ideal model for PD would be one that closely mimics human disease in terms of pathogenesis, progression, histological and molecular changes and that is also easy to use and assess in a standardized manner. While an ideal model for PD is yet to be developed, several animal models have been employed over the past decades with a wide variability in induction methods, advantages and limitations. In the section below, we will discuss rodent and canine PD models as two examples of the most widely models.

1.6.1 Rodent Models

Rodent (mice and rat) PD models have been widely used due to their affordability, accessibility and the availability of rodent molecular analysis reagents. Although rat PD models are still being used, mice PD models have gained remarkable popularity in recent years due to the widespread application of genetic modification techniques in mice more so than in rats. In mice, the rational for PD induction banks on exogenously promoting periodontal pathogens accumulation around teeth by the administration of oral gavages containing known periodontal pathogens or the application of a suture ligature around teeth to encourage intrinsic plaque accumulation (Abe and Hajishengallis 2013; Baker et al. 2000).

A number of studies comparing different models of murine PD (oral gavage, LPS injection, ligature application) have concluded that the ligature model, unlike other models, is effective in inducing inflammatory bone loss and recapitulating histological and cellular changes associated with human PD (de Molon et al. 2014; de Molon et al. 2016). Instead of exogenously boosting periodontal pathogens load in the mouse oral cavity by injection or gavage, the murine ligature PD model relies on sutures ligated around maxillary molars to act as a bacterial plaque retentive niche

capable of initiating a destructive host inflammatory response (Abe and Hajishengallis 2013; Marchesan et al. 2018). Indeed, inflammatory tissue destruction is almost entirely dependent on the presence of periodontal pathogens in specific pathogen free mice (SPF), since ligatures have failed to instigate inflammation and bone loss in germ-free mice (Rovin et al. 1966; Xiao et al. 2017). Additionally, ligature PD allows for studying the resolution of periodontal inflammation, since removal of ligatures results in spontaneous disease recovery and downregulation of pro-inflammatory makers (Kourtzelis et al. 2019). This is a unique advantage of this model as it provides a powerful tool for testing the effectiveness of immunomodulatory therapies in situations that mimic clinical scenarios. As a result, the murine ligature PD model has gained significant popularity amongst several groups in recent years due to its predictability and reproducibility and technical versatility.

Owing to the reported similarities in the mechanism of inflammatory bone loss between PD and other bone destructive diseases (e.g. rheumatoid arthritis) in mice and humans (Detert et al. 2010; Lübcke et al. 2019), the murine ligature PD model can also serve as an exemplar for chronic bone destructive diseases. However, the strain of mice used needs to be taken into consideration when studying and interpreting specific inflammatory pathways in this model. This is because the most widely used strains (C57BL/6 and BALB/C) for murine PD induction exhibit inherent differences in their T-helper cell subsets frequencies and macrophages innate immune responses (Gorham et al. 1996; Watanabe et al. 2004).

1.6.2 Canine Model

Despite the myriad of advantages of employing mice in periodontal translational research, PD models in higher order animals such as dogs are often needed to circumvent the limitations of mice models. Those limitations include the inability to assess the clinical parameters of PD that are routinely used to evaluate human disease (pocket probing depth, clinical attachment loss and bleeding on probing), in addition to the limited working field of mice oral cavity. The latter makes mice PD models unsuitable for testing novel periodontal regenerative techniques and materials.

Beagles are the most commonly used dog breed for the induction of PD. In beagle dogs, PD is induced by the application of suture ligatures around teeth for a period ranging from 3 to 8 weeks (Martuscelli et al. 2000; Shibutani et al. 1997). The similarities in the subgingival plaque composition between beagle dogs and humans and the increased disease severity with age support the clinical relevance of the canine PD model (Kortegaard et al. 2008; Lindhe et al. 1973; Sorensen et al. 1980). Additionally, PD induction in beagle dogs was shown to recapitulate the clinical signs of periodontal inflammation and disease progression observed in humans (edema, bleeding on probing, attachment loss) (Glowacki et al. 2013; Nociti et al. 2001). Finally, beagle dogs have been extensively used for evaluating the efficacy of many periodontal guided regeneration techniques (Koo et al. 2005; Park et al. 1995; Wikesjö et al. 1998).

Despite the many advantages of the canine PD model, several limitations are encountered with its use including the higher cost, the need for daily companionship, frequent maintenance and the requirement for more extensive training of research personnel.

2.0 Specific Aims

In this study, our goal was to evaluate the therapeutic effect of targeting inflammatory pathways driven by macrophages and Th17 cells in murine PD. **Our first hypothesis** was that local sustained delivery of the chemokine CCL2 in diseased murine periodontium would protect against periodontal tissue destruction and enhance healing by restoring local macrophages homeostasis and reversing microbial dysbiotic changes. **Our second hypothesis** was that targeting of the signature Th17 cytokine IL-17A by local sustained delivery of IL-17A antibodies would halt inflammatory bone loss in mice with PD induction. To test these hypotheses, we outlined the following aims:

Specific Aim 1 (SA1): To assess the therapeutic efficacy of CCL2 local sustained delivery as a preventive, interventional and reparative therapy for murine periodontitis. **SA1A:** Sustained release CCL2 PLGA microparticles (MP) will be fabricated, surface characterized, and their release profile will be evaluated. **SA1B:** CCL2 MP will be delivered concurrently with starting murine ligature PD induction (**Preventive therapy**). Alveolar bone loss will be assessed and the mRNA expression of macrophages polarization, inflammatory and bone remodeling markers in the murine periodontium will be analyzed. **SA1C:** CCL2 MP will be delivered 4 days after the start of murine PD induction (**Interventional therapy**). Alveolar bone loss, osteoclast counts and the expression of macrophages polarization, inflammatory and bone remodeling markers and will be evaluated. **SA1D:** CCL2 MP will be delivered at the end of PD induction prior to a brief recovery period (**Reparative therapy**) to assess alveolar bone gain and periodontal ligament fibers organization.

Specific Aim 2 (SA2): To Unravel the changes in periodontal microbiome and phenotype periodontal macrophages at single cell level in response to local delivery of CCL2 in murine ligature periodontitis. **SA2A:** The periodontal microbial load and composition will be assessed following preventive CCL2 MP treatment of murine ligature induced PD. **SA2B:** CD45 enriched cell suspensions isolated from mice gingiva will be used for phenotyping and assessing the gene expression profile of murine periodontal macrophages following preventive CCL2 MP treatment of murine ligature induced PD.

Specific Aim 3 (SA3): To evaluate the bone loss protective effect of targeting IL-17A cytokine secreted in diseased murine periodontium by local sustained release of IL-17A antibodies. SA3A: Sustained release anti-IL-17A PLGA microparticles (MP) will be fabricated, surface characterized, and their release profile will be assessed. **SA3B:** Anti-IL-17A MP will be locally delivered either simultaneously with or 2 days after ligature PD induction in mice. Alveolar bone loss, osteoclastic activity and the mRNA expression of inflammatory markers will be analyzed.

2.1 Specific Aim 1

2.1.1 Introduction and Rationale

Periodontal disease (PD) is one of the most common oral diseases affecting nearly 50% of the United States adult population (Eke et al. 2015b), and its most severe form has global prevalence of 11.2% (Kassebaum et al. 2014). PD is characterized by a microbial dysbiosis that subverts the host microbe homeostasis in the periodontal environment and triggers chronic inflammatory destruction of tooth supporting structures (Hajishengallis 2015). If left untreated, PD can result in progressive alveolar bone loss, tooth loss and compromised masticatory function (Kosaka et al. 2014) . Furthermore, recent preclinical studies have implicated PD as an aggravating factor in a number of systemic conditions such as Alzheimer's and inflammatory bowel disease (Dominy et al. 2019; Kitamoto et al. 2020).

Owing to its chronic and complex nature, the destructive inflammatory process underlying PD lacks the ability to self-resolve and requires therapeutic intervention to control disease progression. In this respect, a myriad of mechanical (scaling and root planning) and chemical measures (antiseptics and antibiotics) have been employed to control PD (Sanz et al. 2015; Teles and Teles 2009). Those measures aim primarily at reducing the load of inflammation-inducing pathogens in the periodontium, thereby dampening the destructive inflammatory response fueling PD. Despite the long history of improvement in periodontal microbial debridement protocols, those protocols have exhibited varying degrees of success, and, in some patients, may fail to halt progressive attachment loss even in the presence of low plaque scores, as in the case of refractory periodontitis (Colombo et al. 1998; Haffajee et al. 1997).

The lack of consistent therapeutic outcomes for current PD treatment protocols has propelled the quest for adjunctive strategies addressing the host response component of the disease. Those strategies circumvent the arduous task of trying to completely eradicate periodontal pathogens and focus more on modulating the deleterious host response, which is responsible for the majority of inflammatory destruction characteristic of PD (Cekici et al. 2014a).

Macrophages are key mediators of the inflammatory response in many tissues including the periodontium. These cells exhibit a wide spectrum of phenotypic subsets with M1 (classically activated) and M2 (alternatively activated) phenotypes representing the extreme ends of the spectrum (Mantovani et al. 2004). Each phenotypic subset performs distinct functions depending on the nature and stage of the inflammatory process. In this regard, the M1 macrophages drive the initial pro-inflammatory responses necessary for host defense against invading pathogens, whereas M2 macrophages exhibit anti-inflammatory effects to promote inflammation resolution and tissue repair following pathogen eradication (Mantovani et al. 2004). Owing to their phenotypic and functional diversity, macrophages are thought to play a crucial role in the initiation, progression, and resolution of chronic inflammation (Oishi and Manabe 2018). Thus, modulating macrophages response has a potential to influence the course and fate of PD.

Several studies have investigated systemic and local approaches to target macrophages response in the periodontium. In this respect, one study showed that daily oral administration of Rosiglitazone, a PPAR-γ agonist, inhibited bone loss and stimulated bone formation by inducing M2 macrophages in murine periodontium (Viniegra et al. 2018). Another study suggested that locally injected dental pulp stem cell exosomes can accelerate periodontal bone healing in mice by

driving M2 macrophages polarization (Shen et al. 2020). Although promising, the aforementioned studies present macrophage-modulatory strategies that require either frequent systemic administration of the therapeutic agent or address only one stage of PD. To the best of our knowledge, there has been no reports to date of a local sustained periodontal therapeutic strategy that tests the feasibility of modulating macrophages response during different stages of periodontal inflammation or disease severity.

Our group has previously investigated local recruitment or induction of specific populations of immune cells into the periodontium to dampen destructive inflammation (Araujo-Pires et al. 2015; Glowacki et al. 2013; Zhuang et al. 2019). We have shown the feasibility of local induction of M2 macrophages in halting periodontal destruction in murine PD models (Zhuang et al. 2019) . The induction of M2 macrophages was achieved by local sustained delivery of the chemokine CCL2, which has been reported to preferentially induce an M2-like macrophages phenotype in several settings (Roca et al. 2009; Sierra-Filardi et al. 2014). In this work, we further examined the therapeutic efficacy of locally delivered CCL2 as a macrophage-modulating agent to treat early and established murine PD, and to induce periodontal healing during disease recovery. In this regard, we employed three clinically relevant therapeutic approaches for initial (preventive), progressing (interventional) and resolving (reparative) murine PD using local sustained delivery of CCL2. We assessed the changes in bone level, osteoclastic activity, periodontal ligament organization and the gene expression profile in murine periodontium. The present study aimed at providing phenotypic and mechanistic insights into the therapeutic potential of CCL2 local sustained delivery as an adjunctive therapy for PD.

2.1.2 Hypothesis

We hypothesized that local sustained delivery of the chemokine CCL2 would prevent murine ligature PD initiation, slow down its progression and accelerate its resolution by favoring a pro-resolving/M2-like macrophages response in the periodontium.

2.1.3 Materials and Methods

2.1.3.1 Fabrication and characterization of sustained release CCL2 Microparticles

Sustained release CCL2 MP were fabricated by encapsulating recombinant mouse CCL2 protein (R&D systems) into Poly-Lactic-co Gylcolic Acid (PLGA) (Sigma) using a standard water-oil-water double emulsion technique as described previously (Glowacki et al. 2013). The first aqueous phase consisted of 200 µl of 10 µg of recombinant mouse CCL2 with 1% bovine serum albumin (BSA) and 15 mmol NaCl. The oil phase was made by dissolving 200 mg PLGA polymer (lactic:glycolide 50:50, Mwt 7000 – 17000) in dichloromethane (organic solvent). The first aqueous and oil phases were sonicated together to obtain an emulsion that was then homogenized with 60 ml of 2% polyvinyl alcohol with 50 mM NaCl (second aqueous phase) to make the second emulsion. The homogenate was then added to 80 ml of 1% polyvinyl alcohol with 50 mM NaCl and stirred for 3 hours to allow for evaporation of dichloromethane. Next, the MP were collected and washed, then resuspended in 5 ml of deionized water and flash frozen in liquid Nitrogen before lyophilization. We also fabricated Blank (unloaded) PLGA MP without recombinant protein following the same protocol.

Following fabrication, the CCL2 MP were surface characterized using a scanning electron microscope (JSM-6335F), and their size distribution was assessed with volume impedance measurements on a Beckman Coulter counter. Next, the release profile of CCL2 protein from the MP was assessed by suspending 10 mg of the MP in 1 ml PBS with 1% BSA and placing the suspension on a tube rotator at 37°C. Supernatants were collected by centrifugation of the MP suspension followed by resuspension in equal amount of fresh PBS/BSA solution. Supernatant collection continued over a period of 30 days. The amount of the soluble CCL2 protein in the supernatant was quantified using an ELISA assay (R&D systems).

2.1.3.2 Murine ligature induced periodontitis

All animal procedures followed a protocol approved by the Institutional Animal Care and Use Committee at the University of Pittsburgh (protocol number: 18042616), and the ARRIVE guidelines for preclinical studies. Male 6-8-week-old Balb/C wild type mice, weighing 25-30 g, were purchased from Charles Rivers and used for the induction of ligature periodontitis around maxillary second molars. Mice were kept in cages (3-4 mice/cage) in a controlled environment with 12-hour dark/light cycles and were fed standard pellet diet and water through the length of each experiment. Mice were allowed an acclimation period of at least 72 hours before starting the experiments. Before placing ligatures in each experiment, mice were randomly assigned to experimental groups that included an age-matched-healthy control group with no ligature placement. For ligature periodontitis induction, mice were first anesthetized by intraperitoneal injection of 80 mg/8 mg/kg Ketamine/Xylazine, then, under a stereomicroscope, 6-0 silk suture (Henry Schein) was ligated around the left maxillary second molar with the knot placed on the palatal side, as previously described (Abe and Hajishengallis 2013).

Depending on the endpoint of each experiment, ligatures were left in place for either 7 (Preventive approach) or 10 days (Interventional approach) before mice sacrifice. Alternatively, ligatures were removed after 10 days then a recovery period of 4 days was allowed before sacrificing the mice (Reparative approach). G*Power 3.1 software was used to estimate the number of mice needed for each experiment. For the preventive approach experiment, a total of 44 mice were used (24 mice for bone loss analysis and 20 mice for gene expression analysis). For the interventional approach experiment, 50 mice were used (30 mice for bone loss analysis and 20 mice for gene expression analysis). Finally, 31 mice were used for the reparative approach experiment. At experimental endpoints, mice were euthanized in CO2 chamber followed by cervical dislocation.

2.1.3.3 Local periodontal delivery of CCL2 or blank PLGA MP

Following ligatures placement on maxillary molars, CCL2 or blank PLGA MP were locally delivered as a single dose at one time point throughout the length of the experiment. The MP delivery time point was determined based on whether a preventive, interventional or reparative therapeutic approach was intended in each experiment. Accordingly, MP were administered on same day of placement, 4 days after placement or on the day of removal of ligatures for the preventive, interventional and reparative therapeutic approaches, respectively (Fig. 1 outlines the experimental end points for each of the therapeutic approaches).

At the time of MP administration, 50 µl of either CCL2 or blank MP suspended in 2% carboxymethylcellulose in PBS (10 mg MP/ml) were locally injected in the buccal and palatal gingiva of the ligated maxillary second molar. 20 µl were injected in the mid-buccal aspect and the remaining 30 µl were distributed on the mesial, middle and distal palatal aspects of the ligated maxillary second molar. For the interventional and reparative approach experiments, mice that

had lost their ligatures at the time of MP delivery with or without ligatures removal were excluded from the study. In each experiment, mice with ligatures only and no MP injection (untreated) or age matching healthy mice with neither ligatures nor MP (healthy control) were included as additional experimental groups. No adverse events were encountered while conducting the animal experiments.

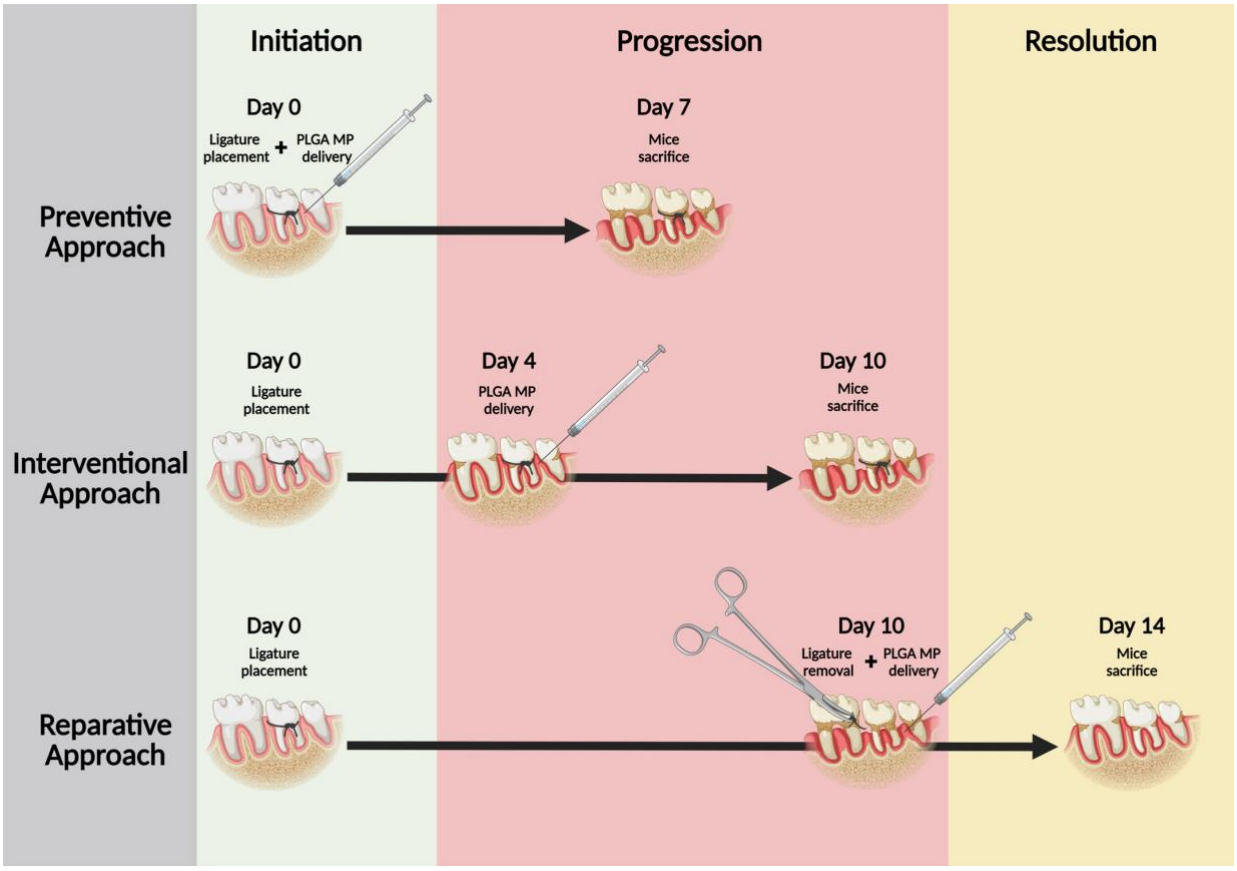

Figure 1. Diagramatic representation of the experimental design describing the 3 therapeutic approahes employed to treat initial, progressing (established) and resolving murine ligature induced periodontal disease (PD).

2.1.3.4 Micro-computed tomography and alveolar bone analysis

At the end of each experiment, mice maxillae were harvested and fixed overnight in 10% neutral buffered formalin then transferred to 70% ethanol for scanning with a micro-computed

tomography system (Scanco μCT 50, Scanco Medical). A resolution of 10μm voxel size, 55KVp, 0.36 degrees rotation step (180 degrees angular range) and a 1200 ms exposure per view were used. All scans were reoriented with DataViewer software (GE Healthcare) to a standardized orientation guided by pre-defined anatomical landmarks. For bone loss evaluation, reoriented images were used to measure the distance between the cementoenamel junction (CEJ) of the maxillary second molar and the level of the alveolar bone crest (ABC) on the mesial, distal, buccal and palatal aspects using CTAN software (Bruker). For mesial and distal measurements, the CEJ to ABC distance were measured on 8 measurement slices with a distance interval of 40 μm in between. For the buccal and palatal measurements, the CEJ to ABC distance were measured on 20 measurement slices with a distance interval of 30 μm in between. The average measurements on each aspect on the ligated side were normalized to the corresponding averages on the healthy side of the same maxilla. In the reparative therapeutic approach experiment, a second normalization to the average measurements from the 10 days ligature only group was performed. The investigator/personnel conducting the measurements was blinded to the treatment received.

2.1.3.5 Histological analysis

Mice maxillae samples were demineralized for 10 days in 10% EDTA, then embedded in paraffin. Embedded tissue samples were then sectioned into 5-μm thick sagittal sections that were used for assessing osteoclastic activity or characterizing the periodontal ligament fibers around the ligated molar using bright field microscopy.

Osteoclasts in tissue sections from the interventional approach experiment were quantified using a TRAP staining kit (Sigma) according to the manufacturer's instructions. In brief, deparaffinized tissue sections were first incubated in a fixative solution (25 ml citrate solution, 65

ml acetone and 8 ml of 37% formaldehyde) for 30 seconds then rinsed thoroughly in deionized water. Next, the slides were incubated in prewarmed reaction solution (45 ml deionized water prewarmed to 37°C, 1 ml diazotized Fast Garnet GBC solution, 0.5 ml Naphthol AS-BI phosphate solution, 2 ml acetate solution and 1 ml tartrate solution) for 1 hour at 37°C while protected from light. Following the 1-hour incubation, the slides were rinsed thoroughly in deionized water then counterstained with Hematoxylin solution for 30-45 seconds. After counterstaining, the slides were rinsed with running tap water for 5 minutes, then air-dried in a fume hood before adding Aqua-Poly/Mount mounting medium (Polysciences) and coverslip.

TRAP+ osteoclasts were identified as multinuclear pattern with red cytoplasm and purple nuclei. For each sample, three tissue sections near the bucco-lingual center and with a distance ladder of 25-30 μm were selected for counting TRAP+ cells. The region of interest was be defined as the area extending from either the mesial or distal alveolar bone crests to the corresponding root apex of the second molar. The total number of TRAP+ cells was normalized by the surface area of the ROI as measured by ImageJ software. The investigator/personnel performing the quantification was blinded to the treatment received.

To assess the pattern of periodontal ligament reorganization during the recovery phase following ligature removal, tissue sections from the reparative approach experiment were stained with a Picrosirius Red stain (Polysciences) following the protocol provided by the manufacturer. Briefly, deparaffinized tissue sections were first stained with Weigert's Hematoxylin solution for 8 minutes then rinsed thoroughly with deionized water. The slides were then incubated with phosphomolybdic acid (Solution A) for 2 minutes then rinsed with deionized water. Next, the

slides were incubated in Picrosirius Red F3B staining solution (Solution B) for 60 minutes. After picrosirius red staining, the slides were incubated in 0.1 N hydrochloride acid (Solution C), then dehydrated in ethanol (70% for 45 seconds once, 95% for 60 seconds twice and 100% for 60 seconds twice). Finally, the slides were incubated in Xylene for 60 seconds per incubation then the mounting medium and coverslips were added.

The orientation and distribution of the periodontal ligament collagen fibers around the ligated molar was visually assessed and compared across the experimental groups.

2.1.3.6 Quantitative polymerase chain reaction (qPCR)

For gene expression analysis, the preventive and interventional therapeutic approach experiments described above were repeated, then gingival tissues surrounding the ligated molar were harvested at predefined endpoints to proceed with RNA extraction, reverse transcription and qPCR analysis. For the preventive approach, local MP injection was done simultaneously with ligatures (day 0) placement then mice were sacrificed 4 days after (ligature PD induction for 4 days). For the interventional approach, MP injection was done 4 days after ligature placement, then mice were sacrificed 6 days (10 days ligature PD induction). Following mice sacrifice, the half-maxillae on the ligated side were harvested and flash frozen in liquid nitrogen then stored in -80 °C until the day of RNA extraction. The half maxillae samples were thawed at 4°C in RNA later solution the night before RNA extraction. Total RNA was extracted from the dissected alveolar gingiva on the ligated side using Trizol reagent (Life technologies, then purified using RNeasy Mini kit (Qiagen). Next, RNA was reverse transcribed to cDNA using High-Capacity RNA-to-cDNA™ Kit (Applied biosystems). Quantitative polymerase chain reaction was conducted using TaqMan™ Gene Expression Master Mix and Taqman primers (Applied Biosystems) on a QuantStudio 6 Flex Real- Time PCR system (Thermo Fisher Scientific). The

gene expression of macrophages polarization, inflammatory and bone remodeling markers (**Table 1**) was assessed. Data analysis was done with the delta-delta Ct method (Livak and Schmittgen 2001).

Table 1 List of Taqman probes used for qPCR analysis

Gene symbol and name	Taqman™ gene expression assay ID
Arg1 - liver arginase	Mm00475988_m1
Il1rn - interleukin 1 receptor antagonist	Mm00446187_m1
Nos2 - inducible nitric oxide synthase 2	Mm00440502_m1
Il6 – interleukin 6	Mm00446190_m1
Tnfsf11 - Tumor necrosis factor superfamily member 11	Mm00441906_m1
Tnfrsf11b - Tumor necrosis factor superfamily member 11b	Mm00435454_m1

2.1.3.7 Statistical analysis

Statistical analysis was performed in GraphPad Prism version 8. One-way ANOVA was used to compare between experimental groups followed by Tukey post-hoc test. Sample size was calculated using G*Power 3.1 software. A power level of 0.8 and an alpha of 0.05 were used in estimating sample size. Results were presented as mean ±SD and statistical significance was considered at $p < 0.05$.

2.1.4 Results

2.1.4.1 Characterization of sustained release CCL2 MP

SEM scanning of the CCL2 MP showed uniformly spherical MP with varying degrees of surface porosity (Fig. 2A). The volume impedance measurement showed that the average particle size was 21.49-±10.02 μm (Fig. 2B). The 30 days cumulative ELISA release profile (Fig. 2C) of rmCCL2 protein from the PLGA MP started with a burst release of about 28% of encapsulated protein, followed by a gradual release of another 23% over the first week. Steady release of about 6-15% of encapsulated CCL2 was observed at 5-7 days increments up to day 30.

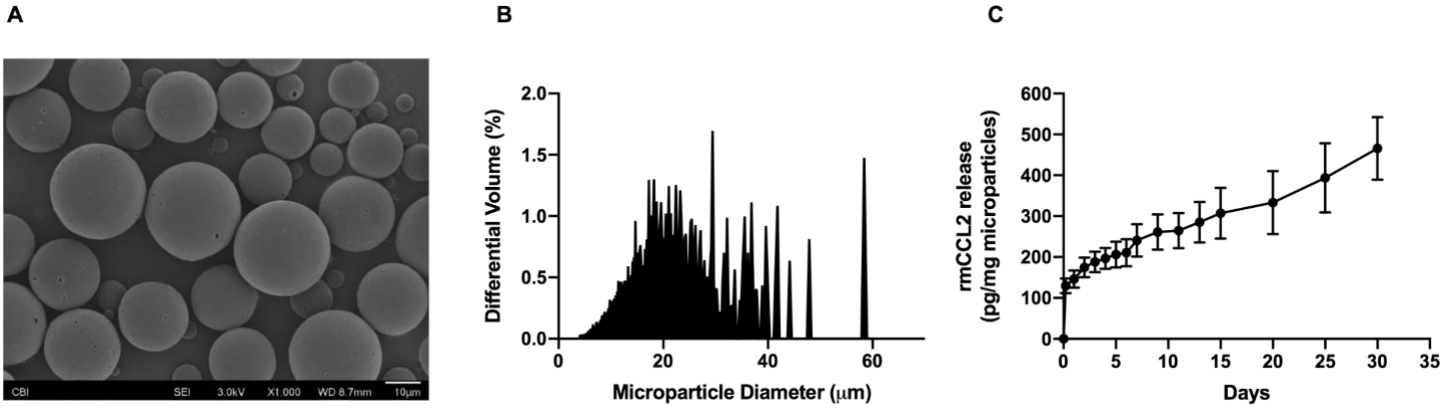

Figure 2. CCL2 PLGA MP characterization, size distribution and release profile assessment

2.1.4.2 Sustained release CCL2 MP inhibit murine PD initiation

To evaluate whether CCL2 local delivery inhibits bone loss initiation in murine PD, we analyzed periodontal bone levels in maxillae samples from mice that underwent ligature PD induction with or without simultaneous CCL2 MP local therapy (Preventive therapeutic approach). Our µCT analysis indicated that preventive CCL2 MP therapy inhibited interdental bone loss by ~32-37% compared to untreated or blank control mice (Fig. 3B). There was no statistically significant difference in buccal and palatal bone loss between groups (Fig. 3C and D).

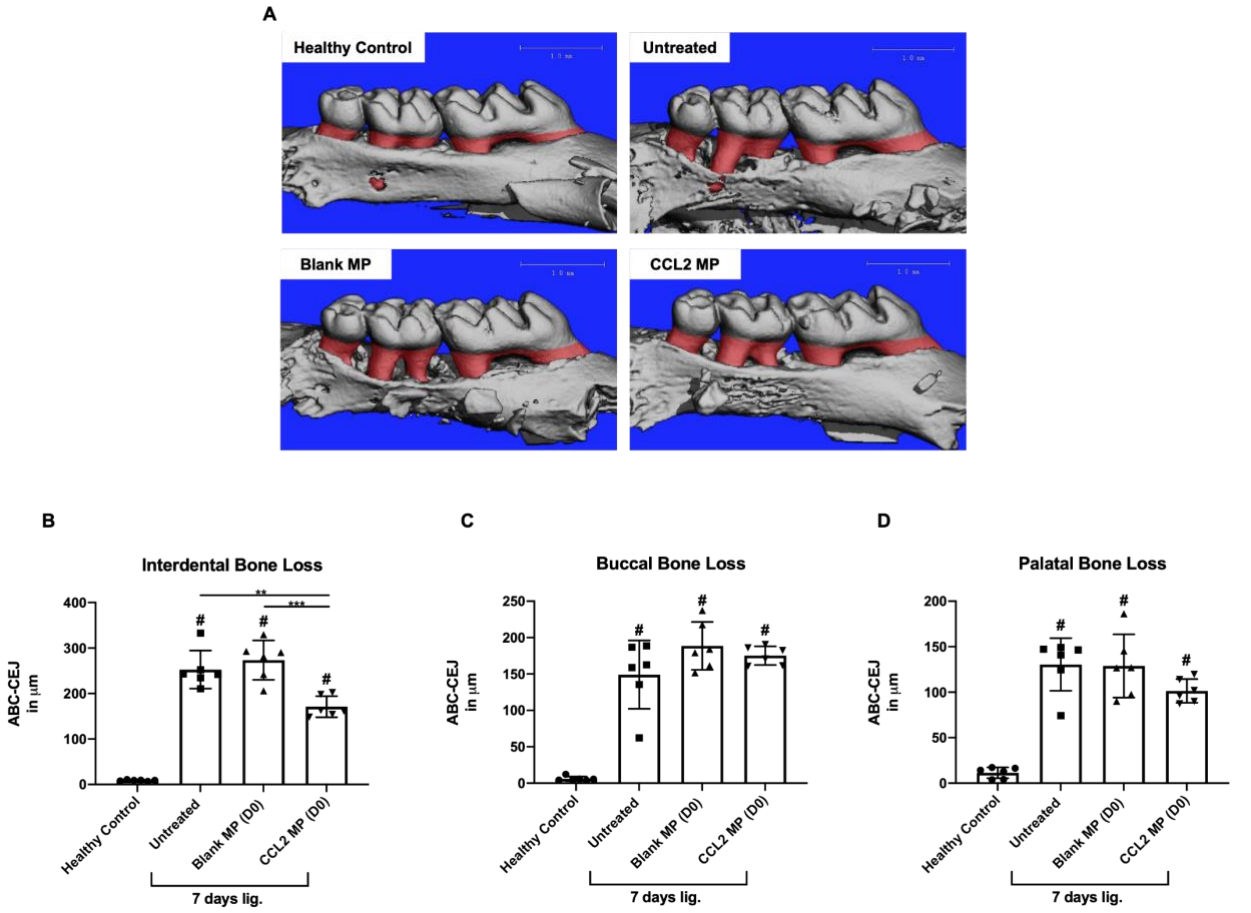

Figure 3. Micro-computed tomography analysis of alveolar bone loss following preventive local sustained release CCL2 MP therapy. CCL2 MP were locally delivered simultaneously with ligature placement in a 7 days ligature induced periodontitis model. Healthy control mice, mice with ligature placement only (untreated) or mice with ligature placement and blank MP (Blank MP) delivery were used as controls. One-way ANOVA with a post hoc Tukey test was performed to determine statistical significance, where *: $p < 0.05$, **: $p < 0.005$, ***: $p < 0.0005$ and ****: $p < 0.0001$ and #: significantly different from "Healthy control group". N = 6 mice.

2.1.4.3 Preventive CCL2 therapy induces a pro-resolving macrophages phenotype and inhibits uncoupled bone remodeling

Using qPCR, we assessed the expression of gingival inflammatory and bone remodeling markers following local delivery of CCL2 MP at the start of the induction of murine ligature PD for 4 days (Preventive therapeutic approach). Compared to ligature only mice or mice that received blank MP, mice treated with CCL2 MP showed an up-regulated mRNA expression of the pro-resolving M2-like macrophages marker *Arg1*, and downregulated expression of the M1 macrophages marker *Nos2* (Fig. 4A, B and C). Furthermore, preventive CCL2 MP therapy decreased the expression of the pro-inflammatory/pro-osteoclastic markers *Il6* and *Tnfsf11*, while *Tnfrsf11b* exhibited no change (Fig. 4 D, E and F).

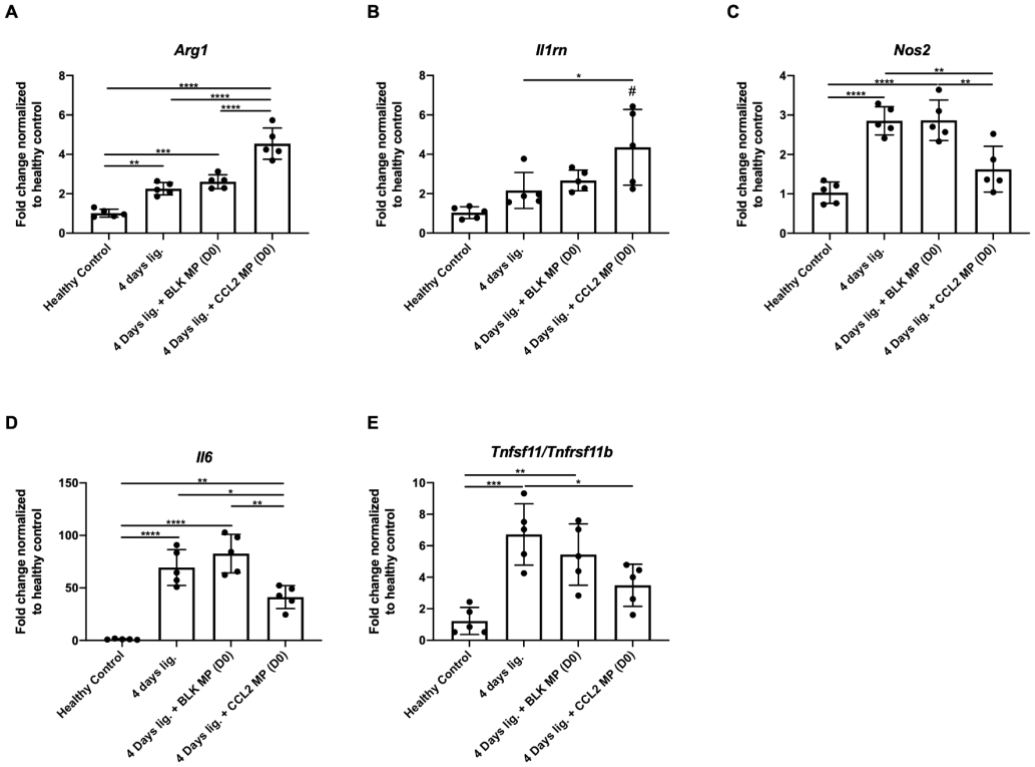

Figure 4. Quantitative polymerase reaction (qPCR) analysis of macrophages, inflammatory and bone remodeling markers at day 4 following ligature placement with or without simultaneous PLGA MP delivery (Preventive therapeutic approach). The mRNA expression of the M2-like macrophages markers *Arg1* and *Il1rn* (A and B), the M1 macrophages marker *Nos2* (C), the proinflammatory marker *Il6* (D) and the ratio of bone remodeling markers *Tnfsf11* (encoding RANKL) and *Tnfrsf11b* (encoding OPG) (E and F) was assessed. One-way ANOVA with a post hoc Tukey test was performed to determine statistical significance, where *: $p < 0.05$, **: $p < 0.005$, ***: $p < 0.0005$ and ****: $p < 0.0001$ with n= 5 mice.

2.1.4.4 Sustained release CCL2 MP restrain murine PD progression

We next sought to investigate whether the activity of PD at the time of CCL2 MP administration influence their protective effect against bone loss. To that end, CCL2 MP were delivered after 4 days from the start of ligature PD induction for 10 days (Interventional therapeutic approach). Our μCT analysis revealed that CCL2 MP suppress further interdental bone loss by ~ 26-29% when delivered in the presence of an active PD in mice (day 4) compared to untreated and blank control mice (Fig. 5B). No difference between groups was observed on the buccal and palatal aspects with interventional CCL2 therapy (Fig. 5C and D).

In line with the bone loss inhibitory effect of local interventional CCL2, TRAP staining of tissue sections from the same experiment revealed a reduction in osteoclast counts in CCL2 MP treated mice compared to untreated and blank MP treated controls (Fig. 6A-K). Additionally, there was a strong positive correlation between interdental bone loss and osteoclast counts as determined by Pearson correlation coefficient ($r = 0.737$, $p < 0.0001$) (Fig. 6L). Collectively, those results indicate that the protective effect of CCL2 local sustained release against bone loss is effective in the presence of an active disease.

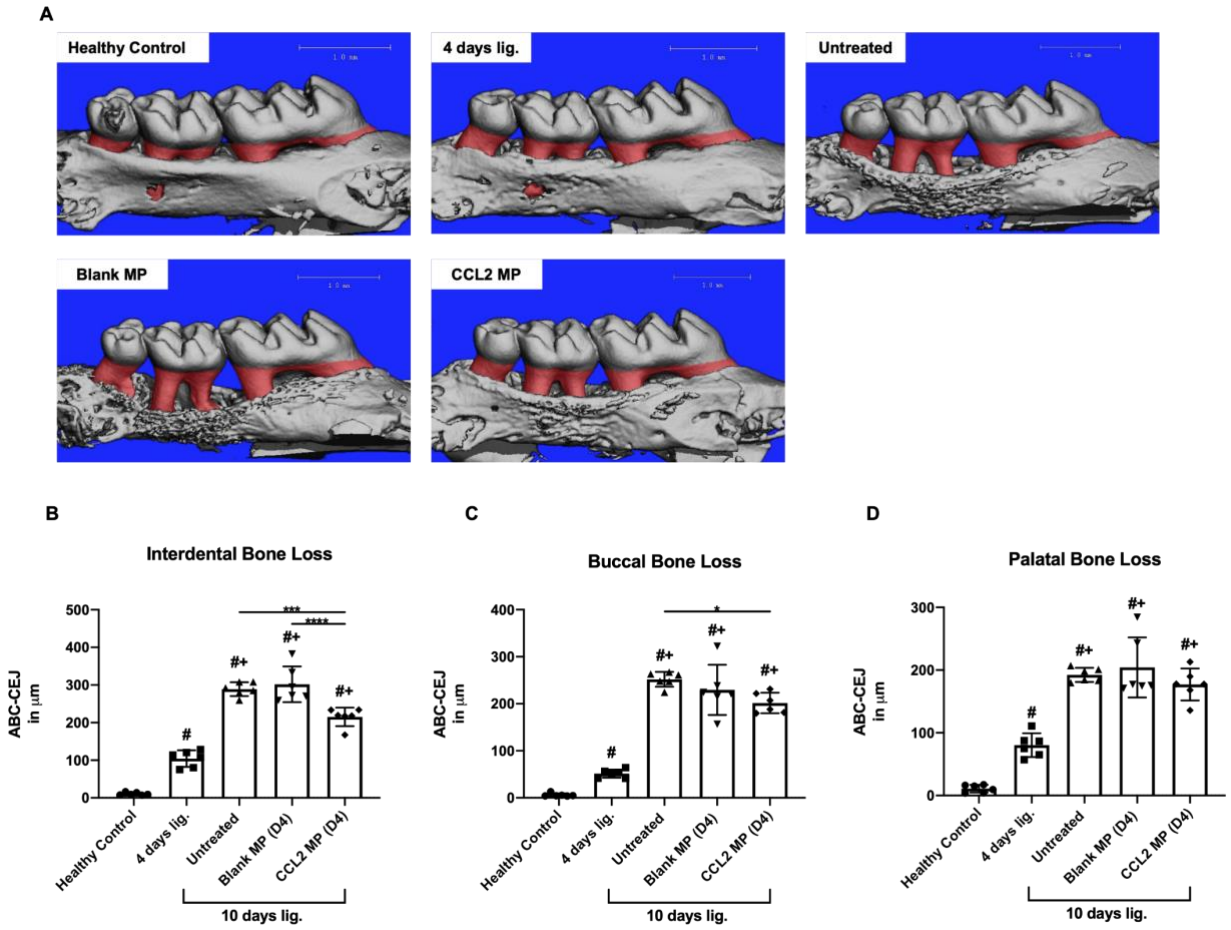

Figure 5. Sustained Release CCL2 MP restrain bone loss in established Murine PD. (A) Representative 3D images of the reconstructed micro-CT scans from each experimental group in the interventional therapeutic approach experiment. Alveolar bone loss was quantified by measuring the CEJ-ABC distance on the interdental (B), buccal (C) and palatal (D) aspects of the ligated maxillary second molar. Age-matched healthy control mice, mice with ligature PD induction only (untreated) or mice with ligature PD induction and blank MP local delivery were used as control. One-way ANOVA with a post hoc Tukey test was performed to determine statistical significance, where *: $p < 0.05$, **: $p < 0.005$, ***: $p < 0.0005$ and ****: $p < 0.0001$, #: significantly different from "Healthy control group" and +: significantly different from the "4 days ligature group". N=6 mice.

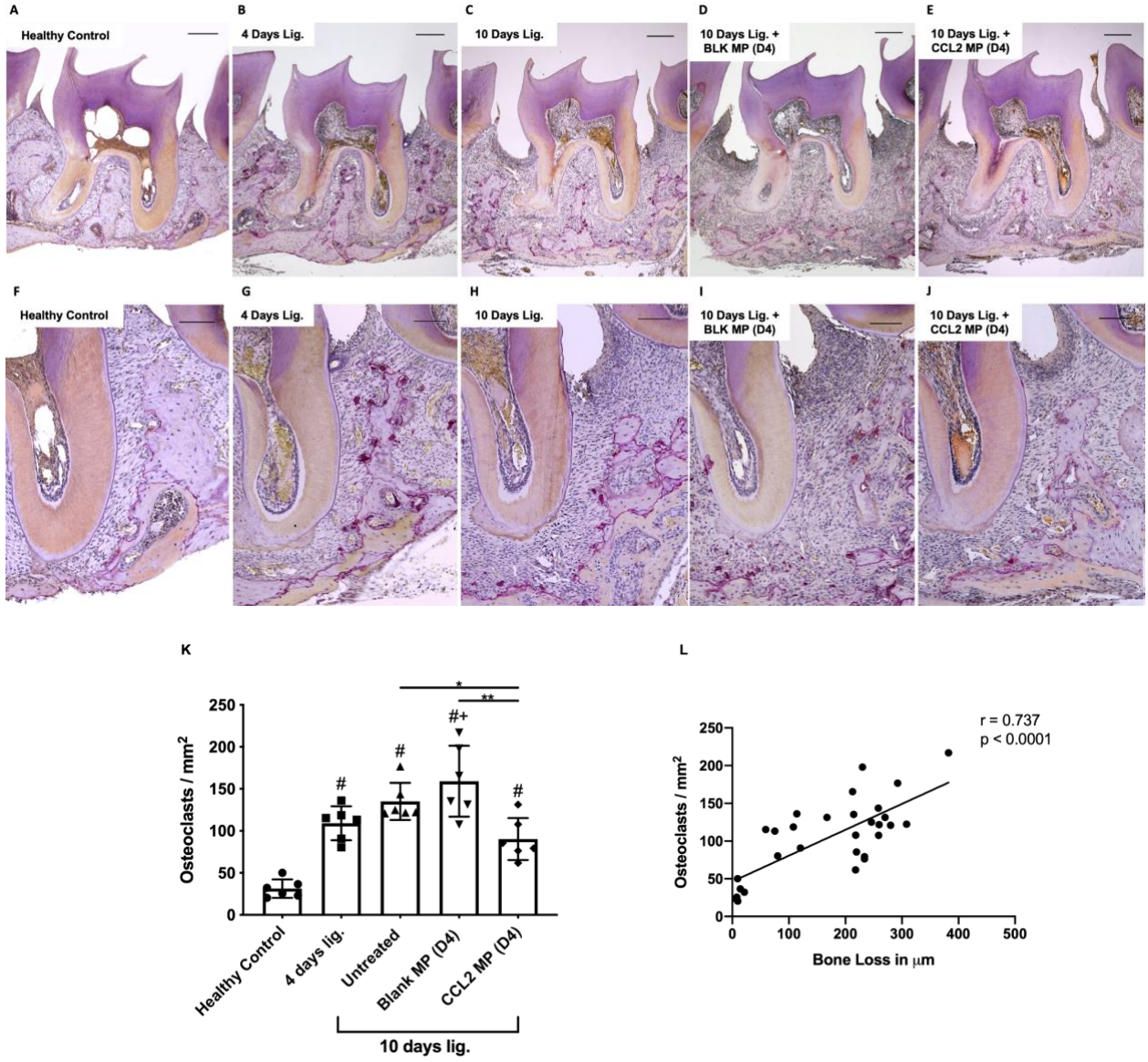

Figure 6. Sustained Release CCL2 MP inhibit osteoclastic activity in established Murine PD. (A-J) Representative images of the TRAP staining of tissues sections from different experimental groups in the interventional therapeutic approach experiment. (A-E) are the 40x magnified bright field images (scale bar = 200 μm), whereas (F-J) are the 100x magnified images (scale bar = 100 μm). (K) Analysis of TRAP positive osteoclast counts on the interdental aspect of the ligated maxillary second molar. One-way ANOVA with a post hoc Tukey test was performed to determine statistical significance, where *: $p < 0.05$, **: $p < 0.005$, ***: $p < 0.0005$ and ****: $p < 0.0001$, #: significantly different from "Healthy control group" and +: significantly different from the "4 days ligature group". N=6 mice. (L) Correlation analysis of osteoclasts number with the severity of bone loss. There was a strong positive correlation between the 2 parameters as determined by Pearson correlation coefficient ($r = 0.737$, $p < 0.0001$). N = 6 mice per group.

2.1.4.5 Interventional CCL2 therapy induces a pro-resolving macrophages phenotype and inhibits uncoupled bone remodeling

Similar to the preventive model, we also assessed the expression of gingival inflammatory and bone remodeling markers by qPCR. Local delivery of CCL2 MP was performed 4 days after the start of murine ligature PD induction for 10 days (Interventional therapeutic approach). Interventional CCL2 MP treatment resulted in an up-regulated mRNA expression of the pro-resolving M2-like macrophages markers *Arg1* and *Il1rn*, and downregulated expression of the M1 macrophages marker *Nos2* compared to the no MP or blank MP delivery (Fig. 7A, B and C). Moreover, interventional CCL2 MP therapy inhibited the expression of the pro-inflammatory/pro-osteoclastic markers *Il6* and *Tnfsf11*, while *Tnfrsf11b* showed no change between all groups where ligature PD was induced (Fig. 7D, E and F).

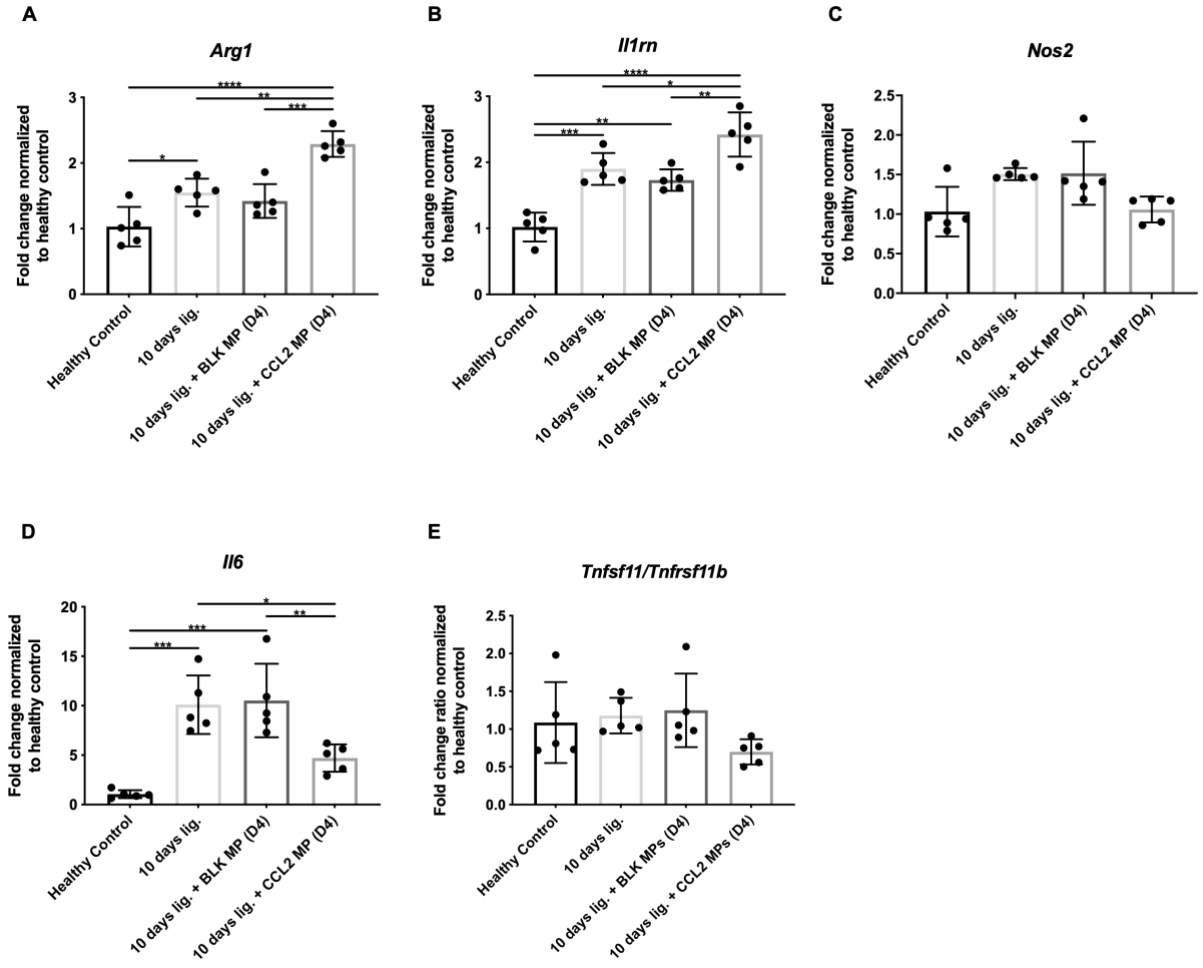

Figure 7. QPCR analysis for the expression of macrophages polarization, inflammatory and bone remodeling markers. Sustained release CCL2 MP were delivered 4 days after ligature placement during the course of a 10 days ligature PD induction (Interventional therapeutic approach). The mRNA expression of the M2 macrophages markers *Arg1* and *Il1rn* (A and B), as well as the M1 macrophages marker *Nos2* (C) was assessed. Additionally, the expression of the pro-inflammatory marker *Il6* and the ratio of bone remodeling markers *Tnfsf11* (encoding RANKL) and *Tnfrsf11b* (encoding OPG) were also evaluated (D-F). One-way ANOVA with a post hoc Tukey test was performed to determine statistical significance, where *: $p < 0.05$, **: $p < 0.005$, ***: $p < 0.0005$ and ****: $p < 0.0001$ with n = 5 mice.

2.1.4.6 Sustained release CCL2 MP accelerate periodontal repair during murine PD resolution

After confirming the effectiveness of our CCL2 local therapeutic strategy during murine PD initiation and progression, we sought to evaluate the potential positive effect of this strategy on periodontal healing during the resolution of murine PD. To that end, CCL2 MP were delivered concurrently with removal of ligatures at the start of a 4 days recovery period after murine PD induction for 10 days (Reparative therapeutic approach).

Analysis of alveolar bone levels revealed that CCL2 MP treated mice exhibited an accelerated interdental bone gain that reached 56% of healthy levels, as opposed to a 17-30% gain observed in untreated and Blank MP treated mice, where no difference in bone gain was observed on the buccal and palatal aspects (Fig. 8B).

Furthermore, picrosirius red staining of periodontal collagen fibers revealed more coronally positioned periodontal fibers in CCL2 treated mice, compared to the untreated of blank control groups (Fig. 9A-J). Additionally, the periodontal fibers in the CCL2 group appeared more organized, uniformly distributed and with even thickness as they insert into the alveolar bone and root cementum. On the other hand, collagen fibers in untreated or blank control groups exhibited a disorganized pattern and uneven distribution with some fibers completely detached from alveolar bone and cementum.

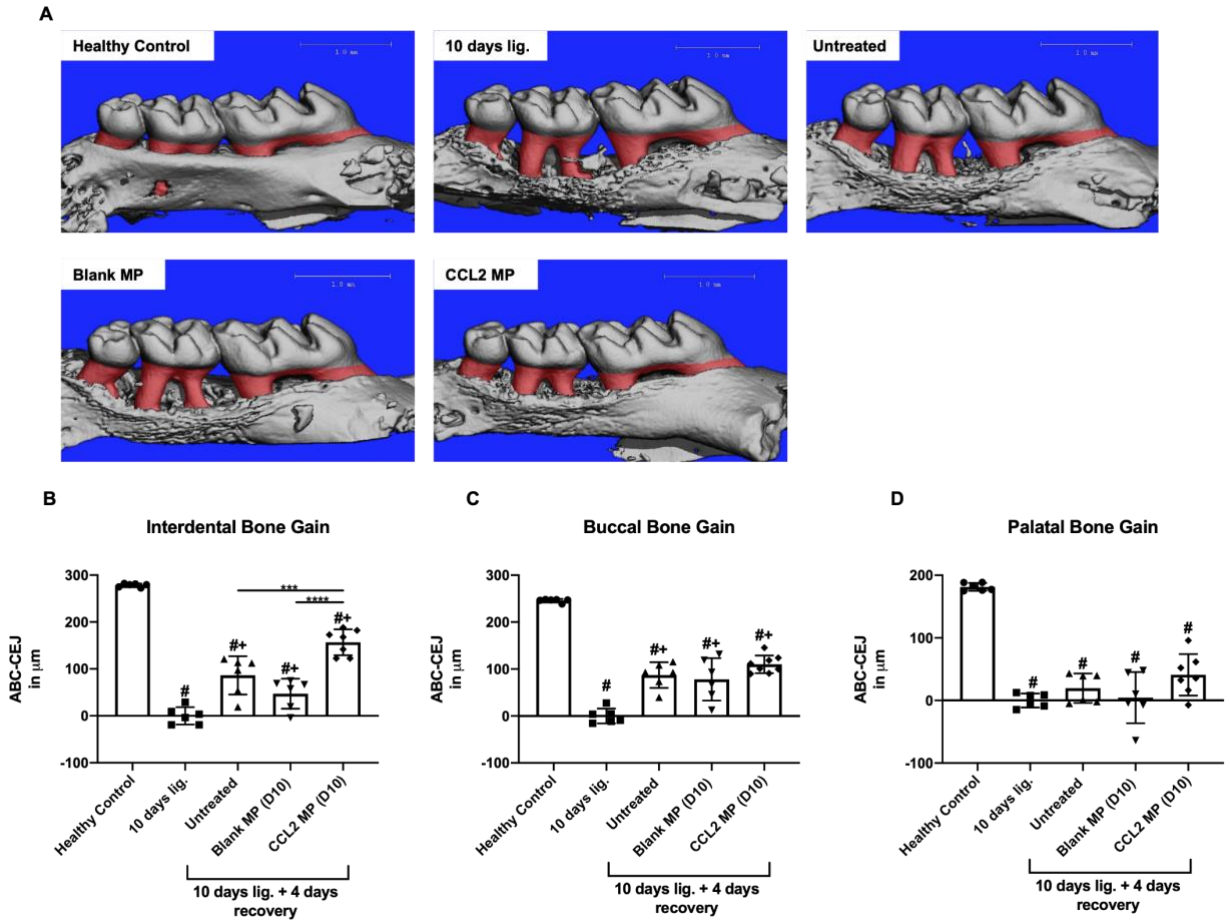

Figure 8. Sustained Release CCL2 MP accelerate periodontal repair during murine PD resolution. (A) Representative 3D images of the reconstructed micro-CT scans from each experimental group in the reparative therapeutic approach experiment. Bone gain was calculated by subtracting the ABC-CEJ measurements in mice that had undergone 4 days recovery from the corresponding average measurements of the 10 days ligature only mice on each aspect. (B-D) Alveolar bone gain quantification on the interdental (B), buccal (C) and palatal aspect of the previously ligated maxillary second molar following the 4 days recovery period. One-way ANOVA with a post hoc Tukey test was performed to determine statistical significance, where *: $p < 0.05$, **: $p < 0.005$, ***: $p < 0.0005$ and ****: $p < 0.0001$, #: significantly different from "Healthy control group" and +: significantly different from the "10 days ligature group". N=6-7 mice.

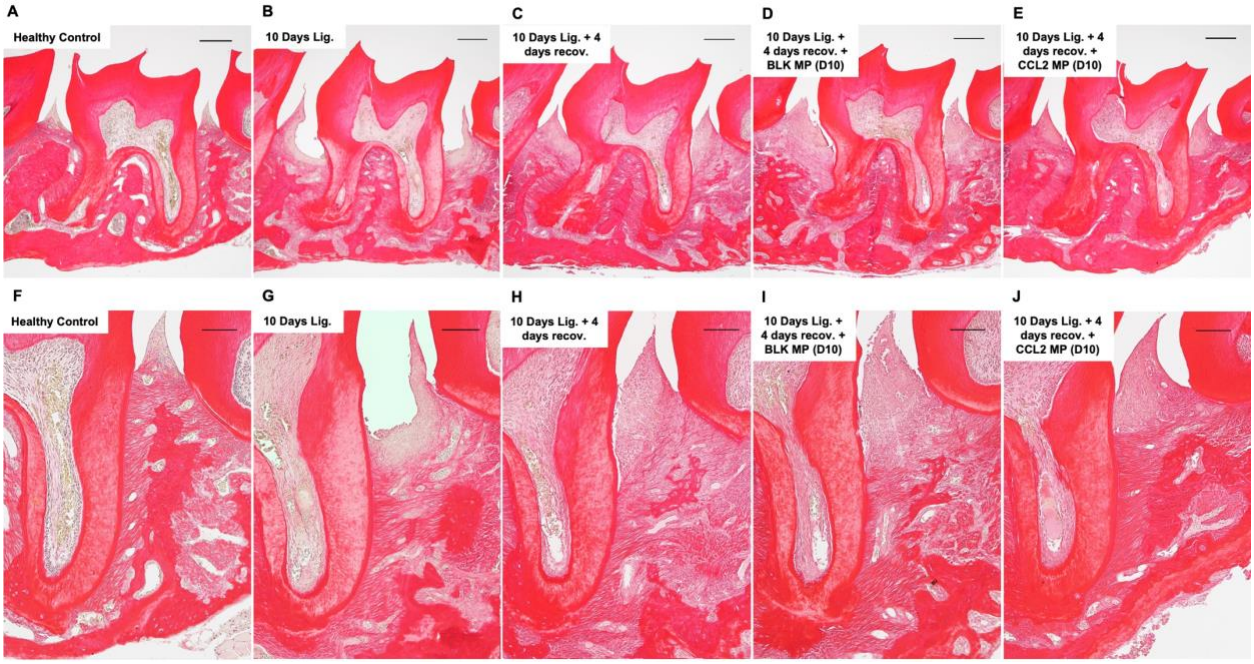

Figure 9. Representative images of the picrosirius red staining of tissue sections from the reparative approach experiment. The structure and organization of periodontal ligament fibers was visually inspected and compared between different experimental groups. (A-E) are representative bright field images at 40x magnification (scale bar= 200 µm). (F-J) are representative bright field images at 100x magnification (scale bar= 100 µm).

2.1.5 Discussion

PD is a chronic inflammatory disease that is associated with progressive destruction of tooth supporting structures and microbial dysbiosis. A number of inflammatory cells belonging to the innate and adaptive immune systems are involved in the periodontal inflammatory response and drive both its destructive and constructive phases. Among those cells, macrophages stand out as crucial members of the innate host response orchestrating PD pathogenesis and determining its fate. These cells comprise 6% of all immune cells in periodontal soft tissue biopsies (Carcuac and Berglundh 2014), and are present in higher numbers in the gingival tissues obtained from periodontitis lesions compared to healthy tissues (Gemmell et al. 2001; Yu et al. 2016). Thus, macrophages represent an attractive therapeutic target for immunomodulatory therapies aiming at controlling the detrimental host response underlying PD.

Our group has previously shown that local sustained delivery of the chemokine CCL2 in diseased murine periodontium at the start of PD induction inhibited periodontal bone loss and up-regulated the expression of M2-like macrophages markers (Zhuang et al. 2019). In this study, we sought to validate and build on our previous findings by investigating the beneficial effects of CCL2 local therapy during different stages of murine ligature PD. To that end, local sustained release of CCL2 was used as a preventive, interventional or reparative periodontal therapy depending on whether CCL2 PLGA MP were delivered at the initiation, progression or resolution stage of murine PD, respectively. This experimental design allowed us to assess the extent of disease protection/amelioration in response to CCL2 local therapy in situations that mimic different clinical scenarios of human PD.

In the preventive therapeutic approach, CCL2 MP were locally delivered at the start of murine ligature PD induction with the intent to dampen the early pro-inflammatory response driving disease initiation and subsequent bone loss. Indeed, preventive CCL2 therapy inhibited interdental bone loss and down-regulated the mRNA expression of the M1 macrophages marker *Nos2* and the pro-inflammatory/pro-osteoclastic markers *Il6* and *Tnfsf11*. Moreover, the M2 macrophages marker *Arg1* was up-regulated in CCL2 MP treated mice. Taken together, those results corroborate our previous findings (Zhuang et al. 2019) and indicate that the suppression of inflammatory bone loss as a result of local preventive CCL2 therapy is associated with changes in both the M1 and M2 macrophages response in favor of an M2-skewed environment.

We next sought to test whether locally delivered CCL2 can halt the progression of an established disease with an ongoing destructive inflammatory process. We have observed an enhanced expression of inflammatory and osteoclastic markers along with alveolar bone loss as early as day 4 post-ligature placement. Thus, delivering CCL2 MP at this time-point can be considered as an interventional administration of treatment during the course of a 10 days ligature induced PD. In this study, interventional CCL2 therapy suppressed interdental bone loss, reduced osteoclasts numbers and down-regulated the mRNA expression of *Il6* and *Tnfsf11*. Moreover, there was an up-regulated expression of the M2 macrophages markers *Arg1* and *Il1rn* in CCL2 MP treated mice. Collectively, those results suggest that CCL2 local therapy maintains its ability to induce an M2-like macrophages response and hinder inflammatory bone loss even in the presence of an active inflammation and ongoing tissue destruction.

The results from the 2 therapeutic approaches outlined above support previous reports pointing to an inverse correlation between osteoclastic activity and the M2 macrophages response during the course of chronic bone destructive diseases (Hannemann et al. 2019; Viniegra et al. 2018). This correlation is further supported by earlier mechanistic studies showing that M2 macrophage secreted cytokines (e.g., IL-1ra and IL-10) inhibit osteoclast formation (Kitazawa et al. 1994; Xu et al. 1995), while M1 macrophages derived cytokines (e.g., IL-6 and TNF- α) promote osteoclastogenesis (Kobayashi et al. 2000; Udagawa et al. 1995). Furthermore, similar to what was observed with local delivery of CCL2 in the present study, another group showed that local delivery of the pro-resolving lipid mediator RevE1 reduced bone loss in both initial and established ligature induced PD in rats (Lee et al. 2016b). RevE1 has been reported to repolarize M1 macrophages towards an IL-10 producing pro-resolving phenotype (Herová et al. 2015), and to inhibit osteoclast differentiation (Herrera et al. 2008). Altogether, the collective results emphasize the dynamic relationship between macrophages polarization and bone remodeling during early and established inflammatory responses.

We also explored the ability of CCL2 local therapy to ameliorate periodontal repair following stimulus removal in murine ligature induced PD. Indeed, several studies have reported spontaneous healing with either an arrest of bone loss or complete bone regeneration within days to weeks from ligatures removal in mice undergoing ligature-induced periodontitis (Kourtzelis et al. 2019; Viniegra et al. 2018; Wong et al. 2017) . To that end, we employed a reparative therapeutic approach where CCL2 MP were locally delivered concurrently with removal of ligatures at the start of a brief 4 days recovery period following 10 days of ligature PD induction. The mice treated with CCL2 MP exhibited an acceleration of interdental bone gain compared to

no treatment or treatment with blank MP. Additionally, the accelerated bone gain in CCL2 MP treated mice was associated with more coronally positioned and organized periodontal ligament fibers, as opposed to the more apical and disorganized periodontal fibers in the untreated and blank MP treated mice. The ability of locally delivered CCL2 to induce an M2-like macrophages response in inflamed periodontium (as we showed in this study) can explain the robust healing effects produced by CCL2 reparative therapy. The CCL2 induced M2-like macrophages can in turn secrete anabolic cytokines (IL-10, IL-1ra and TGF-β) (Mantovani et al. 2004), or factors that support cell proliferation and collagen synthesis (polyamines and L-proline) (Caldwell et al. 2018). Moreover, CCL2 has been reported to enhance apoptotic cell removal (efferocytosis) by macrophages (Tanaka et al. 2010), which is an essential process for inflammation resolution and tissue repair (Poon et al. 2014). The induction of murine periodontal healing by local CCL2 therapy reported here highlights the pivotal role of constructive inflammation in tissue repair following inflammatory damage. Further studies are needed to elucidate the mechanism driving enhanced periodontal healing in response to CCL2 local therapy.

In conclusion, the current study suggests that local sustained delivery of CCL2 favors an M2-like macrophages response and suppresses inflammatory bone loss during the course of early and established murine PD. Local therapy with CCL2 also accelerates periodontal healing during murine PD resolution. The results of the present study provide evidence for the clinical translation potential of immunomodulatory strategies aiming at restoring macrophages homeostasis for treating PD.

2.2 Specific Aim 2

2.2.1 Introduction and Rationale

We have previously shown that local sustained delivery of the chemokine CCL2 inhibited inflammatory bone loss in initial and progressing murine ligature PD (specific aim 1B and 1C). Furthermore, we demonstrated that CCL2 local sustained therapy accelerates bone gain during murine PD resolution (specific aim 1D). Our qPCR analysis revealed that the disease protective/amelioration effects of CCL2 correlated with a macrophage markers expression (*Arg1*, *IL1rn*, *Nos2*, *Il6*) indicative of a pro-resolving/anti-inflammatory macrophage response. Accordingly, we have speculated that CCL2 mediates its therapeutic effect in murine PD, at least in part, by influencing macrophages polarization in the mouse periodontium. However, our speculation was not supported by additional experiments that aim at characterizing murine periodontal macrophages based on their cell surface and intracellular markers expression. Additionally, we have not conducted an in-depth investigation of the pathways involved in the macrophages dependent local therapeutic effect of CCL2 in murine PD. Finally, we have not yet investigated whether murine PD treatment with CCL2 local delivery influences the disease associated changes in periodontal microbial load and composition.

Mouse macrophages have been extensively characterized in almost every tissue during health and disease (lung, heart, kidney, skin, central nervous system, joints) (Gangwar et al. 2020; Lee et al. 2018; Pinto et al. 2012; Wang et al. 2013; Zhang et al. 2008). This characterization has been routinely performed using well-documented macrophages markers assessed via fluorescent activated cell sorting (FACS). Using those markers, the contribution of M1/pro-inflammatory and

M2/anti-inflammatory macrophages has been correlated to disease development or recovery. For instance, during murine acute lung injury (ALI) induction, resident alveolar macrophages ($CD45^{high}$ $CD11b^{low}$) exhibited an M1-like phenotype (expressing ICAM-1), whereas infiltrating alveolar macrophages ($CD45^{high}$ $CD11b^{high}$) showed a mixed M1/M2 like macrophages expression profile (Johnston et al. 2012). During ALI resolution, the recruited macrophages were predominantly M2-like (expressing TfR), while resident macrophages exhibited a mixed M1/M2 expression profile (Johnston et al. 2012). Similarly, in a mouse model of myocardial infarction (MI), M1-like macrophages ($LY6G^{-}CD45^{+}CD11b+F4/80^{+}CD206^{-}$) were dominant in the 1-3 days post-MI induction, while M2 like macrophages ($LY6G^{-}CD45^{+}CD11b+F4/80^{+}CD206^{+}$) made the majority of macrophages after day 5 (Yan et al. 2013). In the same context, the chemokine receptor CCR2 has been previously shown to efficiently distinguish between resident ($CCR2^{-}$) and infiltrating (CCR2+) cardiac macrophages (Lavine et al. 2014). Along the same lines, induction of periodontitis by a porphyromonas gingivalis (Pg-PD) oral gavage was associated with an increase in M1-like macrophages ($LY6G^{-}TCR\beta^{-}B220^{-}CD11b+CD86+$) and a decrease in M2-like macrophages ($LY6G^{-}TCR\beta^{-}B220^{-}CD11b+CD206+$), with no description of the contribution of resident and infiltrating macrophages in those shifts. Apart from the specific markers used to designate M1 versus M2-like macrophages, the results from those animal models indicate that M1-like macrophages contribute to pathological changes associated with disease induction, while M2-like macrophages are associated with disease protection and resolution.

The mouse ALI, MI and Pg-PD models described above are examples of disease models in which different arrays of markers were used to designate the same macrophage polarization state (M1 or M2). This highlights the heterogeneity of macrophages populations and polarization states across different tissue types. This heterogeneity limits the ability of FACS analysis in

uncovering the full range of macrophages phenotypic switches during the transition from a health to disease state or in response to therapeutic intervention. FACS analysis is also limited by the commercial availability of specific fluorescent macrophages markers and its labor-intensive and technique sensitive cell staining protocols.

Single cell RNA sequencing (Sc-RNA seq) is a revolutionary technology that has gained significant popularity in recent years. Since its introduction in 2009 (Tang et al. 2009), Sc-RNA seq has helped to overcome the shortcomings of other transcriptomic analysis techniques such as qPCR analysis and bulk/total RNA sequencing. Those techniques are limited by the fact that gene expression data obtained from total RNA samples represent only the average transcriptional activity of a large population of heterogeneous cells that may differ in functional contribution. By assessing transcriptional similarities and differences at single cell level, Sc-RNA seq allows for uncovering previously overlooked cellular heterogeneity and the identification of rare and hyper-responsive cellular entities (Jaitin et al. 2014; Nguyen et al. 2018; Shalek et al. 2014). In addition, the cell specific differential expression data sets obtained from Sc-RNA seq can be used to identify signaling pathways, upstream regulators and diseases and functions that are associated with the observed phenotypic changes. This can be achieved by inputting the Sc-RNA seq differential expression data into a commercially available pathway analysis platform such as QIAGEN Ingenuity Pathway Analysis (QIAGEN Inc, IPA).

In PD, the disease associated changes in the periodontal microbial communities have been implicated as a triggering factor of destructive inflammation driven by macrophages and other immune cells (Darveau et al. 2012). During the course of PD, the increase in microbial biomass and diversity, as well as the upregulated virulence of individual microbial entities contribute to

breakdown of host microbe homeostasis (Curtis et al. 2020). The shifts in the microbial ecology are further exacerbated by the inflammation-induced changes in the subgingival environment. For instance, the periodontitis associated increase in the flow of the gingival crevicular fluid rich in proteins has been proposed to drive the growth of pathogenic asaccharolytic proteinase producing bacteria (ter Steeg et al. 1987). Similarly, the low redox potential of periodontitis associated plaque and the presence of blood cells in the subgingival pocket could be responsible for the growth of black pigmented anaerobic bacteria that thrive on the hemin derived from hemoglobin (Lewis 2010; Loesche 1991). In addition to the changes in the subgingival ecology, some low abundance disease-associated keystone pathogens such as porphyromonas gingivalis (Pg) can participate in remodeling the periodontal microbiota by targeting the innate and adaptive host defense mechanisms (Hajishengallis 2011). In doing so, Pg impairs immune surveillance and enables low abundance members of microbial community to grow (Hajishengallis and Lamont 2014) . Collectively, all those factors contribute to the dysbiotic changes in the periodontal microbial community and highlight the role of uncontrolled/impaired inflammation in driving periodontal immunopathology. Therefore, interventions that aim at actively controlling local inflammation in the periodontium are expected to also hinder the inflammation-induced shifts in the periodontal microbiota.

In this work, we investigated the effects of locally delivered CCL2 on the transcriptomic changes of murine periodontal macrophages at single cell level during murine PD. We also evaluated the shifts in periodontal microbial communities in response to CCL2 treatment. We hypothesized that CCL2 local delivery would modulate macrophages inflammatory response and reverse the shifts in the periodontal microbiota as a result of murine PD induction.

2.2.2 Hypothesis

We hypothesized that local sustained delivery of CCL2 in diseased murine periodontium would abrogate pro-inflammatory responses by resident and non-resident periodontal macrophages, and reverse inflammation-induced microbial dysbiosis.

2.2.3 Materials and Methods

2.2.3.1 Isolation and purification of murine gingival immune cells

Murine ligature PD was induced for 7 days in 8-10 weeks old male Balb/C mice as described previously (Abe and Hajishengallis 2013). Following ligature placement, mice were split into 3 groups 2 of which received local delivery of either Blank or CCL2 MP around ligated teeth on the same day of ligature placement (Preventive therapeutic approach), while the third group underwent ligature PD induction only (untreated). A 4^{th} group of age matched mice without ligatures placement or MP delivery was used as a healthy control. **Table 2** summarizes the experimental groups for the ScRNA-Seq experiment.

Table 2. Description of the experimental groups used in the Sc-RNA sequencing experiment

Experimental Groups (n = 7-8 mice)	**Healthy control (HCtrl)**	**Untreated (UT)**	**Blank (BLK)**	**CCL2 (CCL2)**
Description	No ligature placement No PLGA MP	Ligature placement only	Ligature placement + Blank MP local delivery	Ligature placement + CCL2 MP local delivery

At the end of the 7 days disease induction period, mice were sacrificed, and the maxillae were harvested for isolation of gingival immune cells on the ligated side as described previously (Dutzan et al. 2016). In brief, alveolar gingival tissues surrounding the ligated tooth in each mouse were dissected and minced in small pieces then digested in 5 ml RPMI with 3.2 mg/ml Collagenase Type IV (Gibco) and 1 mg/ml DNAse for 1 hour (Sigma). Five minutes before the end of digestion, 50 ul of EDTA were added to the digest. Next, 5 ml of RPMI with 1 mg/ml DNAse were added to the collagenase DNAse medium containing digested gingival tissue, and then the mixture was passed through a 70-μm cell strainer to obtain a single cell suspension. The cell suspension was then centrifuged at 1500 xg for 6 minutes in a pre-cooled centrifuge, then the cell pellet was resuspended in PBS with 2% FBS.

Single cell suspensions obtained from each mouse were then incubated with cell hashing antibodies in a known sequence (barcoded oligo-tagged antibodies against cell surface proteins). Following incubation with cell hashing antibodies, cell suspensions from each experimental group were washed three times in PBS with 2%FBS then pooled into one suspension. Next, the pooled cell suspensions were magnetically labelled with a CD45 microbeads kit (Miltenyi Biotec). The CD45-positive cells were then positively selected by passing the magnetically labelled cell suspension through a MACS column placed in the magnetic field of a MACS separator. The unlabeled (CD45-negative) cells passed through the column, while the labelled (CD45-positive) cells were retained in the column. Next, the column was removed from the magnetic field and the retained CD45-positive cells were eluted into a collection tube by flushing appropriate amount of PBS through the column. The flushed CD45 enriched cell suspensions were counted, and their

viability was assessed using an automated cell viability counter (Nexcelom Bioscience) to estimate the number of cells to be for Sc-RNA Seq workflow.

2.2.3.2 Sc-RNA seq workflow

The CD45-enriched live cells were analyzed by ScRNA. In brief, cells pooled from each group were separated into mini-reaction "partitions" or GEMs formed by oil micro-droplets, each containing a gel bead and a cell, by the Chromium instrument (10X Genomics, (Zheng et al. 2017)). Approximately 1000-fold excess of partitions compared to cells assures that most partitions/GEMs will have only one cell/GEM. Gel beads in the GEMs contain a gel bead, scaffold for an oligonucleotide that is composed of an oligodT section for priming reverse transcription, and barcodes for each cell (10X) and each transcript (unique molecular identifier, UMI). 2100 cells were loaded into the instrument to obtain data on ~1200 cells with a rate of ~1.2% of partitions showing more than one cell/partition. The following steps were all be performed using reagents and protocol developed by 10X Genomics. The reaction mixture/emulsion was removed from the Chromium instrument, reverse transcription was performed by incubation of the emulsion at 55 °C for 2 hours. The emulsion was then broken using a recovery agent and following Dynabead and SPRI clean up cDNAs were amplified by PCR (C1000, Bio-Rad). cDNAs was sheared enzymatically. DNA fragments ends were repaired, A-tailed and adaptors ligated. The library was quantified using KAPA Library Quantification Kit (Illumina), and further characterized for cDNA length on a bioanalyzer. RNA-seq was performed on each sample through the University of Pittsburgh Genomics Core. Genes detected (1,000-5,000 genes/cell) plateau at about 200,000 reads/cell (10X Genomics, white paper). Thus, we will typically obtain 200 million reads (NextSeq, Illumina).

2.2.3.3 Sc-RNA seq data analysis

ScRNA-seq raw bcl files were processed to generate library-specific fastq files. Processed reads were examined by quality metrics and mapped to a reference genome using the RNA-seq aligner STAR, implemented through 10X Genomics' Cell Ranger. Cell-gene counting matrices were generated for detailed downstream analyses such as, t-SNE, UMAP, and clustering. This pipeline was previously tested using Cell Ranger and Seurat packages (Satija et al. 2015). T-distributed stochastic neighbor embedding (t-SNE) developed as a machine-learning algorithm has been previously applied very successfully for analyzing single cell transcriptome data (Bushati et al. 2011). Seurat constructs a K-nearest neighbors graph based on Euclidean distance in PCA space. Edge weights were refined by overlap in local neighborhoods (Jacard distance). Finally, cells were clustered using a smart local moving algorithm (SLM) to iteratively group cells (Emmons et al. 2016). Differential gene expression between specific groups and clusters was assessed by implementing the non-parameteric Wilcoxon rank sum test with a bonferroni correction using all features in the dataset. Output includes an unadjusted p value, the log fold-change of a gene's average expression value between the two groups, and the percentage of cells per group expressing the gene of interest.

2.2.3.4 Ingenuity pathway analysis “IPA”

The differentially expressed genes (DEGs) in the two binary comparisons: untreated versus healthy control (UT vs. HCtrl) and CCL2 versus untreated (CCL2 vs. UT) were used for ingenuity pathway analysis “IPA” in the macrophages (Macs) clusters. DEGs used for analysis were filtered so that only those with a fold change greater than 1.1 (upregulation) or less than 0.9 (downregulation) and an expression p value less than 0.05 were included in the analysis. The top canonical pathways and upstream regulators were assessed within the individual groups and

compared between the 2 binary comparisons. As a rule, canonical pathways and upstream regulators were designated as upregulated or downregulated (statistically significant increase of decrease in activity) only when they have an absolute z-score value of two or higher.

2.2.3.5 DNA extraction for evaluation of periodontal microbial load and composition

Murine ligature PD was induced for 7 days in 8-10 weeks old male Balb/C mice, concurrently with preventive CCL2 MP treatment as described in specific aim 1. The experimental groups used in this experiment are described in table 3 below. At the end of disease induction, mice were sacrificed and the half maxillae tissue blocks (molar teeth with ligature in place, gingiva and alveolar bone) on the ligated side was harvested, placed into an Eppendorf tube with Tris-EDTA (TE) buffer then stored at -80 °C until the day of DNA extraction. For DNA extraction, samples were be first thawed on a heated shaking block at 37 °C for 10 minutes. Next, 1 µl of Ready-Lyse lysozyme solution (Epicenter) was added to each sample, followed by incubation at 37 °C for 60 minutes on a heated shaking block. After the lysis step, total DNA was purified from each sample using DNeasy Blood and Tissue Kit (Qiagen) following manufacturer's instructions. A TE buffer control was used in each DNA extraction assay.

Table 3. Experimental groups description for the microbial load and composition analysis experiment

Experimental Groups (n = 7-8 mice)	Healthy/ Healthy 2hr ligature	Untreated	Blank	CCL2
Description	- No ligature placement **or** ligature placement for 2 hours - No PLGA MP	Ligature placement only	Ligature placement + Blank MP local delivery	Ligature placement + CCL2 MP local delivery

2.2.3.6 Analysis of total periodontal microbial load

The total bacterial load per sample was evaluated via qPCR using 16S rRNA gene primers and a TaqMan probe (Nadkarni et al. 2002). A standard curve with a known number of 16S rRNA gene copies was used as a reference. 16S rRNA gene copies were normalized to the sample weight. The detection threshold for the copy number was based on the standard curve and the negative controls (TE buffer only).

2.2.3.7 Evaluation of periodontal microbial composition

The composition of the murine periodontal microbiome was evaluated in different experimental groups using previously described procedures (Abusleme et al. 2017; Dutzan et al. 2018c).

Amplification and sequencing of 16S rRNA gene libraries

Amplicon libraries were prepared using fusion primers, including adaptors, indices, spacers and 16S rRNA gene primers for the V1-V2 region or for the V3-V4 region. Our sequencing strategy is based on the method of Fadrosh et al. (Fadrosh et al. 2014), modified for V1-V2 universal primers 8F 5'- agagtttgatcmtggctcag-3' and 361R 5'-cyiactgctgcctcccgtag-3' or for the V3-V4 universal primers 341F 5'-CCTACGGGNGGCWGCAG-3′ and 785R 5'GACTACHVGGGTATCTAATCC-3'. These two regions were sequenced to minimize the possibility of taxa underrepresentation due to primer recognition bias. PCR reaction set up and amplification conditions have been previously described (Abusleme et al. 2017). PCR products and negative controls (for DNA extraction and PCR) were purified using Agencourt AMPure XP reagents, quantified, pooled and sequenced using the MiSeq Reagent Kit v3 (2 x 300 cycle) (Illumina).

Processing of sequences and taxonomic classification

16S rRNA gene reads were processed in mothur (Schloss et al. 2009). Forward and reverse reads were assembled into contigs followed by removal of primers, barcodes, trimming and removal of chimeric sequences. Individual sequences were classified using The Ribosomal Database Project (RDP) classifier. Reads were clustered at 97% similarity into Operational Taxonomic Units (OTUs). OTUs were classified up to genus and species levels when possible, according to the consensus taxonomy. To enhance the taxonomical resolution of each OTU, the representative sequence was compared using BLAST to the NCBI 16S rRNA sequence database and the best match (with at least 97% similarity and coverage) was also used to identify OTUs. Microbiome diversity (Beta diversity) was determined via the non-parametric Shannon Index and the Jaccard and ThetaYC indices, respectively. Clustering of microbiome communities according to experimental groups was evaluated via principal component analysis (PCA). Differences in taxa across experimental groups were evaluated via LEfSe (Segata et al. 2011).

2.2.4 Results

2.2.4.1 Dimensionality reduction and clustering of the dataset

To visualize and define the different cell clusters in the dataset, we used Uniform Manifold Approximation and Projection (UMAP), which is a novel manifold learning technique for dimension reduction. 2D projection of the UMAP revealed 37 cell clusters, 4 of which were macrophages clusters. The identified macrophages (Macs) clusters were designated as follows: cluster 0: **classically activated/M1 macrophages,** cluster 7: **infiltrating macrophages**, cluster 15: **M2 macrophages** and cluster 16: **resident macrophages**. The M1/classical Macs cluster was characterized by high expression of *Il1b* and *Cxcl2*, infiltrating Macs expressed high levels of *Lyz2*, *Plac8* and *Ccr2*, M1 Macs expressed *Cd80*, *Ccl3* and *Ccl4*, M2 Macs expressed *Mgl2*, *Ccl22* and *Ccl17* and resident Macs expressed *C1qa* and *Cd68*. Since clusters 0 and 7 (M1/classical and infiltrating macrophages) represented the majority of macrophages populations in all experimental groups (~70-90%), we focused our canonical pathways and upstream regulators analysis on these 2 clusters.

Table 4. Total counts of CD45 enriched gingival cells in each experimental group

Experimental group	Cell count
Healthy Control (Hctrl)	1506
Untreated (UT)	671
Blank	652
CCL2	3594

Table 5. Cell counts in each macrophages cluster per experimental group

	Hctrl	UT	Blank	CCL2
Cluster 0 - M1/Classically activated Macs	71	103	81	946
Cluster 7 – Infiltrating Macs	89	27	13	189
Cluster 15 – Cxcl16, CCL17, CCL22, Retnla, Mgl2 M2 Macs	36	16	8	71
Cluster 16 – C1qa/Cd68 Resident Macs	23	10	9	44

A)

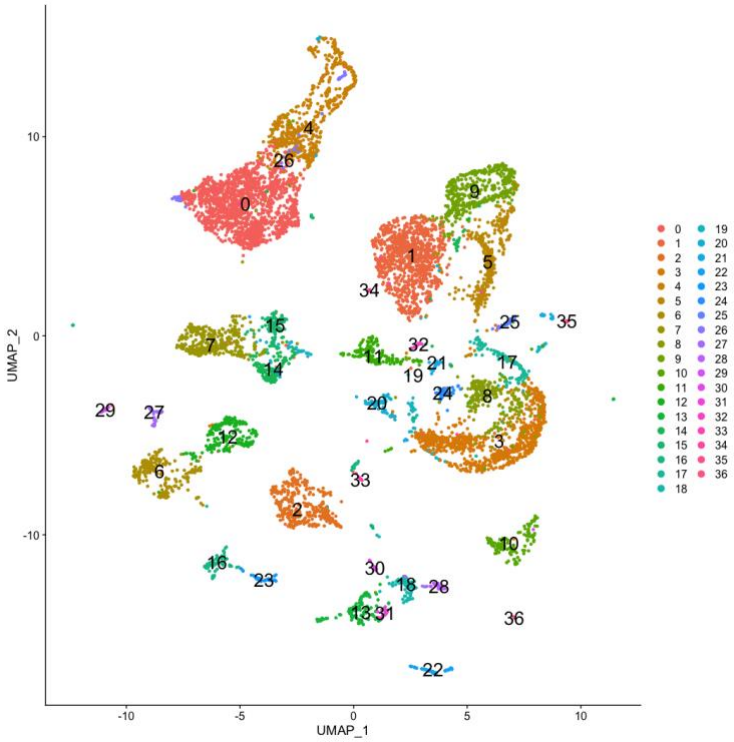

B)

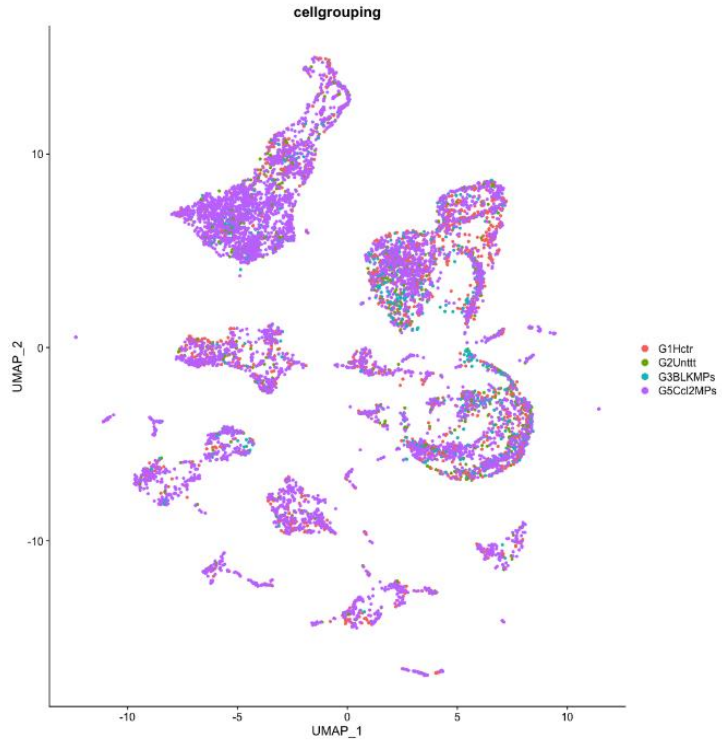

Figure 10. A) UMAP clustering of the total CD45 enriched gingival cells from all experimental groups. B) UMAP clustering of CD45 enriched gingival cells in each experimental group.

A)

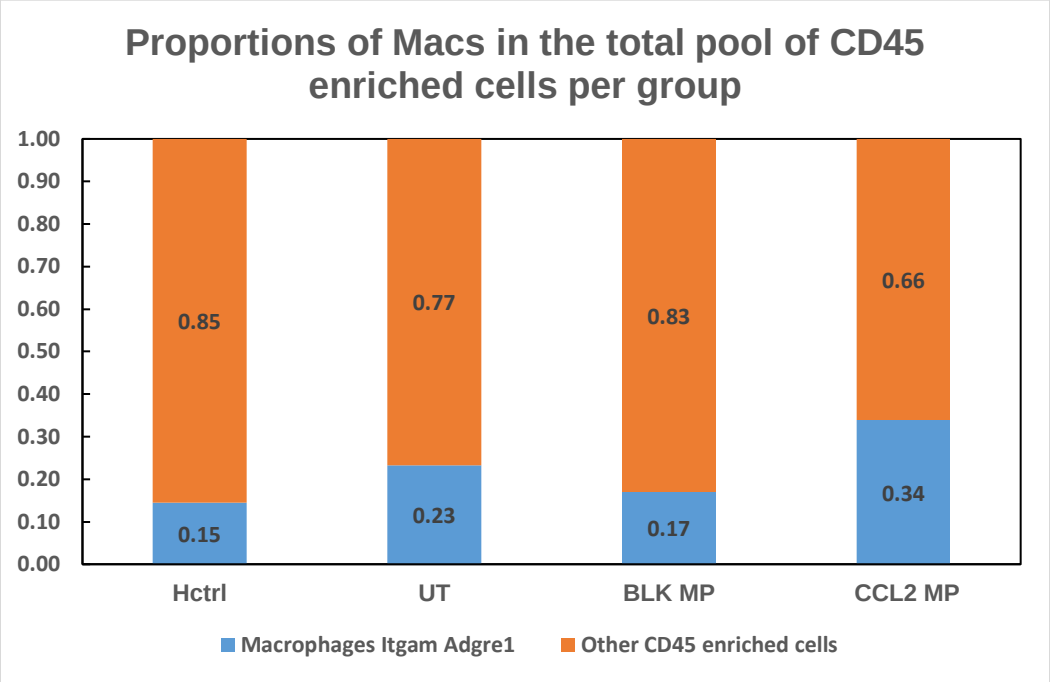

B)

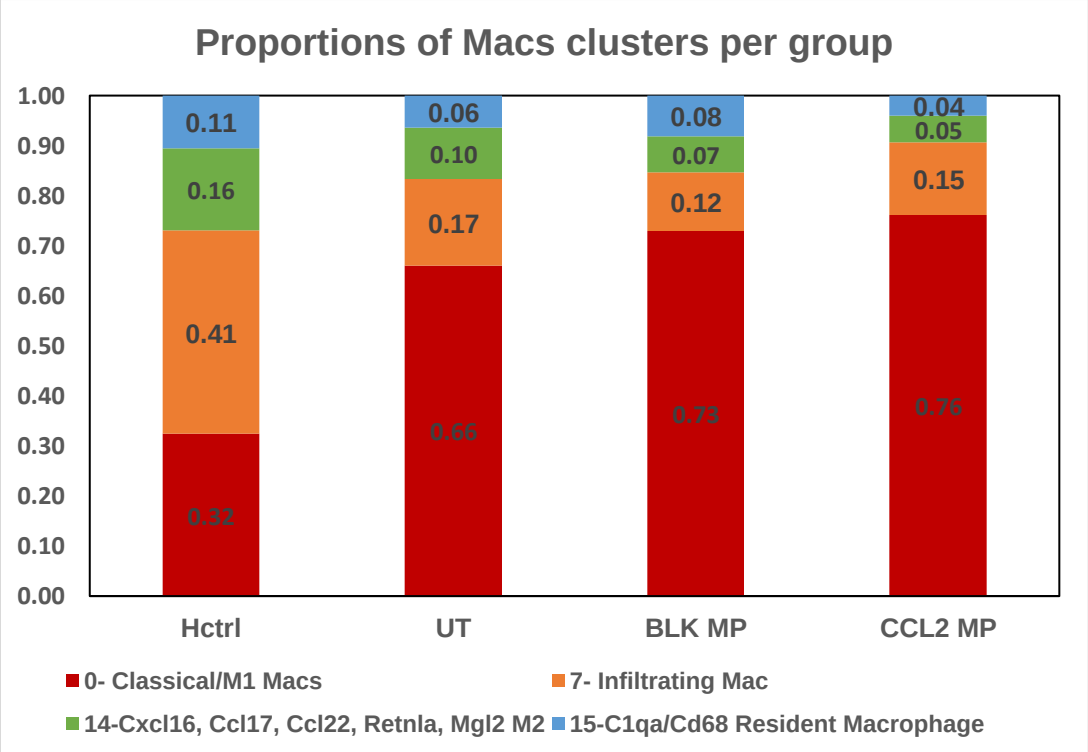

Figure 11. A) Proportion of periodontal macrophages in relation to other CD45 enriched cells in the murine gingiva. B) Proportions of different macrophages substes in relation to each other.

2.2.4.2 Canonical pathway analysis

We first sought to determine the signaling pathways that are activated or inhibited as a result of murine PD induction (UT vs. HCtrl) and following preventive treatment of murine PD with CCL2 MP (CCL2 vs. UT). To that end, the filtered DEGs sets were used to assess the top canonical pathways in the two binary comparisons designating each condition. Using Wilcoxon rank sum test, we identified 221 and 198 DEGs in the classical/M1 Macs cluster, and 351 and 180 DEGs in the infiltrating Macs cluster from the binary comparisons between UT vs. Hctrl and between CCL2 vs. UT, respectively.

Cluster 0 – Classical/M1 macrophages

In the classical/ Macs cluster (Cluster 0), the binary comparison between UT and Hctrl (murine PD induction) revealed 21 canonical pathways that had an absolute z-score of 2 or higher (Fig. 12). Among those 21 canonical pathways, 16 pathways had a positive z-score ≥ 2 and were considered activated (orange bars) and 5 pathways had a negative z-score ≤ -2 denoting inhibition (blue bars). The activated pathways included those related to induction of inflammation (IL-6, TREM1, HMGB1 and Inflammasome pathways), calcified tissue damage (Osteoarthritis pathway), and host defense against pathogens (Acute phase response, LPS/IL-1 mediated inhibition of RXR function and role of pattern recognition receptor in the recognition of bacteria and viruses). Additionally, macrophages specific pro-inflammatory and host defense signaling pathways were activated (MIF mediated glucocorticoid regulation, MIF regulation of innate immunity and iNOS signaling). In the same context, macrophages specific anti-inflammatory pathways were inhibited (PPAR and MSP-RON signaling). EiF2 signaling pathway was also

downregulated in response to murine PD induction. This pathway is part of the host defense system against intracellular pathogen invasion (Shrestha et al. 2012) .

In the comparison between CCL2 and untreated (treatment of murine PD with CCL2 MP), all statistically significant canonical pathways had a z-score ≤ -2, denoting inhibition (Fig. 13). The inhibited pathways in response to CCL2 treatment included TREM1 signaling, which was activated by murine PD induction. The remaining inhibited pathways included those involved in the innate and adaptive immune responses (Crosstalk between Dendritic Cells and Natural killer Cells, fMLP signaling in neutrophils, dendritic cell maturation and IL-17 signaling) and cellular motility and adhesion (Remodeling of epithelial adherens junctions, signaling by Rho family GTPases, integrin, regulation of actin-based motility by Rho and Rac signaling).

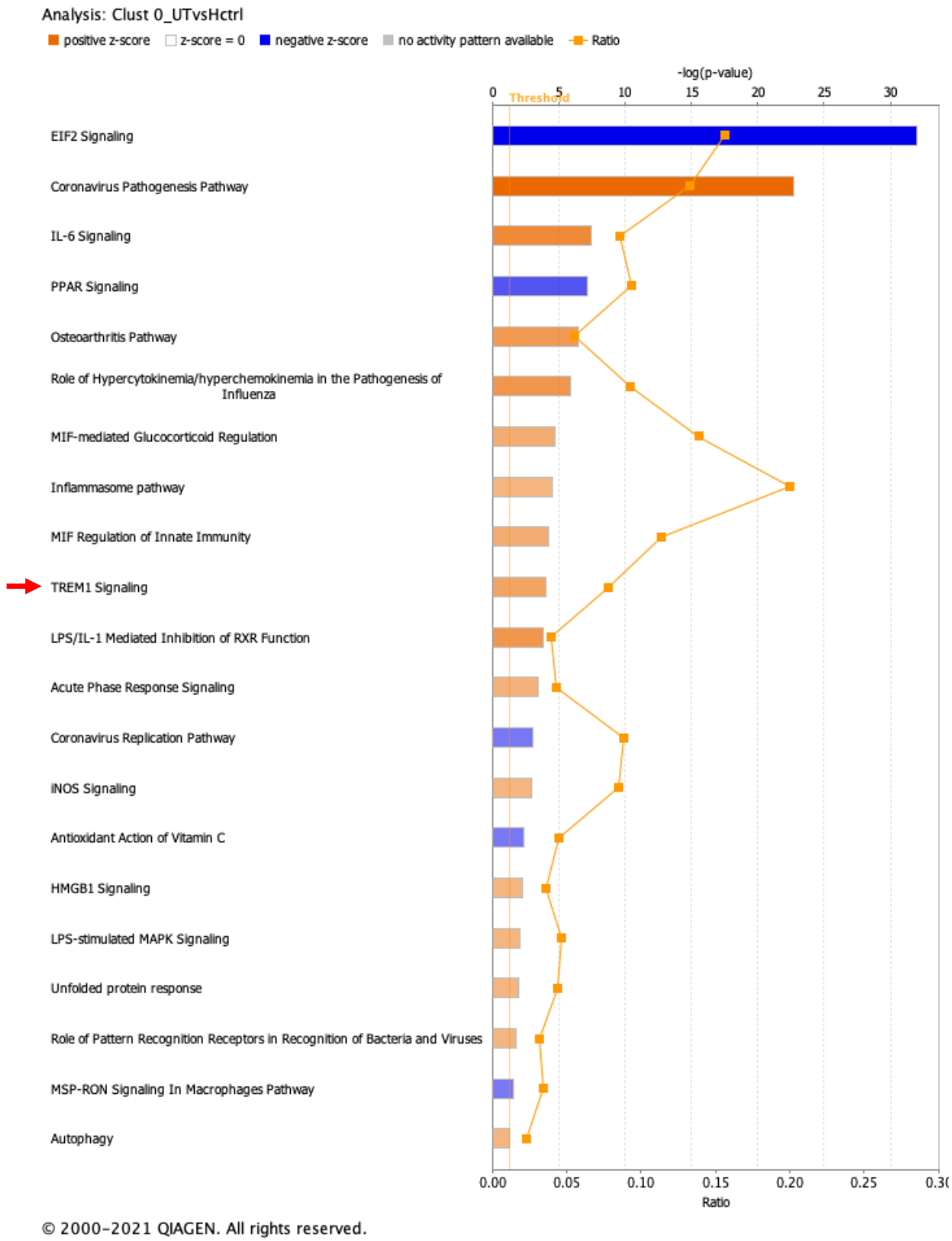

Figure 12. Activated (orange) and inhibited (blue) canonical pathways in classical/M1 macrophages in response to murine ligature PD induction. Those pathways were based on the DEGs between the untreated group when compared to the healthy control group.

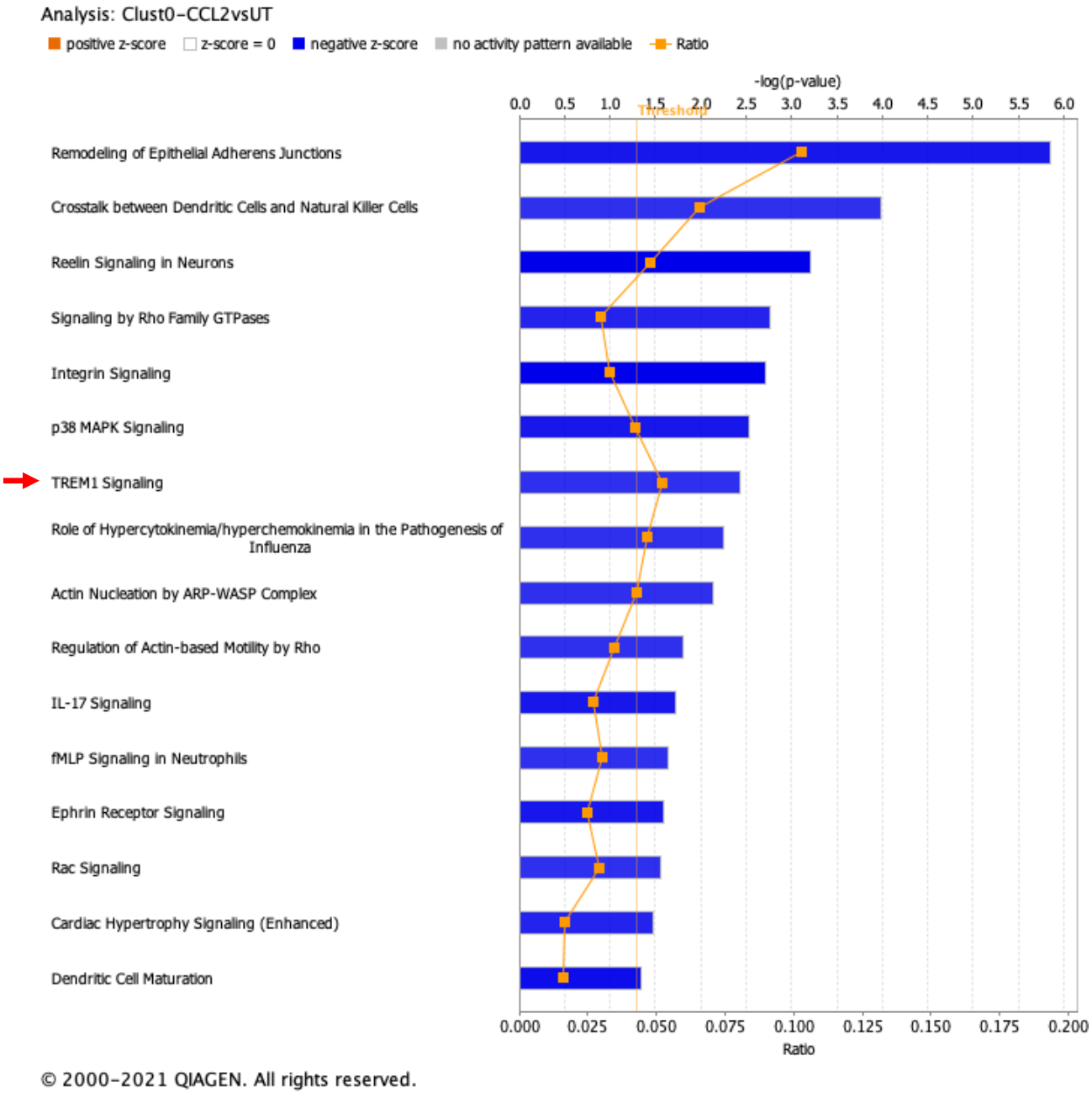

Figure 13. Inhibited (blue) canonical pathways in classical/M1 macrophages in response to preventive CCL2 treatment of murine ligature PD induction. Those pathways were based on the DEGs between the CCL2 group when compared to the untreated control group.

To better visualize the overall trend of canonical pathways activation or inhibition in classical/M1 Macs during murine PD induction and following CCL2 treatment, we performed a comparison analysis of the significant canonical pathways between the two binary comparisons (UT vs. Hctrl and CCL2 vs. UT). Regardless of the z-score significance cutoff of ± 2, our analysis showed that CCL2 treatment reversed the activity of a significant number of the pathways that were upregulated by murine PD induction only (Fig. 14). In addition, we generated gene heatmaps for select pathways that have been reported to contribute to murine PD induction (TREM1, IL-6 and IL-17). Our gene heatmaps showed that murine PD induction upregulated pro-inflammatory M1 macrophages markers in the classical/M1 macrophages cluster (*Il1b*, *Cd14, Ptgs2* and *Cxcl3*), whereas CCL2 treatment downregulates some of those genes (*Il1b* and *Cxcl3*), and other pro-inflammatory genes (*Mmp9* and *Ltb*) (Fig. 12).

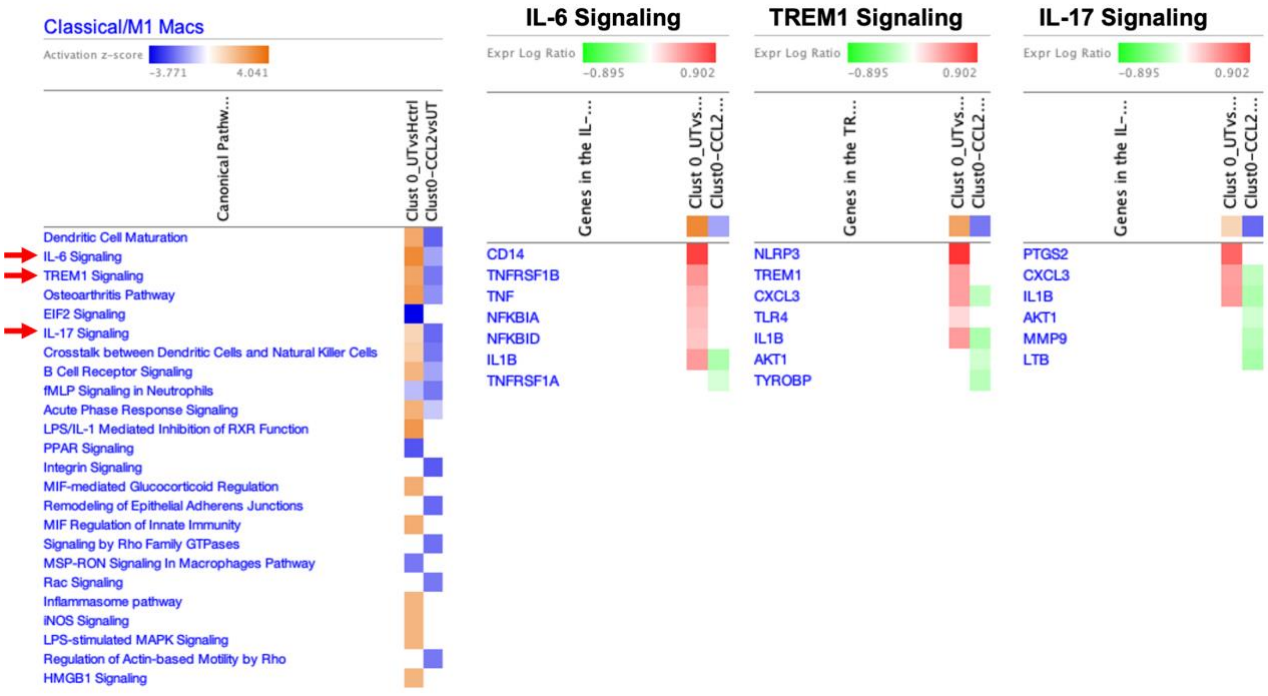

Figure 14. Comparison analysis for the top canonical pathways that are activated or inhibited by murine PD induction or its treatment with CCL2 MP (left panel), and heatmaps for representative DEGs in the IL-6, TREM1, IL-6 and IL-17 signaling pathways (right panel).

Cluster 7 – Infiltrating macrophages

In the infiltrating macrophages cluster (Cluster 7), the binary comparison between UT and Hctrl (murine PD induction) revealed 30 canonical pathways that had an absolute z-score of 2 or higher (Fig. 15). Among those 30 canonical pathways, 29 pathways had a positive z-score ≥ 2 and were considered activated (orange bars) and one pathway had a negative z-score ≤ -2 indicating its inhibition (blue bar). The activated pathways in the infiltrating macrophages included those involved in the induction of inflammation (Acute Phase Response, HMG1 and IL-6 signaling), classical activation of macrophages (GM-CSF signaling) and migration of immune cells (Leukocyte extravasation, IL-8 signaling and fMLP signaling in neutrophils). Other pathways associated with B and T cells activation (CD28 Signaling in T helper cells and B cell receptor signaling), and cellular growth and proliferation (mTOR and FGF signaling) were activated in infiltrating macrophages. Protein Kinase A (PKA) signaling was the only pathway that was downregulated in infiltrating macrophages. PKA mediated signaling has been reported to be essential for inflammation resolution processes driven by macrophages (Kong et al. 2016; Negreiros-Lima et al. 2020).

In the comparison between CCL2 and UT, all pathways had a positive z-score ≥ 2 and were considered activated (orange bars). CCL2 treatment of murine PD activated pathways associated with neutrophils chemotaxis, nervous system signaling and iron dependent cell death (IL-8, Ephrin receptor and Ferroptosis signaling pathways). Furthermore, the PKA signaling pathway involved in inflammation resolution was activated by CCL2 treatment. Thus, CCL2 reversed the effect of murine PD induction (UT vs Hctrl) on PKA signaling in infiltrating macrophages.

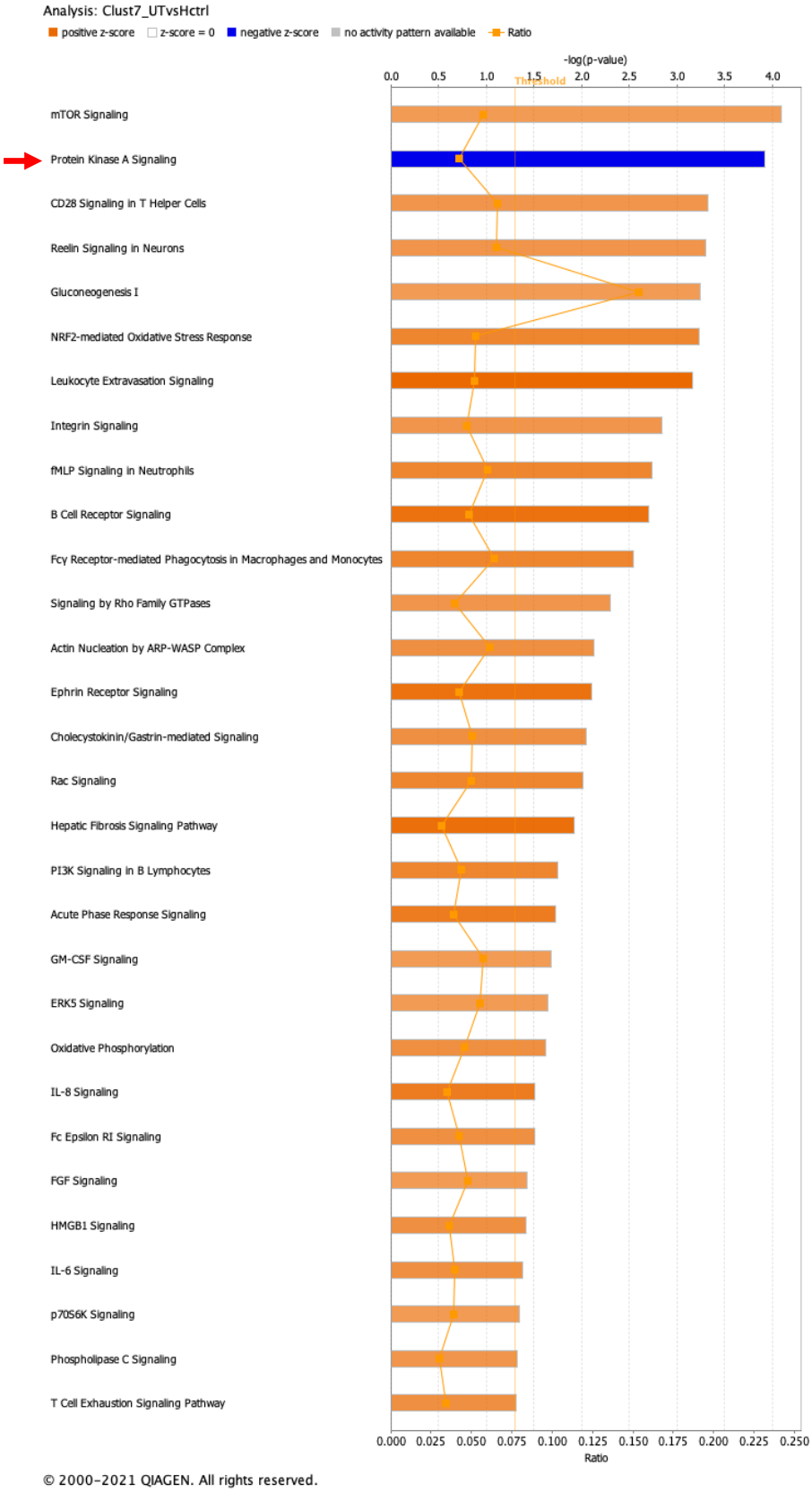

Figure 15. Activated (orange) and inhibited canonical pathways in response to murine ligature PD induction. Those pathways are based on the DEGs between the UT group when compared to the healthy control group.

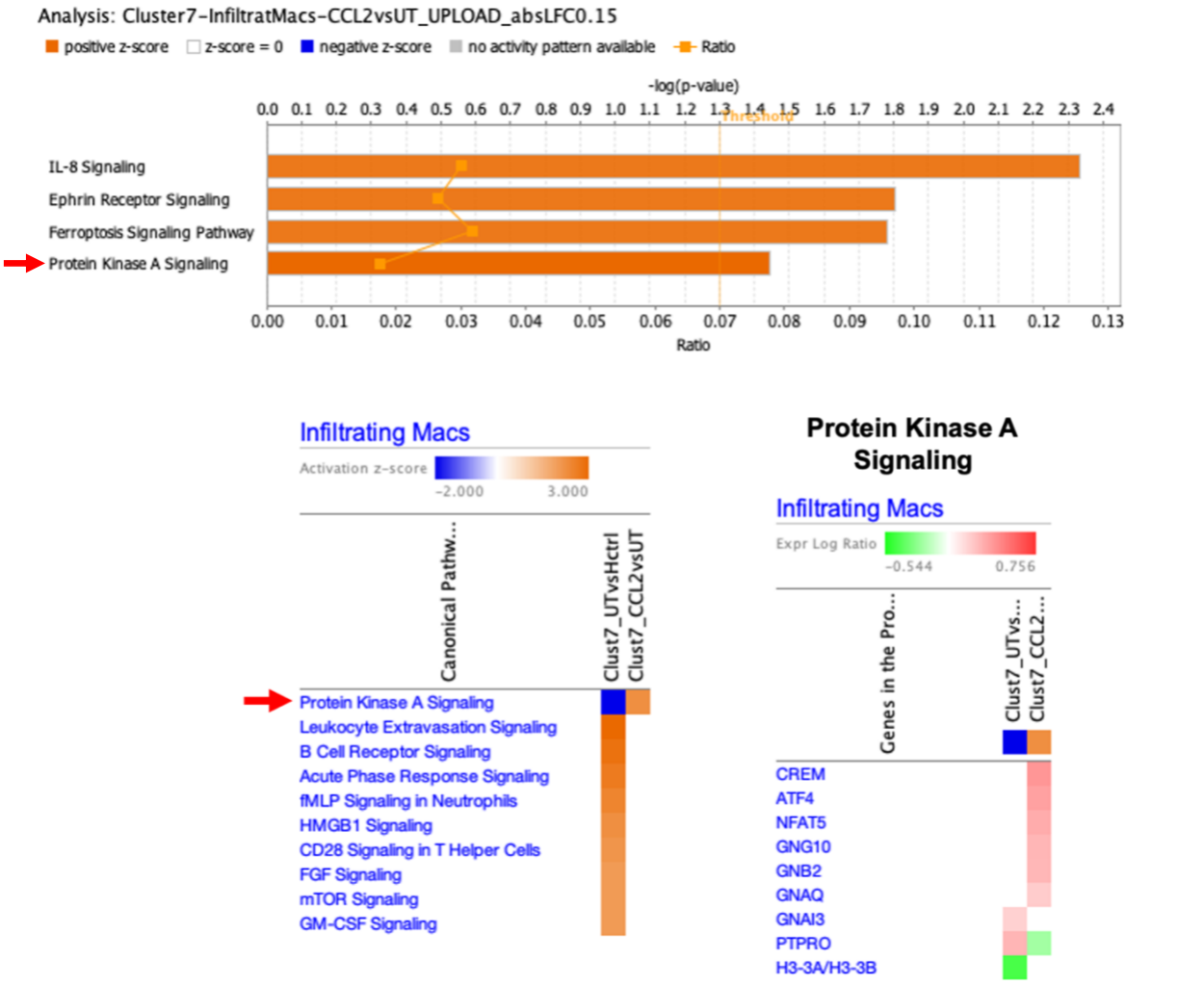

Figure 16. (A) Activated (orange) and inhibited canonical pathways in response to preventive CCL2 treatment of murine ligature PD induction in infiltrating macrophages. Those pathways are based on the DEGs between the CCL2 group when compared to the untreated control group. (B) Comparison analysis for the top canonical pathways that are activated or inhibited by murine PD induction or its treatment with CCL2 MP, and heatmaps for representative DEGs in the Protein Kinase A.

2.2.4.3 Upstream regulator analysis

Our next goal was to identify the upstream regulators that can explain the changes in gene expression observed in our data sets but were not listed among the upregulated or downregulated targets. IPA can predict the activation or inhibition of those upstream regulators by linking information about those regulators from the IPA Knowledge Base to the expression results in our data sets. Next, IPA generates an activation z-score for each of the upstream regulators, where a z-score ≥ 2 indicates predicted activation and a z-score ≤ -2 indicates predicted inhibition. We focused our analysis on upstream regulators that belong to the cytokine, transmembrane receptor and transmembrane receptor categories.

Cluster 0 – Classical/M1 macrophages

In classical/M1 Macs, we identified 113 upstream regulators that have an absolute activation z-score ≥ 2 in either of the two binary comparisons representing murine PD induction (UT vs. Hctrl) and its treatment with CCL2 MP (CCL2 vs. UT). Out of those 113 regulators, we selected 25 that are associated with macrophages polarization, induction of inflammation and pathogen recognition (Fig. 17). We observed that murine PD induction (UT vs. Hctrl) resulted in a predicted activation of upstream regulators designated as pro-inflammatory cytokines or receptors (*Ifng*, *Tnf*, *Osm*, *Il12*, *Il6*, *Il6r* and *Il17a*) and transmembrane pathogen recognition receptors (*Tlr3*, *Tlr4* and *Tlr9*). In addition, the genes for the M1 macrophages associated transcription factor *Stat1* and the osteoclasts differentiation factor *Tnfsf11* (encoding RANKL) exhibited predicted activation with murine PD induction. In contrast, CCL2 treatment of murine PD yielded a predicted inhibition of the cytokines, transmembrane pathogen recognition receptors that were upregulated by murine PD induction only. Moreover, *Stat1* and *Tnfsf11* exhibited

predicted inhibition by CCL2 treatment of murine PD (CCL2 vs. UT). Finally, CCL2 treatment resulted in predicted activation of the anti-inflammatory marker genes *Il1rn* and *Il10ra*, which are associated with a pro-resolving M2 macrophages response.

Figure 17. (Left) Heatmap showing selected upstream regulators that are predicted to be activated (blue) or inihibited (orange) by murine PD induction (UT vs. Hctrl) or its treatment with CCL2 (CCL2 vs. UT). (Hueber et al.) Heatmaps showing representative upregulated (red) and downregulated (green) DEGs contributing to a prediction of activation or inhibition of *Stat1*, *Il1rn*, *Tlr4* and *Il17a*.

Cluster 7 – Infiltrating macrophages

In infiltrating macrophages, we identified 65 upstream regulators that exhibited predicted activation or inhibition (absolute z-score ≥ 2) in the binary comparison between UT and Hctrl (murine PD induction) (Fig. 18). In the comparison between CCL2 and UT (preventive treatment of murine PD with CCL2 MP), none of the identified upstream regulators showed a difference in the predicted activation (absolute z-score < 2). However, we observed a trend of predicted inhibition (negative z-score) with CCL2 treatment in some pro-inflammatory and osteoclastic activity regulators (*Tnsfsf11*, *Il1a* and *Osm*).

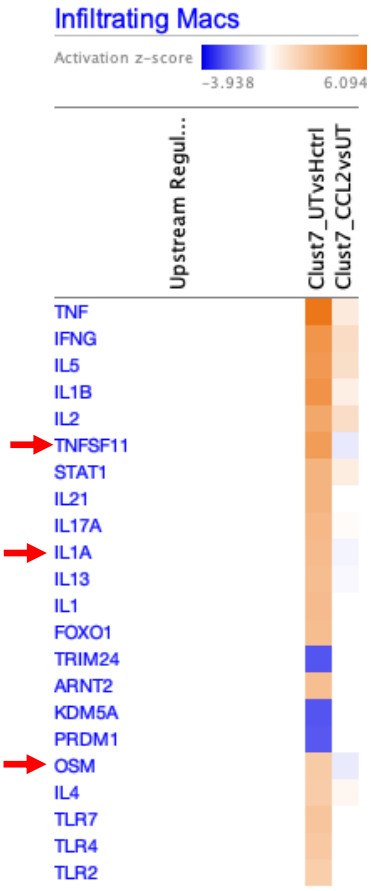

Figure 18. Heatmap depicting representative upstream regulators that are predicted to be activated (orange) or inhibited (blue) in response to murine ligature PD induction (UT vs. Hctrl) or its treatment with CCL2 MP (CCL2 vs. UT).

2.2.4.4 CCL2 sustained delivery does not affect the total microbial load in murine PD

We first evaluated the changes in the total periodontal microbial load (microbial biomass) following murine PD induction or its treatment with IL-4 or CCL2. Except for the healthy 2hr ligature group, all experimental groups (untreated, Blank, IL-4 and CCL2) had an average copy number that was higher than the detection threshold based on the standard curve and the negative control. Our 16SrRNA qPCR data indicated that there was no significant difference in the microbial biomass between all experimental groups that exhibited a copy number above the detection threshold (Fig. 19). Those results suggest that neither murine ligature PD induction nor its treatment with CCL2 MP had an effect on the total microbial load.

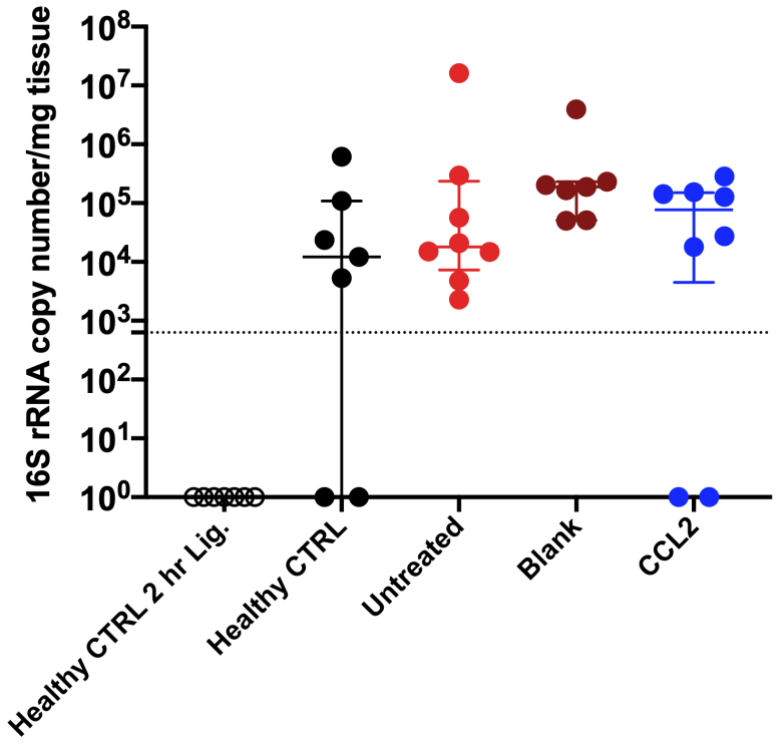

Figure 19. Graph depicts the quantifcation of the total bacterial load in the 5 experimental groups: healthy control with 2 hours ligature (Healthy CTRL 2hr Lig.), healthy control side without ligature (Healthy CTRL), mice with 7 days ligature induced PD only (Untreated), or concurrently with blank or CCL2 MP delivery at day 0 (Blank or CCL2). The bacterial load is presented in term of 16S rRNA copy number as determined by a qPCR assay.

2.2.4.5 CCL2 sustained delivery affects the shifts in microbial composition associated with murine PD

We next sought to determine whether CCL2 local delivery has an effect on the microbial composition shifts associated with murine PD induction. We analyzed the changes in the periodontal microbial communities by evaluating the relative abundance of the top phyla, genera and species in each of the experimental groups. We also assessed the differences in relative abundance for enriched genera and species between experimental groups using LEfSe (linear discriminant analysis of effect size) analysis.

Phylum level analysis revealed that Firmicutes was the most abundant phylum in the healthy murine periodontium, whereas murine PD induction is associated with a dramatic increase in the abundance Proteobacteria and a decrease in Firmicutes (Fig. 20A). Local delivery of CCL2 MP did not have an effect on the disease-associated changes of Firmicutes and Proteobacteria. At the genus level, Lactobacillus was the most abundant health associated genus, while Enterobacteriaceae unclassified dominated following PD induction, which also caused a remarkable decrease in Lactobacillus abundance (Fig. 20B). Local delivery of CCL2 caused a trend of reversal in the disease-associated rise in Enterobacteriaceae unclassified. Similarly, species level analysis showed that murine PD induction resulted in a surge in Enterobacteriaceae unclassified with abrogation of this surge with CCL2 treatment (Fig. 20C).

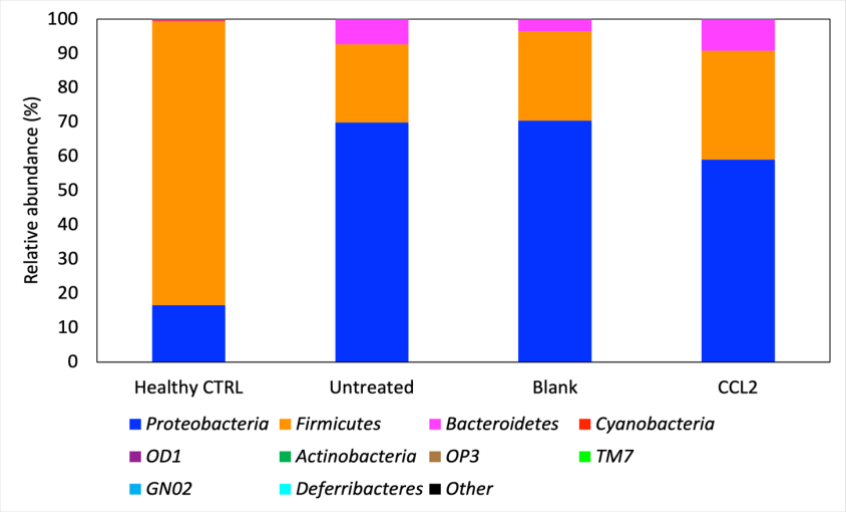

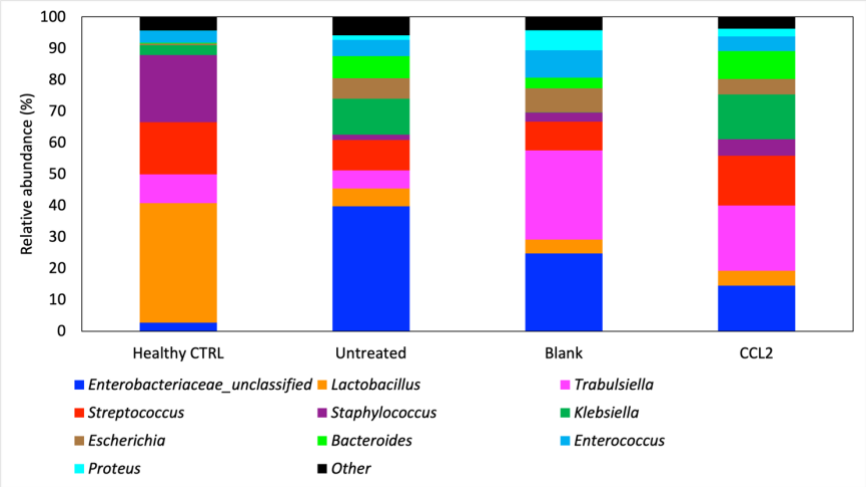

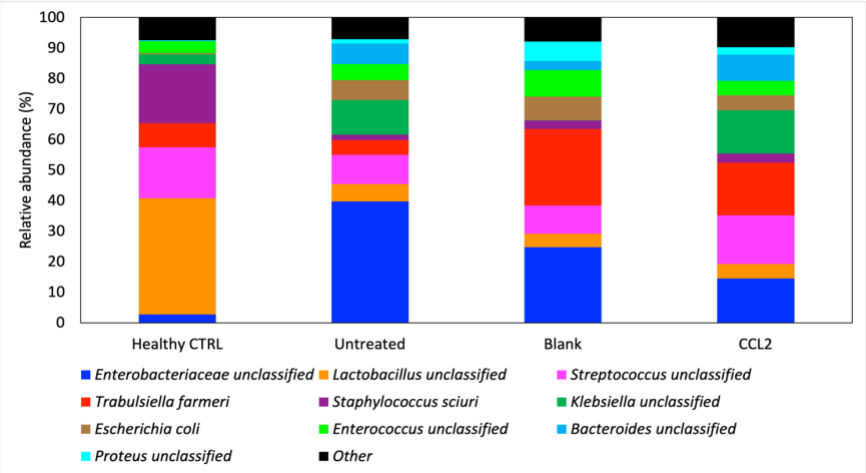

Figure 20. Analysis of the relative abundance of the top phyla (A), genera (B) and species (C) following murine PD induction alone (Untreated), or concurrently with local delivery of blank or CCL2 MP (Blank and CCL2).

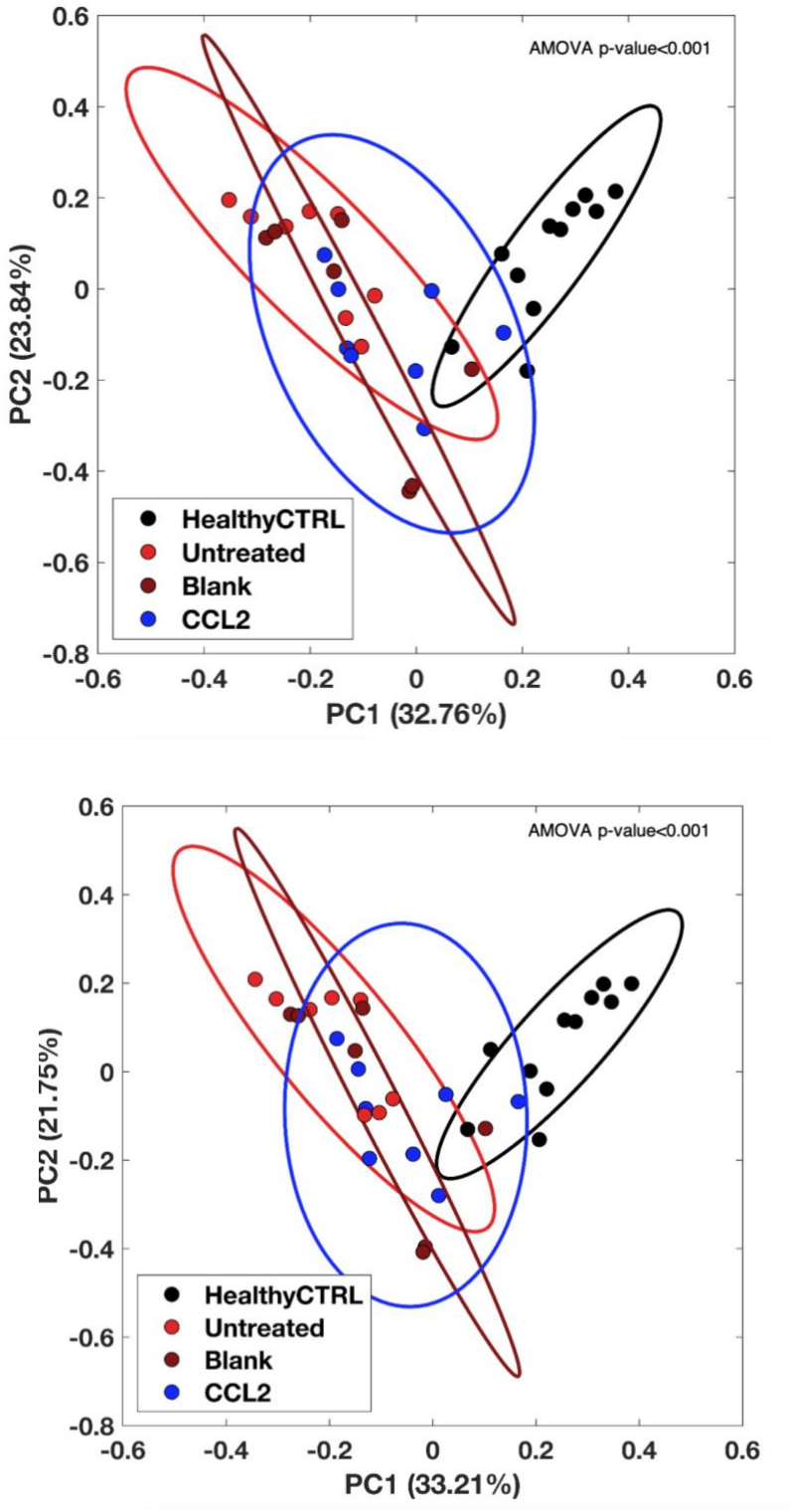

Figure 21. Euclidean beta diversity plots at genus (top panel) and species (bottom panel) levels.

Using LEfSe analysis, we assessed the differences in enriched taxa between healthy control and untreated groups, and between CCL2 and untreated groups at both the genus and species levels. In the comparison between untreated and healthy control groups, we identified 16 genera that were enriched in the untreated group and 11 genera that were enriched in the healthy control group (Fig. 22A). Compared to the untreated group, CCL2 treatment showed a trend similar to the healthy control group by preventing the enrichment in 4 out of the 16 genera associated with murine PD induction (Enterobacteriaceae unclassified, Gluconacetobacter, Anaerococcus and S24_7_unclassified).

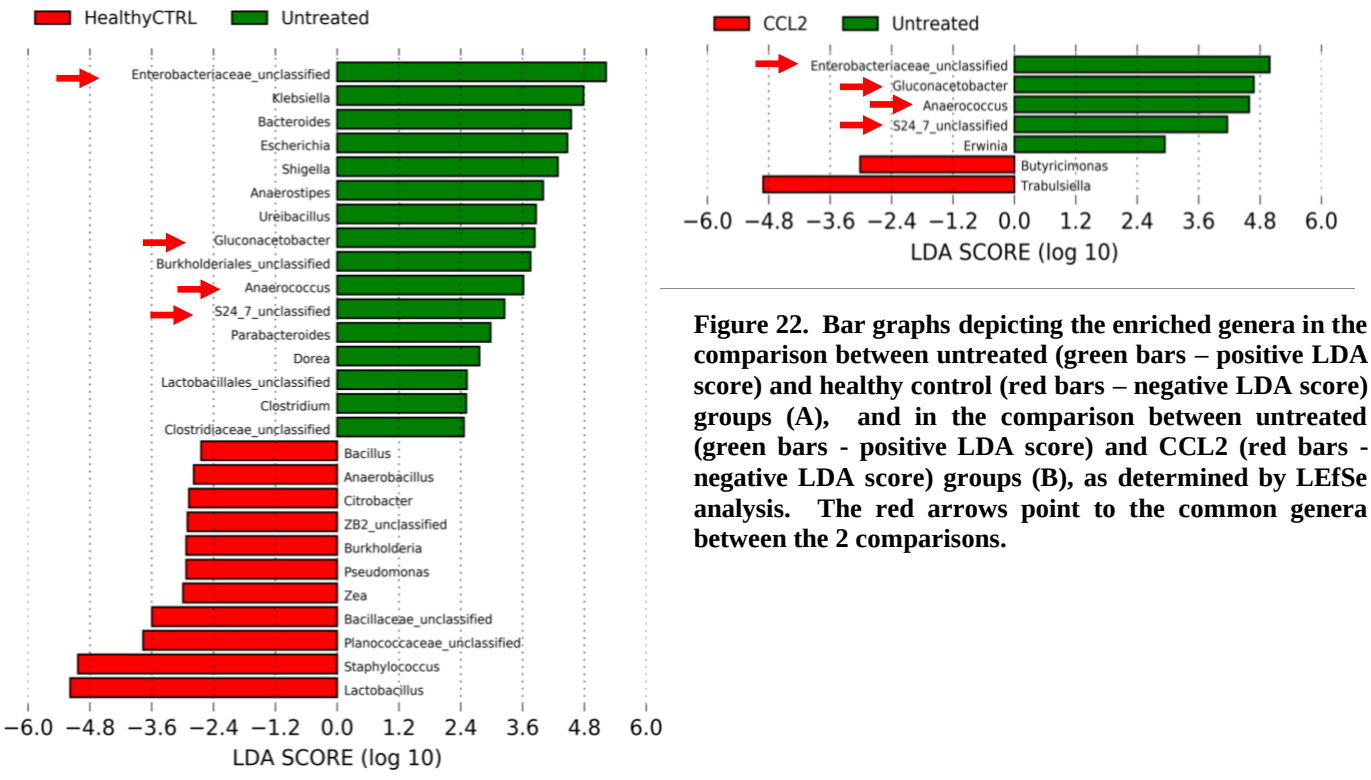

Figure 22. Bar graphs depicting the enriched genera in the comparison between untreated (green bars – positive LDA score) and healthy control (red bars – negative LDA score) groups (A), and in the comparison between untreated (green bars - positive LDA score) and CCL2 (red bars - negative LDA score) groups (B), as determined by LEfSe analysis. The red arrows point to the common genera between the 2 comparisons.

At the species level, LEfSe analysis revealed 33 enriched species in the untreated group and 12 enriched species in the healthy control group when they were compared to each other. CCL2 treatment abrogated the enrichment in 6 out of the 33 species identified in the comparison between healthy control and untreated groups (Enterobacteriaceae_unclassified, S24_7_unclassified, Gluconacetobacter_unclassified, Clostridium_unclassified, Anaerococcus_unclassified and Enterobacter_aerogenes) (Fig. 23).

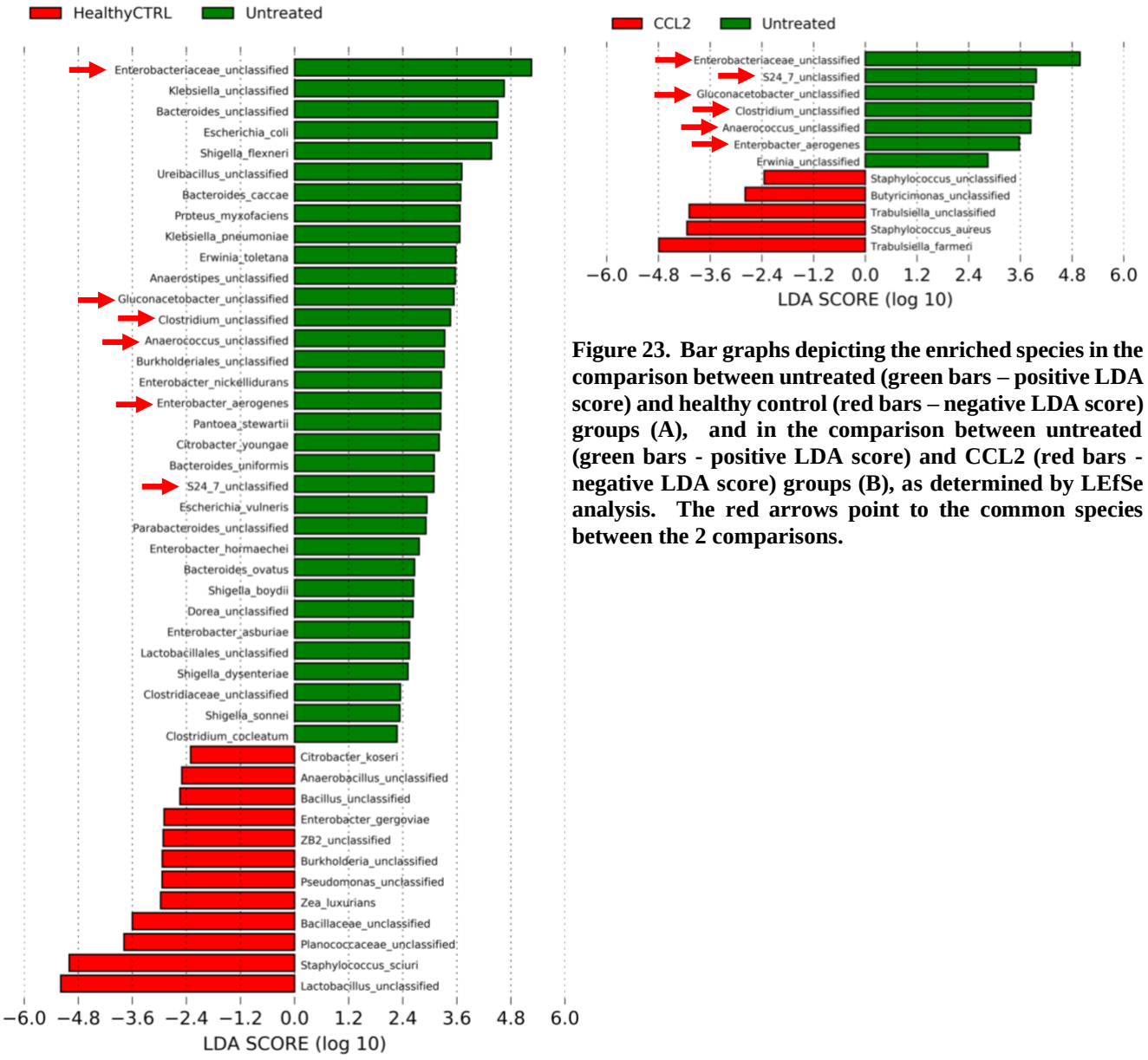

Figure 23. Bar graphs depicting the enriched species in the comparison between untreated (green bars – positive LDA score) and healthy control (red bars – negative LDA score) groups (A), and in the comparison between untreated (green bars - positive LDA score) and CCL2 (red bars - negative LDA score) groups (B), as determined by LEfSe analysis. The red arrows point to the common species between the 2 comparisons.

2.2.5 Discussion

Macrophages are the major phagocytes of the innate immune system. These cells perform a wide range of functions in tissue during health and disease. In human periodontitis, macrophages make 6% of all immune cells in periodontal tissue biopsies (Carcuac and Berglundh 2014). Furthermore, gingival macrophages increase in numbers during the transition from a healthy to diseased periodontium in both humans and mice (Gemmell et al. 2001; Yu et al. 2016). In this work, we aimed to characterize murine gingival macrophages populations and microbial communities in health and following the induction of ligature periodontitis with or without local sustained delivery of the chemokine CCL2. We hypothesized that murine ligature PD induction would induce a pro-inflammatory response by gingival macrophages and its treatment with CCL2 would reverse this response. We also hypothesized that the immune-regulatory effects of CCL2 would abrogate the disease-associated shifts in the periodontal microbial communities.

Macrophages comprise a wide range of subsets that differ in origin and activation states (Italiani and Boraschi 2014). From an origin standpoint, macrophages can be classified as either yolk sac derived or monocyte-derived macrophages. The yolk sac derived macrophages develop during embryogenesis without going through a monocytic stage. These macrophages contribute to a fraction of tissue resident macrophages that are replenished by self-renewal. On the other hand, monocyte-derived macrophages arise from the hematopoietic stem cells in the bone marrow and give rise to infiltrating macrophages and the remaining fraction of tissue resident macrophages. From an activation state standpoint, the classically activated/M1 pro-inflammatory and the alternatively activated/M2 anti-inflammatory macrophages represent the 2 extremes of a

wide continuum of phenotypic subsets that can overlap in functions and marker/cytokine expression (Martinez and Gordon 2014).

Using UMAP clustering, we identified 4 groups/clusters of macrophages in the BALB/C murine gingiva: M1/classically activated (cluster 0), infiltrating (cluster 7), M2 (cluster 15) and resident macrophages (Macs) (cluster 16). Combined, the classical/M1 and infiltrating clusters constituted the majority of macrophages (~70-90%) in the murine gingiva. For this reason, we focused our pathway analysis on these two major clusters since they exhibited significant shifts in their proportions during the transition from a healthy to diseased periodontium and following local delivery of CCL2 MP. Our clustering analysis revealed that murine PD induction is associated with a sharp rise in M1/classical Macs and a decline in infiltrating Macs numbers. Relative to the total macrophages pool, the proportion of M1 Macs in the groups with murine PD (UT, BLK and CCL2) was almost double that of the healthy control. On the other hand, the proportion of infiltrating Macs was reduced by more than 50% following murine ligature PD induction. Studies in many mouse models of inflammation indicated that the majority of M1 Macs in tissue originate from the recruited $Ly6C^{+}$ monocyte derived macrophages that infiltrate the tissue in a CCL2/CCR2 dependent mechanism (Auffray et al. 2007; Li et al. 2018; Tacke et al. 2007). In our study, we speculate that the observed shifts in murine periodontal infiltrating and M1 Macs proportions arise from the polarization of the cells in the infiltrating Macs cluster towards an M1/classical phenotype in response to periodontal microbial challenge. This could explain the expansion of the M1/classical Macs at the expense of the infiltrating Macs in mice with murine PD induction.

M1/classically activated Macs are the prototypical pro-inflammatory Macs subset that secretes a myriad of pro-inflammatory cytokines that are also pro-osteoclastic in nature (IL-6, IL-23 and TNF-a) (Mantovani et al. 2004). Thus, it is expected that an increase in periodontal M1 Macs would correlate with enhanced inflammatory bone loss in PD. In this regard, one study showed that immunofluorescent staining of tissue sections from mice with induced periodontitis revealed a mixed Macs population dominated by cells exhibiting dual expression of M1 and M2 Macs markers (Yu et al. 2016). The authors of this study suggested a switch from an anti-inflammatory M2 to a pro-inflammatory M1 Macs as a potential mechanism driving bone loss in murine PD. In contrast, another study reported that mice with ligature induced PD exhibited less alveolar bone loss following adoptive transfer of M1, rather than M2, Macs with localization of adoptively transferred cells in the murine gingiva (Yamaguchi et al. 2016). The aforementioned studies relied on similar markers to designate M1 Macs in vivo, yet no definitive conclusion about a protective or destructive role for M1 Macs in murine PD can be drawn. Those conflicting reports suggest a more complex role of cells designated as "M1/classically activated macrophages" in the context of inflammatory bone remodeling in the murine periodontium.

Our IPA pathway analysis revealed that murine PD induction upregulates pathways denoting pro-inflammatory response in M1/classical Macs. In particular, TREM1 (Triggering Receptor Expressed on Myeloid Cells 1) was the only murine PD associated pro-inflammatory signaling pathway that was inhibited by CCL2 MP treatment in our study. TREM1 is an immunoglobulin like activating receptor that acts as a potent amplifier of innate immune response induced by pathogen recognition receptors such as Toll-like receptors (Tammaro et al. 2017). TREM1 has been reported as a pivotal inducer of immunopathology in animal models of colitis,

atherosclerosis and autoimmune arthritis (Murakami et al. 2009; Schenk et al. 2007; Zysset et al. 2016). More recently, TREM1 signaling has been implicated as a key driver of periodontal inflammation in humans and mice. In this respect, periodontitis patients exhibited enhanced expression of TREM1 in the gingiva, gingival crevicular fluid and serum (Bisson et al. 2012; Bostanci et al. 2013; Willi et al. 2014). In the same context, a recent study showed that local injection of a TREM1 antagonist in mice with ligature induced PD inhibited alveolar bone loss and gingival IL-17A expression (Bostanci et al. 2019). IL-17A is a signature cytokine of pathogenic Th17 cells that have been suggested to play a crucial role in driving destructive inflammation in human and murine periodontitis (Dutzan et al. 2018a). Consistent with those findings, the observed TREM1 signaling pathway inhibition by CCL2 local delivery in our study correlated with downregulation of IL-17 signaling pathway and IL-17A predicted activity in our canonical pathways and upstream regulators analyses, respectively. Collectively, our Sc-RNA seq data implicate TREM1/IL-17 signaling pathways as potential targets for CCL2 immunomodulatory effects on periodontal M1/classical Macs.

M1/classical Macs secrete a number of pro-inflammatory cytokines that are crucial for homeostatic and pathogenic Th17 cells differentiation and expansion. Notably, both IL-6 and IL-23 were shown to be essential for pathogenic Th17 cells expansion in murine ligature periodontitis (Dutzan et al. 2018a). In murine collagen induced arthritis, targeted depletion of pro-inflammatory M1 Macs ($DR5^+$ with high expression of IL-23) was associated with a reduction in lymph node and synovial Th17 cells, an inhibition in joints osteoclastic activity and a decrease in arthritis severity (Li et al. 2012). Similarly, pathogenic Th17 cells can potentiate M1 Macs response by their secretion of high levels of GM-CSF and IL-17A. GM-CSF has been reported as a potent

inducer of human M1 Macs differentiation (Fleetwood et al. 2007; Verreck et al. 2004), whereas IL-17A was shown to favor M1 Macs polarization in human and murine with bisphosphonate related osteonecrosis of the jaw (Zhang et al. 2013). Altogether, the collective data point to a bidirectional positive feedback loop between M1/classical Macs and Th17 cells (Li et al. 2013). Along with the predicted inhibition IL-17A, our upstream regulators analysis showed predicted inhibition of M1 Macs associated markers (*Stat1*, *Cxcl3*, *Il1b*, *Tnf*, *Tlr4* and *Il6*) in the M1/classical Macs cluster. Those results further corroborate the anti-inflammatory influence of locally delivered CCL2 on murine periodontal Macs and highlight the dynamic relationship between Macs and Th17 cells in murine PD.

The infiltrating macrophages cluster exhibited minimal differences between PD induction and following treatment with CCL2 local delivery in our canonical and upstream regulator analyses. Expectedly, murine PD induction alone (UT group) upregulated pathways related to immune cells migration, induction of inflammation and M1 Macs differentiation in infiltrating Macs cluster. Protein Kinase A signaling was the only pathway that was inhibited in the untreated group while activated in the CCL2 treated group. Several studies indicated that PKA mediated signaling could play a role in the inflammation resolution processes mediated by Macs. In this respect, binding of a PKA subunit to the transmembrane domain of IFN-γ receptor hindered STAT-1 dependent M1 Macs polarization (Kong et al. 2016). Additionally, PKA was shown to mediate cyclic AMP mediated reprogramming of M1 Macs to the M2 phenotype, and its inhibition abrogated the resolution of LPS induced pleurisy (Negreiros-Lima et al. 2020). Those results suggest that infiltrating Macs in the CCL2 MP treated group are less prone to adopt a pro-inflammatory M1 phenotype as they contribute to the classical/M1 macrophages pool in the murine

periodontium. This could explain, at least in part, the suppressed expression of pro-inflammatory markers in the periodontal M1/classical Macs cluster.

Previous reports suggested a bidirectional interaction between the host response and the microbial communities in the periodontium. In this respect, periodontal microbial challenge triggers a dysregulated host inflammatory response that fuels periodontal microbial dysbiosis, which further subverts the host response (Hajishengallis 2014). The sequence of events leading to periodontal immune subversion and microbial dysbiosis is only starting to be described, and there is little evidence supporting the notion that inflammation precedes dysbiosis (Sima et al. 2016; Tanner et al. 2007) . Nevertheless, the current consensus is that both processes positively reinforce each other during the pathogenesis of periodontitis (Curtis et al. 2020; Hajishengallis 2015).

After we showed that CCL2 sustained delivery dampened Macs pro-inflammatory response and bone loss in murine PD, we sought to assess whether CCL2 immuno-modulatory effects would abrogate the disease-associated shifts in the murine periodontal microbiome. Our microbial composition analysis revealed that CCL2 local sustained delivery abrogated the enrichment of some of the genera and species associated with murine ligature PD induction (Enterobacteriaceae_Unclassified, Anaerococcus, Gluconacetobacter and S24_7_Unclassified). Furthermore, additional taxa exhibited negative enrichment by CCL2 compared to the untreated group at the species level (clostridium unclassified and Enterobacter Aerogenes). To the best of our knowledge, there are no studies to date describing the involvement of those specific genera/species in murine inflammatory bone loss. Therefore, those results can only, at best, support the notion that Macs modulation by CCL2 sustained delivery overturns some of the

disease-associated changes in the murine periodontal microbiota. Two potential mechanisms can explain the observed effects of CCL2 on the murine periodontal microbiota. The first mechanism relies on the reported role of CCL2 in driving immune cells bacterial killing and phagocytic activity in animal infection models (DePaolo et al. 2005; Gomes et al. 2013). The second mechanism suggests an indirect effect of CCL2 where it reverses the inflammation induced changes in the murine periodontal microbiome by suppressing macrophages pro-inflammatory responses as described in our Sc-RNA sequencing analysis earlier. In our study, we observed no difference in the periodontal microbial load between the untreated and CCL2 treated groups. Therefore, it is likely that the trend of reversal observed in periodontal microbial composition is the result of the local immunomodulatory effects of CCL2, rather than an antibacterial activity. Our data are in line with a previous report showing that active inflammation regulation can reverse the disease associated shifts in the composition of rodents' periodontal microbiota (Lee et al. 2016b).

In conclusion, our Sc-RNA sequencing analysis suggested that CCL2 local sustained delivery reprogramed murine pro-inflammatory Macs to a hypo-inflammatory phenotype during the course of ligature-induced PD. Those hypo-inflammatory Macs exhibited suppressed expression of pro-inflammatory and pro-osteoclastic cytokines, which could explain the inhibition of inflammatory bone loss observed in our previous studies. Finally, our 16sRNA sequencing analysis indicated that CCL2 treatment reversed the PD associated shifts in the murine periodontal microbial composition by modulating local inflammation rather than activating immune defense mechanisms against pathogens.

2.3 Specific Aim 3

2.3.1 Introduction and Rationale

Periodontal disease (PD) is a chronic inflammatory condition that affects supporting tooth structures forming the periodontium. Although PD is triggered by keystone pathogens and pathobionts that colonize the tooth surface (Hajishengallis 2014), it is the dysregulated host immune response against those pathogens that causes periodontal tissue destruction (Taubman et al. 2005). This dysregulated host response is fueled by an array of mediators that induce inflammatory osteolysis in the periodontium (Kinane et al. 2011). Among those mediators are pro-inflammatory cytokines such as IL-6 and TNF-α. These cytokines and others are released by both immune and structural cells (e.g., lymphocytes, macrophages or fibroblasts and epithelial cells) in response to bacterial invasion in the periodontium. IL-6 and TNFα have been associated with enhanced osteoclastic activity and progressive alveolar bone loss in animal models of PD (Graves et al. 2011).

IL-17A is a key driver of pathogenic host response in a number of chronic inflammatory conditions where bone loss is a characteristic feature, such as psoriatic arthritis (PsA) and PD (Dutzan et al. 2018b; Jandus et al. 2008; Leipe et al. 2010). In both conditions, chronic expansion and activation of IL-17A-producing lymphocytes (broadly called "Type 17", including $CD4^+$ T cells, γδ-T cells, ILC3s and NKT cells) is triggered by locally upregulated IL-23, IL-1β and IL-6 and results in progressive bone destruction (Bunte and Beikler 2019; Dutzan et al. 2018a; Dutzan et al. 2018b).

A number of studies have indicated that IL-17A mediates bone loss through a combination of osteoblast, osteocyte and osteoclast functions. In osteoblast cultures, IL-17A stimulates the expression of the major osteoclast-differentiating factor RANKL in a dose-dependent manner (Kotake et al. 1999). Similarly, the ability of IL-17A to upregulate RANKL extends to osteocytes in an animal model of hyperparathyroidism-induced bone loss (Li et al. 2019). In osteoclasts, IL-17A can either promote the generation of osteoclasts from monocytes in the absence of RANKL (Yago et al. 2009) or enhance the sensitivity of osteoclasts precursors to RANKL by upregulating the expression of its receptor (Adamopoulos et al. 2010). In addition to acting on cells directly involved in the bone remodeling process, IL-17A indirectly influences bone loss by acting on stromal and epithelial cells to upregulate pro-osteoclastogenic cytokines, particularly IL-6 (Fossiez et al. 1996; You et al. 2012). IL-17A also synergizes potently with other cytokines, especially TNFα, thus serving as a rheostat for local inflammation (Amatya et al. 2017; Shen and Gaffen 2008). Thus, on balance, the overall effect of IL-17A upregulation in chronic inflammatory conditions of bone is destructive, where it supports uncoupled bone remodeling by favoring osteoclastic activity through both direct and indirect mechanisms.

Interestingly, numerous studies have pointed out a protective role for IL-17A mediated inflammation against pathogen-induced tissue damage, including in PD. In the oral environment, IL-17 receptor signaling mediates host defense against *P. gingivalis* induced bone loss (Yu et al. 2007), as well as oral *Candida albicans* infection in mice (Conti et al. 2009). In both models of oral infection, IL-17A-mediated tissue protection is explained by its vital role in orchestrating neutrophil expansion and recruitment to the infection site (Roussel et al. 2010). This process contrasts with long-term PD or arthritic settings where the dominant effect of IL-17A seems to be

a key driver of hard tissue destruction. Collectively, the aforementioned reports indicate that the end result of IL-17A driven inflammation depends on the nature of the inflammatory response produced in tissue and is dictated in part by the inflammatory setting.

In light of the reported roles of IL-17A in inflammatory diseases, systemic anti-IL-17A therapies have been investigated and exhibited varying degrees of success. In this respect, anti-IL-17A therapy is highly effective at improving clinical outcomes and quality of life in PsA patients (McInnes et al. 2014). While the clinical efficacy of IL-17A neutralizing Abs was reported for RA patients in some clinical trials (Genovese et al. 2010; Hueber et al. 2010), other trials showed no clinical benefit of IL-17A blockade (Dokoupilová et al. 2018; Mease et al. 2018). Therefore, anti-IL-17A therapy is not equally effective in all bone-destructive disease settings.

In this aim, we investigated local, sustained release of IL-17A Abs as a therapeutic strategy for murine ligature PD as a model for chronic bone destructive diseases driven by IL-17A. We hypothesized that modulating the activity of IL-17A locally by antibody neutralization would halt periodontal bone loss. To this end, poly (lactic-co-glycolic) acid (PLGA) microparticles (MP) were used to encapsulate and sustainably release IL-17A Abs in diseased murine periodontium. This study demonstrated proof of principle that local anti-IL-17A therapy is a viable strategy for preventing bone loss in conditions associated with IL-17A-mediated pathology.

2.3.2 Hypothesis

We hypothesized that local sustained delivery of anti-IL-17A antibodies in inflamed murine periodontium would modulate IL-17A cytokine activity and inhibit bone loss caused by IL-17A mediated inflammation.

2.3.3 Materials and Methods

2.3.3.1 Anti-IL-17A microparticles (Anti-IL-17A MP) fabrication and characterization

Poly lactic-co-glycolic acid (PLGA) microparticles loaded with the anti-IL-17A antibody (Anti-IL-17A MP), were formulated using a standard water-oil-water double emulsion procedure as described previously (Jhunjhunwala et al. 2012). The aqueous phase contained 1 mg/

ml of anti-mouse IL-17A monoclonal antibody (eBioscience -16717385) in phosphate buffered saline (PBS), while the oil phase was made of PLGA dissolved in dichloromethane as an organic solvent. Blank MP (Unloaded MP) were fabricated following the same procedure, except that the aqueous solution consisted only of PBS. MP were surface characterized using a scanning electron microscope (SEM, JSM-6330F; JEOL) and the release profile of the anti-IL-17A antibody (anti-IL-17A) was determined over 2 weeks using an enzyme-linked immunosorbent assay (ELISA). The surface characterization of MP surface morphology was carried out using a scanning electron microscope (JSM-6330F; JEOL). The release profile of the antibody was determined by suspending the anti-IL-17A MP (~ 7mg) in 1 ml of PBS, the suspension was placed on a tube rotator at 37^{o}C and the supernatants was collected and replaced daily for two weeks. The amount (and structural integrity) of anti-IL-17A in the supernatant was quantified using a standard

enzyme-linked immunosorbent assay (ELISA). In brief, a recombinant mouse IL-17A ELISA standard (Biolegend – 576009) was reconstituted in 1% BSA in PBS then coated on an ELISA microlplate (10 ng/100 µl/well), then the plate was incubated at room temperature overnight. Following overnight incubation, the plate was washed with PBS-Tween then blocked with 3% BSA in PBS and incubated with the supernatants collected daily from the anti-IL-17A MP suspension for 2 hours at room temperature. Serial dilutions of the stock anti-mouse IL-17A solution used for MP fabrication were used as standards for the assay. Next, the plate was washed then incubated with a secondary antibody that constituted of goat-anti-mouse IgG-AP conjugated (Santa Cruz - 2047) at room temperature for 1 hour. Finally, 100 µl of 1 step PNPP (Thermo Scientific – 37621) was added to each well then incubated for 30 minutes at room temperature followed by the addition of 50 µl of 2N NaOH to stop the reaction. The absorbance was detected in a micro-plate reader at 405 nm, then the concentration of anti-IL-17A released at each timepoint was calculated using standard curve.

2.3.3.2 Murine ligature-induced periodontal disease

Six to eight weeks old male BALB/c mice (Jackson Laboratory, Bar Harbor, ME) were used in this study. Mice were maintained under a 12/12h light/dark cycle at 23–25°C with free access to water and commercial food. The study was approved by Institutional Animal Care and Use Committee (IACUC) of the University of Pittsburgh (Protocol # 15053781).

The murine ligature PD model employed in this study was previously described (Abe and Hajishengallis 2013). Briefly, mice were anaesthetized with a mixture of Ketamine (80mg/kg) and Xylazine (8mg/kg), then a sterile 6-0 silk suture (Henry Schein®) was ligated around the maxillary second molar at the level of the gingival sulcus to induce plaque accumulation. The contralateral non-ligated maxillary molar served as an internal control.

2.3.3.3 Experimental design, Anti-IL17A MP local delivery and samples collection

After ligature placement, the animals were divided into three experimental groups: (1) Untreated: ligature placement with no MP injection, (2) anti-IL-17A MP – day 0: ligature placement with Anti-IL-17A MP injection on the same day and (Kitamoto et al.) IL-17A MP – day 2: ligature placement with Anti-IL-17A MP injection after 48 hours. All mice were sacrificed on the 8th day after ligation (n=5 mice). For the second and third groups, anti-IL-17A MP suspended in PBS with 2% carboxymethylcelulose (25 mg/ml) were locally delivered using a 28.5-gauge insulin syringe into four different sites (10-15 ul/site) in the buccal and palatal gingiva surrounding the ligated tooth under a stereomicroscope.

To rule out the possibility that PLGA may exert an effect on bone loss, we conducted an independent experiment where alveolar bone loss was compared between mice with ligature placement only (no MP injection) and mice with ligature and local injection of unloaded (Blank) MP (Supplementary figure1). At the end of the experiment, mice were euthanized, and the maxillae were harvested and placed in either 10% Formaldehyde for fixation then alveolar bone loss and histological analysis, or in liquid nitrogen followed by storage at 80°C for RNA extraction and qPCR analysis.

2.3.3.4 Alveolar bone loss quantification

To quantify alveolar bone loss, the fixed mice maxillae, were transferred to 70% ethanol for micro-computed tomography (µCT) scanning using a viva CT 40 microCT system (SCANCO Medical, Brüttisellen, Switzerland) at a resolution of 10.5 µm and 55 µA kVp. The scans were reoriented so that a horizontal line crossed the cementoenamel junction (CEJ) of the first and second molars in the sagittal plane, while a vertical line crossed the center of the pulp chamber of all molars in the transaxial plane. After reorientation, linear bone resorption was assessed by

measuring the distance between the CEJ and the alveolar bone crest (ABC) using Image J software. On the buccal and palatal aspects, the ABC-CEJ distance was measured in 47 coronal sections spanning all molars, with 52.5 µm intervals in between successive sections. On the interdental aspects, bone loss was assessed in 11 sagittal sections, with 52.5 µm intervals in between, on both the mesial and distal sides of the second molar. The interdental bone loss was calculated as the average of mesial and distal measurements. Measurements were performed on both the ligated (experimental) and non-ligated (healthy) sides of the maxillae. For each aspect, data were presented as the differences between the average values on the ligated and non-ligated sides. The investigator conducting the measurements was blinded from the treatment received in the experimental group being analyzed.

2.3.3.5 Histological analysis

The fixed maxillae were demineralized in 10% EDTA for 15 days at 4^{o}C and processed for paraffin embedding histological analysis. Paraffin embedded half-maxillae were sectioned in serial 4 µm thick sections in a buccal-palatal direction. Sections were stained for tartrate resistant acid phosphatase (TRAP; Sigma– Aldrich, Saint Louis, MO, USA) and counterstained with hematoxylin for quantifcation of osteoclasts. Only the sections in which the pulp chamber and the two roots of the 2nd molar could be visualized were selected for further analysis. For each sample, four maxillae sections, at a distance of at least 16 µm intervals, were utilized for identifying and counting of osteclasts at 400x magnification. In selected sections, the coronal two thirds of the mesial and distal alveolar bone crest adjacent to the maxillary 2nd molar and furcation area was demarcated using Image J software as regions of interest (ROIs). Osteoclasts were identified as TRAP-positive, multinucleated cells with purple cytoplasm situated on the marginal alveolar bone

of the demarcated areas. Results were presented as the average number of osteoclasts divided by the surface are of the ROIs in mm^2 in each experimental group.

2.3.3.6 Quantitative polymerase chain reaction (qPCR)

The frozen maxillae samples were first crushed in liquid nitrogen then RNA extraction was performed using RNeasy Mini Kit (Qiagen, Valencia, CA). The gene expression of interleukin-17A (IL-17A), interleukin-6 (IL-6), tumor necrosis factor alpha (TNF-α) and receptor activator of nuclear factor kappa-B ligand (RANKL) was assessed by qPCR using TaqMan probes (Applied Biosystems, Foster City, CA). Real-time PCR was performed using QuantStudioTM 6 Flex Real-Time PCR system (Thermo Fisher Scientific). Data were analyzed using the delta-delta Ct method and presented as the mean fold change normalized to the healthy control group.

2.3.3.7 Statistical Analysis

Results were presented as means ± SD of 5-6 mice per group. Differences between means were evaluated using one-way ANOVA followed by Tukey (bone loss and osteoclastic activity) or Holm-Sidak (gene expression) post-hoc multiple comparison tests. P-value of less than 5% ($p<0.05$) was considered statistically significant. Statistics were performed using GraphPad Prism.

2.3.4 Results

2.3.4.1 Sustained release profile of functionally active anti-IL-17A Abs from PLGA MP

Release of anti-IL-17A from PLGA MP included an initial burst release of 0.7 ng/ml, followed by a relatively steady release of additional 0.1 ng/ml per day, continuing until day 11. An increase in the anti-IL-17A release rate took place starting day 12 with 0.2ng/ml being released until day 14 (Fig. 19A). Total loading of anti-IL-17A in PLGA was 20% of the amount initially used in the fabrication. SEM images revealed spherically shaped non-porous anti-IL-17A MP with an average diameter of 17.8µm, which is within the known effective size range for PLGA MP intended for drug delivery (Fig. 19B, C). Although PLGA MP smaller than 10 µm are more susceptible to phagocytosis by immune cells, MP larger than 10 µm will remain in the extracellular matrix tissue releasing encapsulated proteins locally at the site of depot.

It should be noted that these ELISA results confirm not only the quantity of IL-17A Abs released from the PLGA MP, but also that the structural integrity of the Abs was maintained, given that this assay is based on the binding of functionally active IL-17A antibody to its epitope on IL-17A. Thus, it is likely that the released IL-17A Abs will exert neutralizing activity upon local delivery.

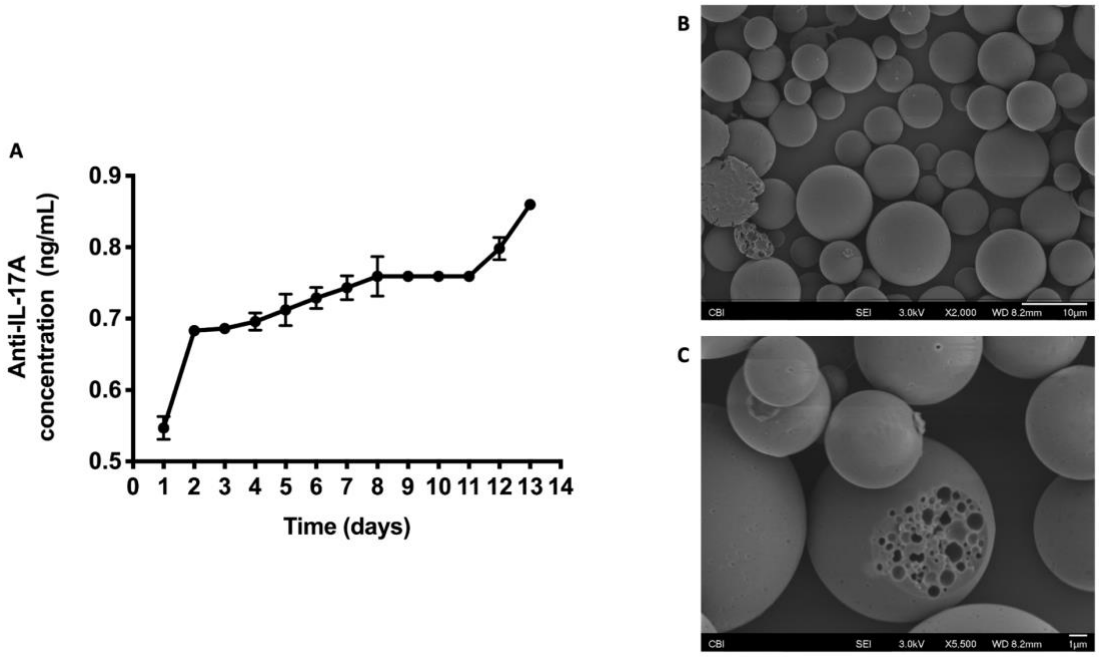

Figure 24. Characterization of PLGA microparticles encapsulating IL-17[a] antibody. Cumulative fraction of IL-17Ab released from PLGA MP for 14 days, determined by ELISA (a). Scanning Eletron Microscopy image of IL-17AbMP, x2000 (b) and x5500 (c).

2.3.4.2 Anti-IL-17A MP inhibited alveolar bone loss and reduced osteoclasts counts in murine PD

To determine the impact of local sustained delivery of anti-IL17A on periodontal bone loss, we employed a standard ligature-induced mouse model of PD (Abe and Hajishengallis 2013). Anti-IL-17A MP were administered contemporaneously with or 2 days after the start of PD induction (Anti-IL-17A D0 or D2). Compared to untreated controls, the anti-IL-17A MP D2 group showed inhibition of alveolar bone loss on the buccal and interdental aspects of the ligated molar as determined by µCT analysis (Figure 20). Additionally, the osteoclast count in the anti-IL-17A MP D2 group was lower than the untreated group, particularly evident on the mesial aspect of the ligated molar as determined by TRAP staining (Fig. 21). Administration of unloaded PLGA MP did not alter the extent of bone loss or osteoclastic activity compared to the untreated/ ligature

control group (Fig. 22), confirming that the PLGA delivery system does not impact alveolar bone loss in ligature PD.

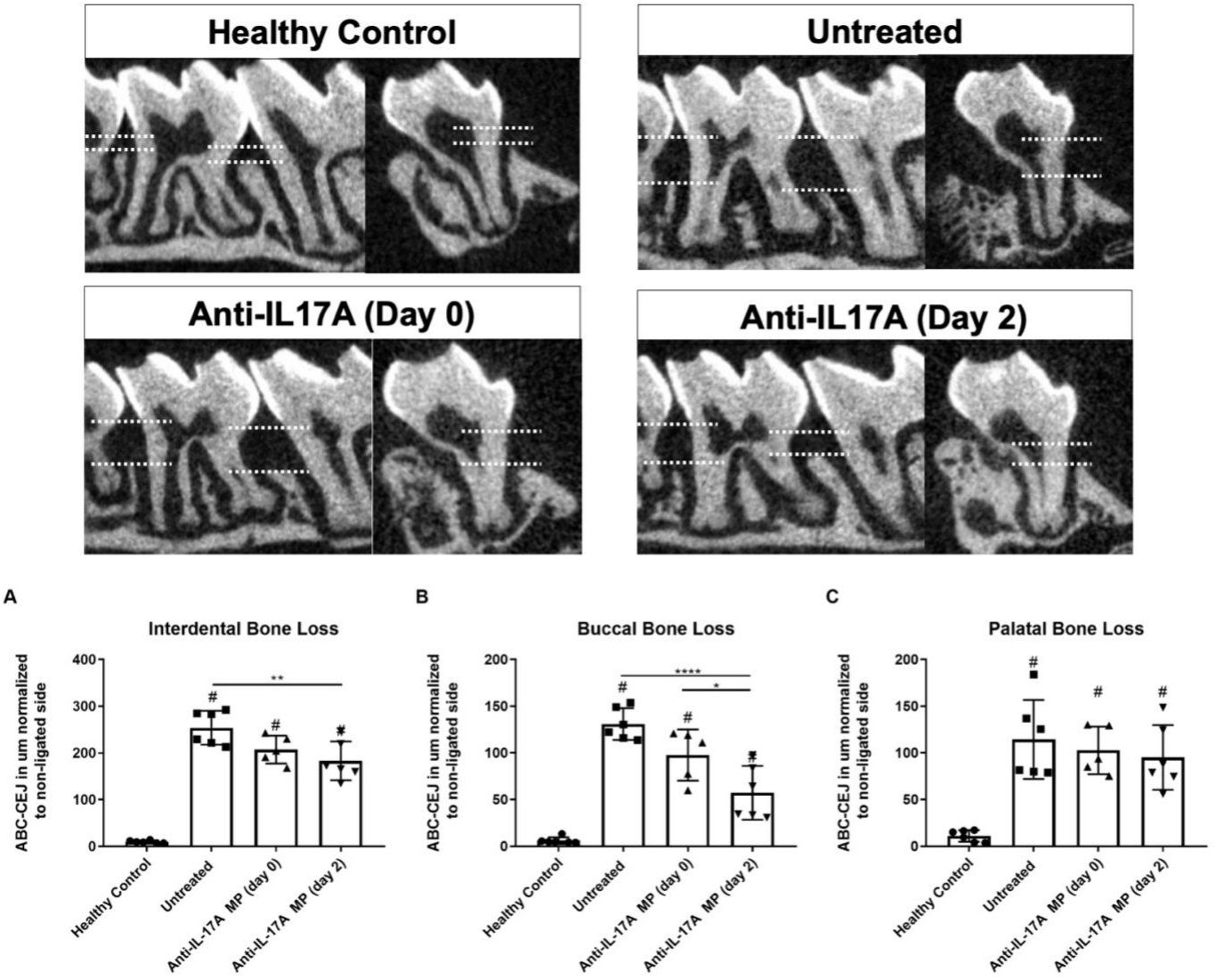

Figure 25. Microtomographic (microCT) evaluation of alveolar bone loss in mice. Microparticles (MP) were injected into gingival tissue surrounding the ligated tooth on either day 0 or day 2, after ligature placement. Representative 2D microCT images from sagittal and transaxial slices of mice hemi-maxilla: healthy group, untreated group, and groups treated with anti-IL-17ª MP at day 0 and day 2. Quantification of alveolar bone loss represented by the linear bone loss between the CEJ and ABC (dashed red lines) along the interdental (A), buccal (B) and palatal (C) sides. Values (mean ± SD) obtained from 5-6 animals per group. P values were determined by one-way ANOVA followed by Tukey's multiple-comparisons test, where *: $p < 0.05$, **: $p < 0.005$, ***: $p < 0.0005$ and ****: $p < 0.0001$.

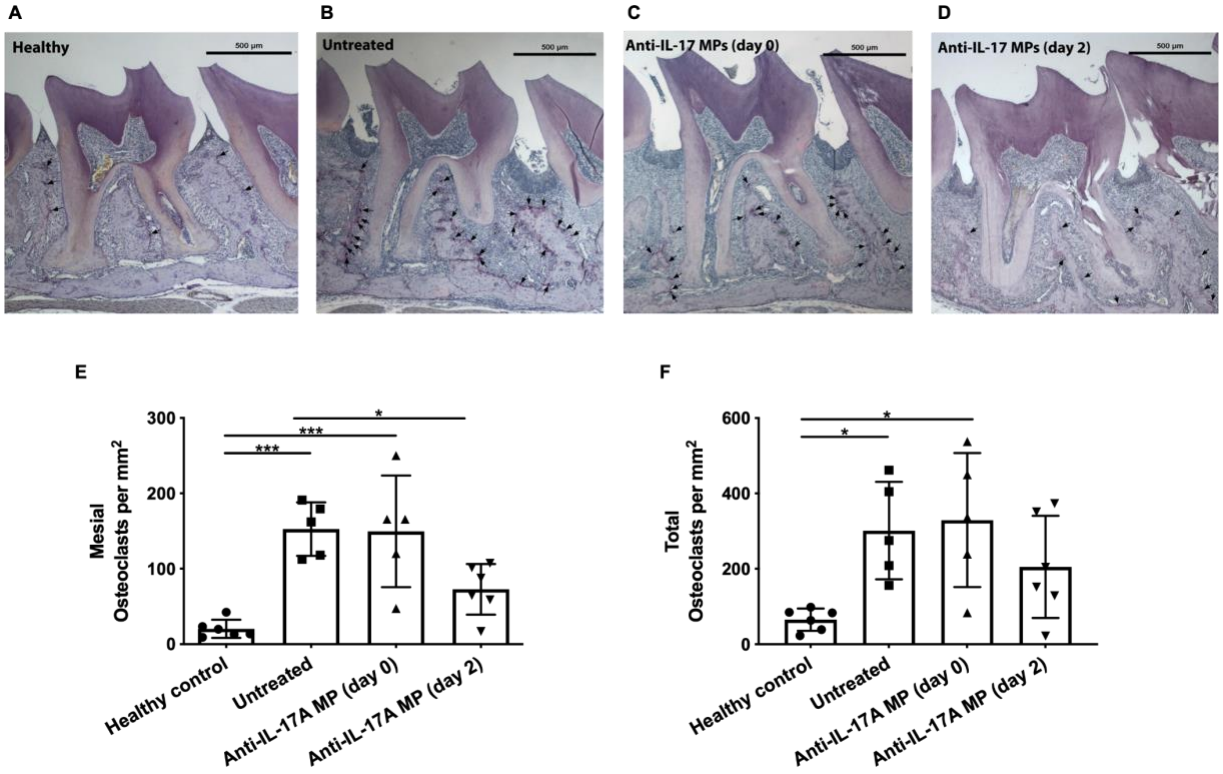

Figure 26. Effect of Anti-IL-17A MP on the number of alveolar bone-associated osteoclasts. (A) Histological representation of healthy, untreated, and IL-17AMP – day 0 and day 2 groups. Hemi-maxilla samples were stained for TRAP, as described in Material and Methods section. The arrows show TRAP-positive multinucleated osteoclasts associated to alveolar bone (Magnification: 400 ×, scale bar: 100 µm). (E) Quantification of the total TRAP-positive multinucleated alveolar bone-associated osteoclasts and on the mesial aspect separately (F). Anti-IL-17A MP at day 2 significantly decreased the number of osteoclasts per mm^2 in the alveolar bone in comparison to untreated group. Values (mean ± SD) obtained from 5-6 animals per group. P values were determined by one-way ANOVA followed by Tukey's multiple-comparisons test, where *: p < 0.05, **: p < 0.005, ***: p < 0.0005 and ****: p < 0.0001.

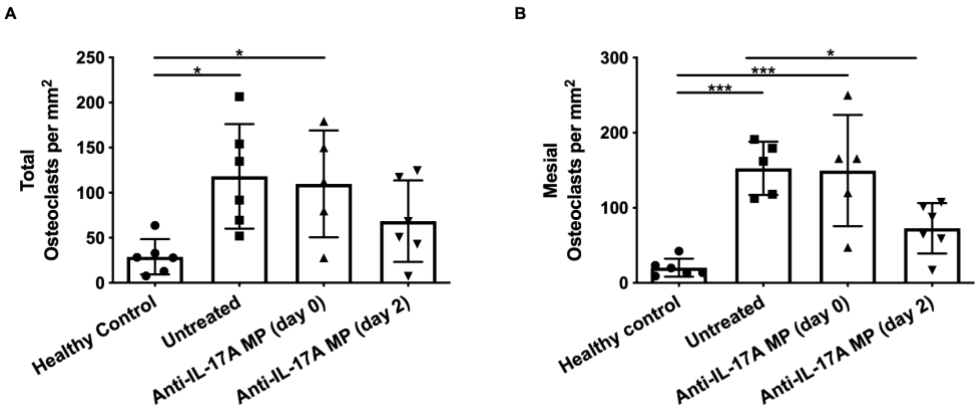

Figure 27. (A) Quatification of total bone loss following ligature PD induction for 8 days only (untreated) or ligature PD induction with blank PLGA MP local delivery (Blank MP), compared to the healthy control group (Healthy). (B) Total osteoclasts analysis represents the sum of TRAP-positive cells on the mesial, distal and furcation areas in untreated and Blank MP treated mice compared to healthy control mice.. Values (mean ± SD) from 6 animals per group. P values were determined by one-way ANOVA followed by Tukey's multiple-comparisons test, where *: p < 0.05, **: p < 0.005, ***: p < 0.0005 and ****: p < 0.0001.

2.3.4.3 Cytokine expression profiles following Anti-IL-17A MP administration

To determine the expression profile of *Il17*a and its dependent genes during ligature induced PD, we extracted RNA from periodontal tissues at different time points days following ligature placement (Fig. 23). We observed upregulation of *Il17a* mRNA expression starting at day 2 post-ligature placement, evident at day 4 and peaking at day 8. The gradually increasing expression profile of *Il17a* during murine ligature induced PD prompted us to deliver the anti-IL-17A MP 2 days after, instead of concurrent with, placing ligatures for all subsequent experiments.

Expression of *Il6*, *Tnfa* and *Tnfsf11* (RANKL) mRNA in periodontium was evaluated at either day 4 or day 8 after ligature placement. At day 4, the untreated/ligature-only group showed elevated *Il6* and *Tnfsf11* compared to controls. Anti-IL-17A MP administration reversed upregulation of *Il6* but not *Tnfsf11* (Figure 24A and C). *Tnfa* was not different among experimental groups (Figure 24B). At day 8, *Tnfsf11* showed sustained upregulation in the untreated group compared to controls. Mice given anti-IL-17A MP exhibited no differences in the expression of *Il-6*, *Tnfa* and *Tnfsf11* mRNA compared to the heathy controls or the untreated groups at day 8 (Figure 24 D and F). Collectively, these data show that local neutralization of IL-17A in diseased periodontium inhibits *Il6* mRNA expression, recapitulating the previously reported effect of IL-17A on *Il6* expression.

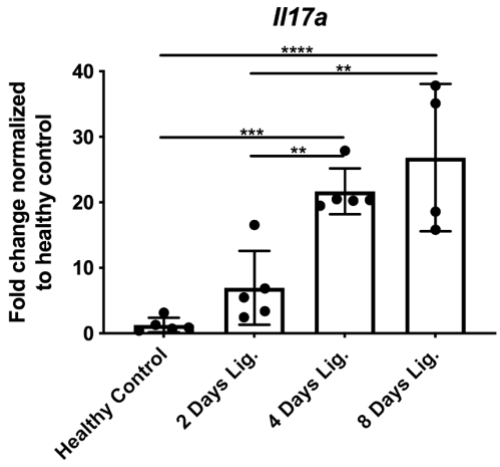

Figure 28. Expression of *Il17a* gene in the gingiva around the ligated maxillart second molar during the course of the 8 days ligature induced periodontitis model. Data represents the mean fold change analyzed by delta-delta CT method from 4-5 mice. P values were determined by one-way ANOVA followed by Holm-Sidak's multiple-comparisons test, where *: p < 0.05, **: p < 0.005, ***: p < 0.0005 and ****: p < 0.0001.

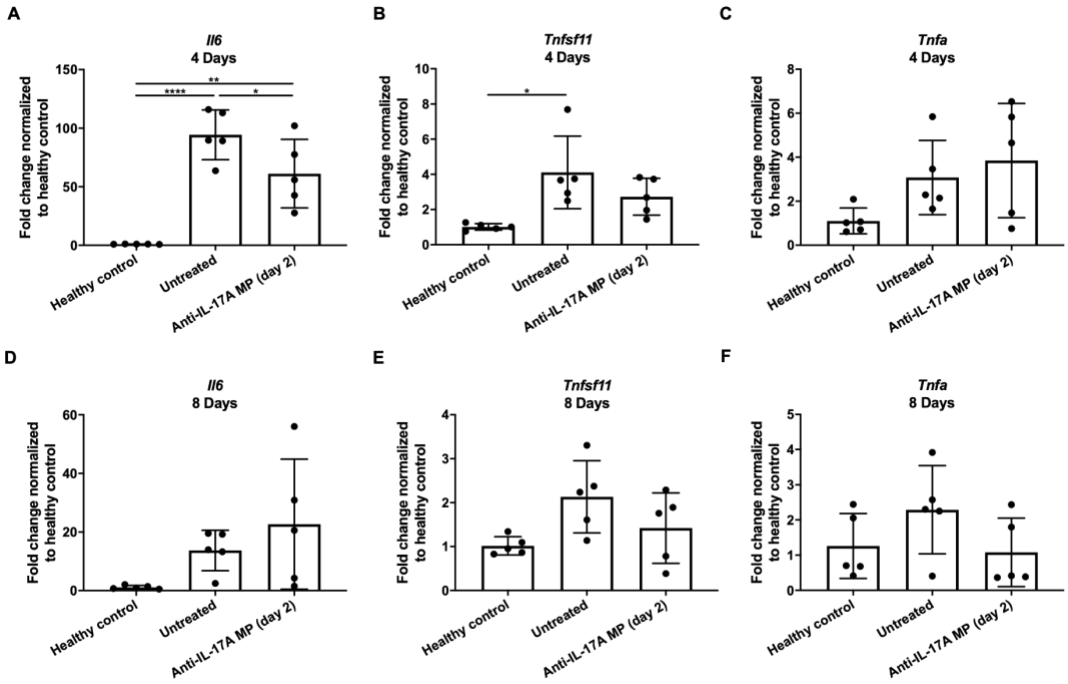

Figure 29. Expression of pro-inflammatory markers in periodontal tissues of mice. *Il6* , *Tnfa* and *Tnfsf11* (RANKL) expression in the periodontal tissues was compared by the value of $2^{(-\Delta\Delta Ct)}$ (n = 5 mice). Microparticles were injected into the maxillary gingiva on day 2 after ligation and the biochemical markers were assessed at 4th (A, B and C) and 8th (D, E and F) day after ligature placement. Periodontal tissues from untreated group showed an increase in *Il6* and *Tnfsf11* levels at 4 days. Anti-IL-17A MP injection decreased the levels of *Il6* when evaluated in the 4th but not in the 8th day after ligature placement. *Tnfsf11* expression did not change by IL-17A MP delivery at 4 or 8 days. Ligature placement and 17A MP injection did not affect *Tnfa* expression in the periodontal tissues at both timepoints. P values were determined by one-way ANOVA followed by Holm-Sidak's multiple-comparisons test, where *: p < 0.05, **: p < 0.005, ***: p < 0.0005 and ****: p < 0.0001.

2.3.5 Discussion

A healthy periodontium depends on an intricate balance between the host response and the periodontal microbiota. In PD, changes in the periodontal microbial load or composition (dysbiosis) provokes inflammation-driven tissue destruction (Hajishengallis 2014). Because periodontal damage is primarily caused by an uncontrolled host inflammatory response to a dysbiotic microbiota (Lamont and Hajishengallis 2015)**,** host modulation has become an attractive therapeutic approach for PD in recent years. In this regard, our group previously demonstrated that recruitment of Tregs (Glowacki et al. 2013) or induction of pro-resolving M2 macrophages (Zhuang et al. 2019) in murine periodontium can protect against inflammatory bone loss.

IL-17A is the signature cytokine of Th17 cells, as well as innate lymphocytes such as γδ-T cells, NKT and ILC3s (Sutton et al. 2012). In the present study, we evaluated the therapeutic efficacy of modulating IL-17A in murine ligature PD as an exemplar for chronic osteolytic diseases. Our goal was to provide a proof of concept for the application of this therapeutic strategy to ameliorate bone destructive diseases involving IL-17A. To that end, we developed a formulation that sustainably releases functionally-active IL-17A Abs to suppress the destructive effects of IL-17A in murine periodontium. This formulation was intended for local administration as a single-dose therapy over the course of murine PD. This translational approach builds on an earlier report pointing to a protective effect of daily local administration of an IL-17A monoclonal antibody against inflammatory bone loss in mice undergoing experimental periodontitis (Eskan et al. 2012).

In the present study, we observed an inhibition in alveolar bone loss when anti-IL-17A MP were delivered 2 days after, but not simultaneously with, PD induction. One possible explanation for this observation is the difference in timing between the secretion of IL-17A in the inflamed periodontium and the release of the IL-17A Abs from the MP (Figure 1A). Our qPCR data showed that *Il17a* mRNA expression in murine periodontal tissues following PD induction is modest at day 2 then sharply increases at day 4, remaining elevated up to day 8 (Supplementary figure 2). We speculate that the rise in *Il17a* from day 2 to day 4 marks the emergence of a pathogenic, rather than homeostatic, subset of IL-17A-producing cells in the inflamed periodontal environment, denoting a switch from a protective to a destructive IL-17A driven inflammation. This switch to a destructive IL-17A driven inflammation could explain the previously reported acceleration in bone loss 3-5 days after ligature placement in the murine ligature-induced PD model (Abe and Hajishengallis 2013; Kourtzelis et al. 2019). Thus, it is expected that a therapeutic strategy that targets IL-17A activity would be most effective as IL-17A is produced in the periodontium (2 days after ligature placement). To that end, we designed our experiment so that the anti-IL-17A burst release takes place just before the emergence of pathogenic IL-17A-producing cells. This temporal synchrony between the anti-IL-17A burst release and the hypothesized window for IL-17A hyperactivity may explain the protective effect of delivering anti-IL-17A MP 2 days after ligature placement and not earlier.

The magnitude of inflammatory bone loss inhibition achieved with delivery of anti-IL-17A MP ranged from ~25% on the interdental aspect to ~50% on the buccal aspect, compared to the untreated group. A similar range of efficacy/bone loss protection is of clinical significance in terms of human disease, where a 20-30% difference in bone loss marks the transition from

mild/moderate to severe disease, based on the newly introduced classification (Tonetti et al. 2018). This further supports the clinical translation potential of anti-IL-17A therapeutics for periodontal disease. Moreover, it is likely that a larger magnitude of bone loss inhibition can be achieved by delivering higher doses of anti-IL-17A using our delivery system. This is because *Il17a* expression has been shown to correlate with the severity of bone loss in previous studies employing the murine ligature PD model (Eskan et al. 2012; Kourtzelis et al. 2019).

The IL-17A targeted approach outlined here is of clinical significance since IL-17A-producing cells present at periodontal sites are not always pathogenic in nature. On one hand, one study suggested that a homeostatic subset of Th17 cells arise in the gingiva as a result of physiological forces of mastication, and this population is essential for immune surveillance and host defense at oral barrier sites (Dutzan et al. 2017). On the other hand, a pathogenic Th17 cell subset expands locally in response to microbial dysbiosis and drives inflammatory damage in murine ligature PD (Dutzan et al. 2018a). The latter report suggested that the destructive inflammatory response in murine PD is induced by IL-17A-dependent signaling. Thus, it is evident that the effects of IL-17A and its producing cells in tissue can be context dependent. Therefore, an understanding of IL-17A dynamic and divergent functions should form the basis for deploying IL-17A targeted therapies in a specific clinical setting.

Osteoclastic bone resorption is a hallmark of PD and is regulated by diverse signals within the bone microenvironment (Bartold et al. 2010; Boyle et al. 2003; Kotake et al. 1999; Teitelbaum 2000). In line with the findings of alveolar bone loss suppression, we observed a reduction in the number of osteoclasts in the alveolar bone crest area in the group that received local anti-IL-17A

MP 2 days after ligature placement. Indeed, IL-17A can upregulate the pro-osteoclastogenic cytokines IL-6 and IL-8, either alone or in synergy with other cytokines such as IL-1β and TNF-α (Noack et al. 2019). The synergistic interaction between IL-17A and TNF-α was suggested as a predictor of early joint damage in RA patients (Kirkham et al. 2006). Similarly, IL-1 β was shown to potentiate the IL-17A effect on bone bone destruction in explants from RA patients (Chabaud et al. 2001). Therefore, blockade of IL-17A may indirectly inhibit the effects of other inflammatory cytokines by mitigating their synergistic interactions (McGeachy et al. 2019).

IL-6 has been shown to be indispensable for pathogenic Th17 cell expansion leading to IL-17A overproduction and bone loss in ligature-induced periodontitis (Dutzan et al. 2018b). Moreover, IL-6 is a signature gene induced by IL-17A signaling in many cell types, thus establishing a feed-forward amplification cycle of local inflammation (Onishi and Gaffen 2010). Consistent with this, we saw that the local delivery of anti-IL-17A MP downregulated *Il6* mRNA expression in periodontal tissues, which may be central to its efficacy, interfering with this inflammatory loop in the periodontal tissues.

In conclusion, the current work demonstrates that local and sustained release of IL-17A Abs can halt inflammatory bone loss in murine PD, which served as a model for chronic osteolytic diseases. Accordingly, this approach may represent a promising therapeutic strategy for conditions in which inflammatory bone loss is driven by IL-17A mediated inflammation.

3.0 Conclusions

In this dissertation, we provided proof of concept for the therapeutic efficacy of two local sustained delivery strategies aiming at modulating destructive inflammation in diseased murine periodontium. We leveraged sustained drug release, single cell RNA sequencing and 16S rRNA sequencing technologies to shed the light on the mechanisms underlying the disease protective effects of our therapeutic strategies. We also maximized the benefits of the highly versatile and predictable murine ligature induced periodontitis model throughout our experiments.

The first strategy was geared toward modulating macrophages response in the murine periodontium by local sustained delivery of the chemokine CCL2. Using murine ligature induced periodontitis model, we showed that locally delivered CCL2 inhibited murine alveolar bone loss in early and established periodontitis, and accelerated bone gain during periodontitis resolution. The bone loss protective effect of locally delivered CCL2 local correlated with a suppression of pro-inflammatory pathways in the periodontal M1/classically activated macrophages as determined by pathway analysis of single cell RNA sequencing data. In particular, TREM1 and IL-17 signaling pathways were identified as potential targets for CCL2 mediated immunosuppression. Furthermore, local sustained delivery of CCL2 reversed the microbial composition shifts associated with murine periodontitis induction by abrogating the increase in the relative abundance of specific microbial taxa.

The second strategy focused on modulating the activity of the IL-17A cytokine derived from pathogenic Th17 cells by local sustained delivery of anti-IL-17A antibodies. We proved the

efficacy of this approach in halting alveolar bone loss and osteoclastic activity during the course of murine ligature induced periodontitis. Those effects correlated with downregulated mRNA expression of IL-6. Those results provided proof of principle for the therapeutic potential of local anti-IL-17A therapies for chronic bone destructive diseases.

Our collective results point to the classical/M1macrophages as crucial downstream effectors of locally delivered CCL2 and anti-IL-17A antibodies. On the one hand, it is well established that classical/M1 macrophages are potent producers of IL-6 and IL-23. Both cytokines haven been shown to be essential for pathogenic Th17 expansion in the murine gingiva (Dutzan et al. 2018a). On the other hand, pathogenic Th17 cells secrete high levels of their signature cytokine IL-17A in the gingiva, which has been shown to potentiate pro-inflammatory responses by classical macrophages in the oral environment (Zhang et al. 2013). This dynamic and mutually beneficial interaction between classical/M1 macrophages and Th17 cells has been also highlighted in the context of rheumatoid arthritis (Li et al. 2013). Thus, it is likely that local suppression of classical/M1 macrophages pro-inflammatory responses would also hinder pathogenic Th17 cells activity and vice versa. Our pathway analysis results supported the plausibility of this concept in the periodontal environment. To that end, CCL2 local delivery resulted in simultaneous inhibition of IL-6 and IL-17 at the canonical pathways and upstream regulators levels in classical macrophages. Similarly, local delivery of anti-IL-17A inhibited gingival mRNA expression of IL-6, which could be derived from both Th17 cells and M1/classical macrophages. The latter mechanism has not yet been supported by in vivo single cell RNA sequencing data. Taken together, the data presented in this dissertation warrant further studies aiming at elucidating the relationship between CCL2 and IL-17A signaling in the context of chronic osteolytic diseases.

Bibliography

Abe T, Hajishengallis G. 2013. Optimization of the ligature-induced periodontitis model in mice. J Immunol Methods. 394(1-2):49-54.

Abusleme L, Hong BY, Hoare A, Konkel JE, Diaz PI, Moutsopoulos NM. 2017. Oral microbiome characterization in murine models. Bio Protoc. 7(24).

Adamopoulos IE, Chao C-c, Geissler R, Laface D, Blumenschein W, Iwakura Y, McClanahan T, Bowman EP. 2010. Interleukin-17a upregulates receptor activator of nf-κb on osteoclast precursors. Arthritis Res Ther. 12(1):R29.

Amatya N, Garg AV, Gaffen SL. 2017. Il-17 signaling: The yin and the yang. Trends in immunology. 38(5):310-322.

Araujo-Pires AC, Vieira AE, Francisconi CF, Biguetti CC, Glowacki A, Yoshizawa S, Campanelli AP, Trombone AP, Sfeir CS, Little SR et al. 2015. Il-4/ccl22/ccr4 axis controls regulatory t-cell migration that suppresses inflammatory bone loss in murine experimental periodontitis. Journal of bone and mineral research : the official journal of the American Society for Bone and Mineral Research. 30(3):412-422.

Auffray C, Fogg D, Garfa M, Elain G, Join-Lambert O, Kayal S, Sarnacki S, Cumano A, Lauvau G, Geissmann F. 2007. Monitoring of blood vessels and tissues by a population of monocytes with patrolling behavior. Science (New York, NY). 317(5838):666-670.

Baker PJ, Dixon M, Roopenian DC. 2000. Genetic control of susceptibility to porphyromonas gingivalis-induced alveolar bone loss in mice. Infect Immun. 68(10):5864-5868.

Bartold PM, Cantley MD, Haynes DR. 2010. Mechanisms and control of pathologic bone loss in periodontitis. Periodontology 2000. 53:55-69.

Bartold PM, Van Dyke TE. 2013. Periodontitis: A host-mediated disruption of microbial homeostasis. Unlearning learned concepts. Periodontology 2000. 62(1):203-217.

Beertsen W, Piscaer M, Van Winkelhoff AJ, Everts V. 2001. Generalized cervical root resorption associated with periodontal disease. J Clin Periodontol. 28(11):1067-1073.

Bhavsar NV, Trivedi SR, Dulani K, Brahmbhatt N, Shah S, Chaudhri D. 2016. Clinical and radiographic evaluation of effect of risedronate 5 mg as an adjunct to treatment of chronic periodontitis in postmenopausal women (12-month study). Osteoporos Int. 27(8):2611-2619.

Bisson C, Massin F, Lefevre PA, Thilly N, Miller N, Gibot S. 2012. Increased gingival crevicular fluid levels of soluble triggering receptor expressed on myeloid cells (strem) -1 in severe periodontitis. J Clin Periodontol. 39(12):1141-1148.

Bostanci N, Abe T, Belibasakis GN, Hajishengallis G. 2019. Trem-1 is upregulated in experimental periodontitis, and its blockade inhibits il-17a and rankl expression and suppresses bone loss. J Clin Med. 8(10):1579.

Bostanci N, Oztürk V, Emingil G, Belibasakis GN. 2013. Elevated oral and systemic levels of soluble triggering receptor expressed on myeloid cells-1 (strem-1) in periodontitis. J Dent Res. 92(2):161-165.

Bosurgi L, Cao YG, Cabeza-Cabrerizo M, Tucci A, Hughes LD, Kong Y, Weinstein JS, Licona-Limon P, Schmid ET, Pelorosso F et al. 2017. Macrophage function in tissue repair and

remodeling requires il-4 or il-13 with apoptotic cells. Science (New York, NY). 356(6342):1072-1076.
Boyce BF, Xing L. 2008. Functions of rankl/rank/opg in bone modeling and remodeling. Arch Biochem Biophys. 473(2):139-146.
Boyle WJ, Simonet WS, Lacey DL. 2003. Osteoclast differentiation and activation. Nature. 423(6937):337-342.
Bunte K, Beikler T. 2019. Th17 cells and the il-23/il-17 axis in the pathogenesis of periodontitis and immune-mediated inflammatory diseases. Int J Mol Sci. 20(14):3394.
Bushati N, Smith J, Briscoe J, Watkins C. 2011. An intuitive graphical visualization technique for the interrogation of transcriptome data. Nucleic acids research. 39(17):7380-7389.
Caldwell RW, Rodriguez PC, Toque HA, Narayanan SP, Caldwell RB. 2018. Arginase: A multifaceted enzyme important in health and disease. Physiological reviews. 98(2):641-665.
Carcuac O, Berglundh T. 2014. Composition of human peri-implantitis and periodontitis lesions. J Dent Res. 93(11):1083-1088.
Caton JG. 1999. Evaluation of periostat for patient management. Compend Contin Educ Dent. 20(5):451-456, 458-460, 462; quiz 463.
Cekici A, Kantarci A, Hasturk H, Van Dyke TE. 2014a. Inflammatory and immune pathways in the pathogenesis of periodontal disease. Periodontology 2000. 64(1):57-80.
Cekici A, Kantarci A, Hasturk H, Van Dyke TE. 2014b. Inflammatory and immune pathways in the pathogenesis of periodontal disease. Periodontology 2000. 64(1):57-80.
Chabaud M, Lubberts E, Joosten L, van Den Berg W, Miossec P. 2001. Il-17 derived from juxta-articular bone and synovium contributes to joint degradation in rheumatoid arthritis. Arthritis research. 3(3):168-177.
Cho MI, Garant PR. 2000. Development and general structure of the periodontium. Periodontology 2000. 24:9-27.
Cochran DL. 2008. Inflammation and bone loss in periodontal disease. J Periodontol. 79(8 Suppl):1569-1576.
Colombo AP, Haffajee AD, Dewhirst FE, Paster BJ, Smith CM, Cugini MA, Socransky SS. 1998. Clinical and microbiological features of refractory periodontitis subjects. J Clin Periodontol. 25(2):169-180.
Conti HR, Shen F, Nayyar N, Stocum E, Sun JN, Lindemann MJ, Ho AW, Hai JH, Yu JJ, Jung JW et al. 2009. Th17 cells and il-17 receptor signaling are essential for mucosal host defense against oral candidiasis. The Journal of experimental medicine. 206(2):299-311.
Cullinan MP, Seymour GJ. 2013. Periodontal disease and systemic illness: Will the evidence ever be enough? Periodontology 2000. 62(1):271-286.
Curtis MA, Diaz PI, Van Dyke TE. 2020. The role of the microbiota in periodontal disease. Periodontology 2000. 83(1):14-25.
Darveau RP, Hajishengallis G, Curtis MA. 2012. Porphyromonas gingivalis as a potential community activist for disease. J Dent Res. 91(9):816-820.
de Molon RS, de Avila ED, Boas Nogueira AV, Chaves de Souza JA, Avila-Campos MJ, de Andrade CR, Cirelli JA. 2014. Evaluation of the host response in various models of induced periodontal disease in mice. J Periodontol. 85(3):465-477.
de Molon RS, Mascarenhas VI, de Avila ED, Finoti LS, Toffoli GB, Spolidorio DM, Scarel-Caminaga RM, Tetradis S, Cirelli JA. 2016. Long-term evaluation of oral gavage with

periodontopathogens or ligature induction of experimental periodontal disease in mice. Clinical oral investigations. 20(6):1203-1216.
DePaolo RW, Lathan R, Rollins BJ, Karpus WJ. 2005. The chemokine ccl2 is required for control of murine gastric salmonella enterica infection. Infection and Immunity. 73(10):6514.
Detert J, Pischon N, Burmester GR, Buttgereit F. 2010. The association between rheumatoid arthritis and periodontal disease. Arthritis Res Ther. 12(5):218-218.
Diekwisch TG. 2001. The developmental biology of cementum. Int J Dev Biol. 45(5-6):695-706.
Dokoupilová E, Aelion J, Takeuchi T, Malavolta N, Sfikakis PP, Wang Y, Rohrer S, Richards HB. 2018. Secukinumab after anti-tumour necrosis factor-α therapy: A phase iii study in active rheumatoid arthritis. Scandinavian Journal of Rheumatology. 47(4):276-281.
Dominy SS, Lynch C, Ermini F, Benedyk M, Marczyk A, Konradi A, Nguyen M, Haditsch U, Raha D, Griffin C et al. 2019. Porphyromonas gingivalis in alzheimer's disease brains: Evidence for disease causation and treatment with small-molecule inhibitors. Science advances. 5(1):eaau3333.
Dutzan N, Abusleme L, Bridgeman H, Greenwell-Wild T, Zangerle-Murray T, Fife ME, Bouladoux N, Linley H, Brenchley L, Wemyss K et al. 2017. On-going mechanical damage from mastication drives homeostatic th17 cell responses at the oral barrier. Immunity. 46(1):133-147.
Dutzan N, Abusleme L, Konkel JE, Moutsopoulos NM. 2016. Isolation, characterization and functional examination of the gingival immune cell network. Journal of visualized experiments : JoVE. (108):53736.
Dutzan N, Kajikawa T, Abusleme L, Greenwell-Wild T, Zuazo CE, Ikeuchi T, Brenchley L, Abe T, Hurabielle C, Martin D et al. 2018a. A dysbiotic microbiome triggers t(h)17 cells to mediate oral mucosal immunopathology in mice and humans. Sci Transl Med. 10(463).
Dutzan N, Kajikawa T, Abusleme L, Greenwell-Wild T, Zuazo CE, Ikeuchi T, Brenchley L, Abe T, Hurabielle C, Martin D et al. 2018b. A dysbiotic microbiome triggers t(h)17 cells to mediate oral mucosal immunopathology in mice and humans. Sci Transl Med. 10(463):eaat0797.
Dutzan N, Kajikawa T, Abusleme L, Greenwell-Wild T, Zuazo CE, Ikeuchi T, Brenchley L, Abe T, Hurabielle C, Martin D et al. 2018c. A dysbiotic microbiome triggers th17 cells to mediate oral mucosal immunopathology in mice and humans. Sci Transl Med. 10(463).
Dutzan N, Vernal R, Vaque JP, García-Sesnich J, Hernandez M, Abusleme L, Dezerega A, Gutkind JS, Gamonal J. 2012. Interleukin-21 expression and its association with proinflammatory cytokines in untreated chronic periodontitis patients. J Periodontol. 83(7):948-954.
Eke PI, Dye BA, Wei L, Slade GD, Thornton-Evans GO, Borgnakke WS, Taylor GW, Page RC, Beck JD, Genco RJ. 2015a. Update on prevalence of periodontitis in adults in the united states: Nhanes 2009 – 2012. Journal of periodontology. 86(5):611-622.
Eke PI, Dye BA, Wei L, Slade GD, Thornton-Evans GO, Borgnakke WS, Taylor GW, Page RC, Beck JD, Genco RJ. 2015b. Update on prevalence of periodontitis in adults in the united states: Nhanes 2009 to 2012. J Periodontol. 86(5):611-622.
Emmons S, Kobourov S, Gallant M, Börner K. 2016. Analysis of network clustering algorithms and cluster quality metrics at scale. PLOS ONE. 11(7):e0159161.

Eskan MA, Jotwani R, Abe T, Chmelar J, Lim JH, Liang S, Ciero PA, Krauss JL, Li F, Rauner M et al. 2012. The leukocyte integrin antagonist del-1 inhibits il-17-mediated inflammatory bone loss. Nature immunology. 13(5):465-473.

Evans KE, Fox SW. 2007. Interleukin-10 inhibits osteoclastogenesis by reducing nfatc1 expression and preventing its translocation to the nucleus. BMC Cell Biology. 8:4.

Fadrosh DW, Ma B, Gajer P, Sengamalay N, Ott S, Brotman RM, Ravel J. 2014. An improved dual-indexing approach for multiplexed 16s rrna gene sequencing on the illumina miseq platform. Microbiome. 2(1):6.

Faizuddin M, Tarannum F, Korla N, Swamy S. 2012. Association between long-term aspirin use and periodontal attachment level in humans: A cross-sectional investigation. Aust Dent J. 57(1):45-50.

Fleetwood AJ, Lawrence T, Hamilton JA, Cook AD. 2007. Granulocyte-macrophage colony-stimulating factor (csf) and macrophage csf-dependent macrophage phenotypes display differences in cytokine profiles and transcription factor activities: Implications for csf blockade in inflammation. Journal of immunology (Baltimore, Md : 1950). 178(8):5245-5252.

Fossiez F, Djossou O, Chomarat P, Flores-Romo L, Ait-Yahia S, Maat C, Pin JJ, Garrone P, Garcia E, Saeland S et al. 1996. T cell interleukin-17 induces stromal cells to produce proinflammatory and hematopoietic cytokines. The Journal of experimental medicine. 183(6):2593-2603.

Gangwar RS, Vinayachandran V, Rengasamy P, Chan R, Park B, Diamond-Zaluski R, Cara EA, Cha A, Das L, Asase C et al. 2020. Differential contribution of bone marrow-derived infiltrating monocytes and resident macrophages to persistent lung inflammation in chronic air pollution exposure. Scientific Reports. 10(1):14348.

Gao L, Faibish D, Fredman G, Herrera BS, Chiang N, Serhan CN, Van Dyke TE, Gyurko R. 2013. Resolvin e1 and chemokine-like receptor 1 mediate bone preservation. Journal of immunology (Baltimore, Md : 1950). 190(2):689-694.

Gemmell E, McHugh GB, Grieco DA, Seymour GJ. 2001. Costimulatory molecules in human periodontal disease tissues. J Periodontal Res. 36(2):92-100.

Genovese MC, Van den Bosch F, Roberson SA, Bojin S, Biagini IM, Ryan P, Sloan-Lancaster J. 2010. Ly2439821, a humanized anti-interleukin-17 monoclonal antibody, in the treatment of patients with rheumatoid arthritis: A phase i randomized, double-blind, placebo-controlled, proof-of-concept study. Arthritis Rheum. 62(4):929-939.

Glowacki AJ, Yoshizawa S, Jhunjhunwala S, Vieira AE, Garlet GP, Sfeir C, Little SR. 2013. Prevention of inflammation-mediated bone loss in murine and canine periodontal disease via recruitment of regulatory lymphocytes. Proc Natl Acad Sci U S A. 110(46):18525-18530.

Gomes RN, Teixeira-Cunha MG, Figueiredo RT, Almeida PE, Alves SC, Bozza PT, Bozza FA, Bozza MT, Zimmerman GA, Castro-Faria-Neto HC. 2013. Bacterial clearance in septic mice is modulated by mcp-1/ccl2 and nitric oxide. Shock. 39(1):63-69.

Gorham JD, Güler ML, Steen RG, Mackey AJ, Daly MJ, Frederick K, Dietrich WF, Murphy KM. 1996. Genetic mapping of a murine locus controlling development of t helper 1/t helper 2 type responses. Proceedings of the National Academy of Sciences of the United States of America. 93(22):12467-12472.

Graves DT, Li J, Cochran DL. 2011. Inflammation and uncoupling as mechanisms of periodontal bone loss. J Dent Res. 90(2):143-153.

Guo Q, Wang Y, Xu D, Nossent J, Pavlos NJ, Xu J. 2018. Rheumatoid arthritis: Pathological mechanisms and modern pharmacologic therapies. Bone Res. 6:15.
Haffajee AD, Cugini MA, Dibart S, Smith C, Kent RL, Jr., Socransky SS. 1997. The effect of srp on the clinical and microbiological parameters of periodontal diseases. J Clin Periodontol. 24(5):324-334.
Haffajee AD, Socransky SS, Gunsolley JC. 2003. Systemic anti-infective periodontal therapy. A systematic review. Ann Periodontol. 8(1):115-181.
Hajishengallis G. 2011. Immune evasion strategies of porphyromonas gingivalis. J Oral Biosci. 53(3):233-240.
Hajishengallis G. 2014. Immunomicrobial pathogenesis of periodontitis: Keystones, pathobionts, and host response. Trends in immunology. 35(1):3-11.
Hajishengallis G. 2015. Periodontitis: From microbial immune subversion to systemic inflammation. Nature reviews Immunology. 15(1):30-44.
Hajishengallis G, Lamont RJ. 2014. Breaking bad: Manipulation of the host response by porphyromonas gingivalis. Eur J Immunol. 44(2):328-338.
Hannemann N, Cao S, Eriksson D, Schnelzer A, Jordan J, Eberhardt M, Schleicher U, Rech J, Ramming A, Uebe S et al. 2019. Transcription factor fra-1 targets arginase-1 to enhance macrophage-mediated inflammation in arthritis. The Journal of clinical investigation. 129(7):2669-2684.
Hasturk H, Kantarci A, Goguet-Surmenian E, Blackwood A, Andry C, Serhan CN, Van Dyke TE. 2007. Resolvin e1 regulates inflammation at the cellular and tissue level and restores tissue homeostasis in vivo. The Journal of Immunology. 179(10):7021.
Hasturk H, Kantarci A, Ohira T, Arita M, Ebrahimi N, Chiang N, Petasis NA, Levy BD, Serhan CN, Van Dyke TE. 2006. Rve1 protects from local inflammation and osteoclast- mediated bone destruction in periodontitis. FASEB journal : official publication of the Federation of American Societies for Experimental Biology. 20(2):401-403.
Heitz-Mayfield LJ, Trombelli L, Heitz F, Needleman I, Moles D. 2002. A systematic review of the effect of surgical debridement vs non-surgical debridement for the treatment of chronic periodontitis. J Clin Periodontol. 29 Suppl 3:92-102; discussion 160-102.
Herová M, Schmid M, Gemperle C, Hersberger M. 2015. Chemr23, the receptor for chemerin and resolvin e1, is expressed and functional on m1 but not on m2 macrophages. Journal of immunology (Baltimore, Md : 1950). 194(5):2330-2337.
Herrera BS, Ohira T, Gao L, Omori K, Yang R, Zhu M, Muscara MN, Serhan CN, Van Dyke TE, Gyurko R. 2008. An endogenous regulator of inflammation, resolvin e1, modulates osteoclast differentiation and bone resorption. British journal of pharmacology. 155(8):1214-1223.
Huang YH, Ohsaki Y, Kurisu K. 1991. Distribution of type i and type iii collagen in the developing periodontal ligament of mice. Matrix. 11(1):25-35.
Hueber W, Patel DD, Dryja T, Wright AM, Koroleva I, Bruin G, Antoni C, Draelos Z, Gold MH, Durez P et al. 2010. Effects of ain457, a fully human antibody to interleukin-17a, on psoriasis, rheumatoid arthritis, and uveitis. Science Translational Medicine. 2(52):52ra72.
Italiani P, Boraschi D. 2014. From monocytes to m1/m2 macrophages: Phenotypical vs. Functional differentiation. Frontiers in immunology. 5:514-514.
Jaitin DA, Kenigsberg E, Keren-Shaul H, Elefant N, Paul F, Zaretsky I, Mildner A, Cohen N, Jung S, Tanay A et al. 2014. Massively parallel single-cell rna-seq for marker-free decomposition of tissues into cell types. Science (New York, NY). 343(6172):776-779.

Jandus C, Bioley G, Rivals JP, Dudler J, Speiser D, Romero P. 2008. Increased numbers of circulating polyfunctional th17 memory cells in patients with seronegative spondylarthritides. Arthritis Rheum. 58(8):2307-2317.

Jhunjhunwala S, Balmert SC, Raimondi G, Dons E, Nichols EE, Thomson AW, Little SR. 2012. Controlled release formulations of il-2, tgf-β1 and rapamycin for the induction of regulatory t cells. Journal of controlled release : official journal of the Controlled Release Society. 159(1):78-84.

Johnson RB, Wood N, Serio FG. 2004. Interleukin-11 and il-17 and the pathogenesis of periodontal disease. J Periodontol. 75(1):37-43.

Johnston LK, Rims CR, Gill SE, McGuire JK, Manicone AM. 2012. Pulmonary macrophage subpopulations in the induction and resolution of acute lung injury. Am J Respir Cell Mol Biol. 47(4):417-426.

Kassebaum NJ, Bernabé E, Dahiya M, Bhandari B, Murray CJL, Marcenes W. 2014. Global burden of severe periodontitis in 1990-2010: A systematic review and meta-regression. Journal of Dental Research. 93(11):1045-1053.

Katz J, Yang QB, Zhang P, Potempa J, Travis J, Michalek SM, Balkovetz DF. 2002. Hydrolysis of epithelial junctional proteins by porphyromonas gingivalis gingipains. Infect Immun. 70(5):2512-2518.

Kim YG, Lee CK, Nah SS, Mun SH, Yoo B, Moon HB. 2007. Human cd4+cd25+ regulatory t cells inhibit the differentiation of osteoclasts from peripheral blood mononuclear cells. Biochemical and biophysical research communications. 357(4):1046-1052.

Kinane DF, Preshaw PM, Loos BG. 2011. Host-response: Understanding the cellular and molecular mechanisms of host-microbial interactions--consensus of the seventh european workshop on periodontology. J Clin Periodontol. 38 Suppl 11:44-48.

Kirkham BW, Lassere MN, Edmonds JP, Juhasz KM, Bird PA, Lee CS, Shnier R, Portek IJ. 2006. Synovial membrane cytokine expression is predictive of joint damage progression in rheumatoid arthritis: A two-year prospective study (the damage study cohort). Arthritis Rheum. 54(4):1122-1131.

Kitamoto S, Nagao-Kitamoto H, Jiao Y, Gillilland MG, 3rd, Hayashi A, Imai J, Sugihara K, Miyoshi M, Brazil JC, Kuffa P et al. 2020. The intermucosal connection between the mouth and gut in commensal pathobiont-driven colitis. Cell. 182(2):447-462.e414.

Kitazawa R, Kimble RB, Vannice JL, Kung VT, Pacifici R. 1994. Interleukin-1 receptor antagonist and tumor necrosis factor binding protein decrease osteoclast formation and bone resorption in ovariectomized mice. The Journal of clinical investigation. 94(6):2397-2406.

Kobayashi K, Takahashi N, Jimi E, Udagawa N, Takami M, Kotake S, Nakagawa N, Kinosaki M, Yamaguchi K, Shima N et al. 2000. Tumor necrosis factor alpha stimulates osteoclast differentiation by a mechanism independent of the odf/rankl-rank interaction. The Journal of experimental medicine. 191(2):275-286.

Kong D, Shen Y, Liu G, Zuo S, Ji Y, Lu A, Nakamura M, Lazarus M, Stratakis CA, Breyer RM et al. 2016. Pka regulatory iiα subunit is essential for pgd2-mediated resolution of inflammation. The Journal of experimental medicine. 213(10):2209-2226.

Koo KT, Polimeni G, Qahash M, Kim CK, Wikesjö UM. 2005. Periodontal repair in dogs: Guided tissue regeneration enhances bone formation in sites implanted with a coral-derived calcium carbonate biomaterial. J Clin Periodontol. 32(1):104-110.

Kortegaard HE, Eriksen T, Baelum V. 2008. Periodontal disease in research beagle dogs--an epidemiological study. J Small Anim Pract. 49(12):610-616.

Kosaka T, Ono T, Yoshimuta Y, Kida M, Kikui M, Nokubi T, Maeda Y, Kokubo Y, Watanabe M, Miyamoto Y. 2014. The effect of periodontal status and occlusal support on masticatory performance: The suita study. J Clin Periodontol. 41(5):497-503.

Kotake S, Udagawa N, Takahashi N, Matsuzaki K, Itoh K, Ishiyama S, Saito S, Inoue K, Kamatani N, Gillespie MT et al. 1999. Il-17 in synovial fluids from patients with rheumatoid arthritis is a potent stimulator of osteoclastogenesis. The Journal of clinical investigation. 103(9):1345-1352.

Kourtzelis I, Li X, Mitroulis I, Grosser D, Kajikawa T, Wang B, Grzybek M, von Renesse J, Czogalla A, Troullinaki M et al. 2019. Del-1 promotes macrophage efferocytosis and clearance of inflammation. Nature immunology. 20(1):40-49.

Kurgan S, Kantarci A. 2018. Molecular basis for immunohistochemical and inflammatory changes during progression of gingivitis to periodontitis. Periodontology 2000. 76(1):51-67.

Lamont RJ, Hajishengallis G. 2015. Polymicrobial synergy and dysbiosis in inflammatory disease. Trends in molecular medicine. 21(3):172-183.

Lamont RJ, Koo H, Hajishengallis G. 2018. The oral microbiota: Dynamic communities and host interactions. Nature Reviews Microbiology. 16(12):745-759.

Lavine KJ, Epelman S, Uchida K, Weber KJ, Nichols CG, Schilling JD, Ornitz DM, Randolph GJ, Mann DL. 2014. Distinct macrophage lineages contribute to disparate patterns of cardiac recovery and remodeling in the neonatal and adult heart. Proceedings of the National Academy of Sciences of the United States of America. 111(45):16029-16034.

Lee CT, Teles R, Kantarci A. 2016a. Resolvin e1 reverses experimental periodontitis and dysbiosis. 197(7):2796-2806.

Lee CT, Teles R, Kantarci A, Chen T, McCafferty J, Starr JR, Brito LC, Paster BJ, Van Dyke TE. 2016b. Resolvin e1 reverses experimental periodontitis and dysbiosis. Journal of immunology (Baltimore, Md : 1950). 197(7):2796-2806.

Lee SA, Noel S, Sadasivam M, Allaf ME, Pierorazio PM, Hamad ARA, Rabb H. 2018. Characterization of kidney cd45intcd11bintf4/80+mhcii+cx3cr1+ly6c- "intermediate mononuclear phagocytic cells". PLOS ONE. 13(6):e0198608.

Leipe J, Grunke M, Dechant C, Reindl C, Kerzendorf U, Schulze-Koops H, Skapenko A. 2010. Role of th17 cells in human autoimmune arthritis. Arthritis Rheum. 62(10):2876-2885.

Lester SR, Bain JL, Johnson RB, Serio FG. 2007. Gingival concentrations of interleukin-23 and -17 at healthy sites and at sites of clinical attachment loss. J Periodontol. 78(8):1545-1550.

Lewis JP. 2010. Metal uptake in host-pathogen interactions: Role of iron in porphyromonas gingivalis interactions with host organisms. Periodontology 2000. 52(1):94-116.

Li J, Hsu H-C, Mountz JD. 2013. The dynamic duo-inflammatory m1 macrophages and th17 cells in rheumatic diseases. J Orthop Rheumatol. 1(1):4-4.

Li J, Hsu HC, Yang P, Wu Q, Li H, Edgington LE, Bogyo M, Kimberly RP, Mountz JD. 2012. Treatment of arthritis by macrophage depletion and immunomodulation: Testing an apoptosis-mediated therapy in a humanized death receptor mouse model. Arthritis Rheum. 64(4):1098-1109.

Li J-Y, Yu M, Tyagi AM, Vaccaro C, Hsu E, Adams J, Bellido T, Weitzmann MN, Pacifici R. 2019. Il-17 receptor signaling in osteoblasts/osteocytes mediates pth-induced bone loss and enhances osteocytic rankl production. Journal of Bone and Mineral Research. 34(2):349-360.

Li L, Wei W, Li Z, Chen H, Li Y, Jiang W, Chen W, Kong G, Yang J, Li Z. 2018. The spleen promotes the secretion of ccl2 and supports an m1 dominant phenotype in hepatic macrophages during liver fibrosis. Cellular Physiology and Biochemistry. 51(2):557-574.
Lindhe J, Hamp S, Löe H. 1973. Experimental periodontitis in the beagle dog. J Periodontal Res. 8(1):1-10.
Lindhe J, Hamp SE, Loe H. 1975. Plaque induced periodontal disease in beagle dogs. A 4-year clinical, roentgenographical and histometrical study. J Periodontal Res. 10(5):243-255.
Livak KJ, Schmittgen TD. 2001. Analysis of relative gene expression data using real-time quantitative pcr and the 2(-delta delta c(t)) method. Methods (San Diego, Calif). 25(4):402-408.
Loesche WJ. 1991. Role of anaerobic bacteria in periodontal disease. Ann Otol Rhinol Laryngol Suppl. 154:43-45.
Loesche WJ, Grossman NS. 2001. Periodontal disease as a specific, albeit chronic, infection: Diagnosis and treatment. Clinical microbiology reviews. 14(4):727-752, table of contents.
Lovegrove JM. 2004. Dental plaque revisited: Bacteria associated with periodontal disease. Journal of the New Zealand Society of Periodontology. (87):7-21.
Lübcke PM, Ebbers MNB, Volzke J, Bull J, Kneitz S, Engelmann R, Lang H, Kreikemeyer B, Müller-Hilke B. 2019. Periodontal treatment prevents arthritis in mice and methotrexate ameliorates periodontal bone loss. Scientific Reports. 9(1):8128.
Mahajan AC, Kolte AP, Kolte RA, Agrawal AA. 2017. Dimensional evaluation of root resorption areas in differing severity of chronic periodontitis: A scanning electron microscopic study. Contemp Clin Dent. 8(3):433-438.
Mantovani A, Sica A, Sozzani S, Allavena P, Vecchi A, Locati M. 2004. The chemokine system in diverse forms of macrophage activation and polarization. Trends in immunology. 25(12):677-686.
Marchesan J, Girnary MS, Jing L, Miao MZ, Zhang S, Sun L, Morelli T, Schoenfisch MH, Inohara N, Offenbacher S et al. 2018. An experimental murine model to study periodontitis. Nature protocols. 13(10):2247-2267.
Marsh PD. 1994. Microbial ecology of dental plaque and its significance in health and disease. Advances in dental research. 8(2):263-271.
Martinez FO, Gordon S. 2014. The m1 and m2 paradigm of macrophage activation: Time for reassessment. F1000Prime Rep. 6:13-13.
Martuscelli G, Fiorellini JP, Crohin CC, Howell TH. 2000. The effect of interleukin-11 on the progression of ligature-induced periodontal disease in the beagle dog. J Periodontol. 71(4):573-578.
Matesanz-Pérez P, García-Gargallo M, Figuero E, Bascones-Martínez A, Sanz M, Herrera D. 2013. A systematic review on the effects of local antimicrobials as adjuncts to subgingival debridement, compared with subgingival debridement alone, in the treatment of chronic periodontitis. J Clin Periodontol. 40(3):227-241.
McGeachy MJ, Cua DJ, Gaffen SL. 2019. The il-17 family of cytokines in health and disease. Immunity. 50(4):892-906.
McInnes IB, Sieper J, Braun J, Emery P, van der Heijde D, Isaacs JD, Dahmen G, Wollenhaupt J, Schulze-Koops H, Kogan J et al. 2014. Efficacy and safety of secukinumab, a fully human anti-interleukin-17a monoclonal antibody, in patients with moderate-to-severe psoriatic arthritis: A 24-week, randomised, double-blind, placebo-controlled, phase ii proof-of-concept trial. Annals of the Rheumatic Diseases. 73(2):349.

Mease PJ, Jeka S, Jaller JJ, Kitumnuaypong T, Louthrenoo W, Mann H, Matsievskaia G, Soriano ER, Jia B, Wang C et al. 2018. Cnto6785, a fully human antiinterleukin 17 monoclonal antibody, in patients with rheumatoid arthritis with inadequate response to methotrexate: A randomized, placebo-controlled, phase ii, dose-ranging study. The Journal of Rheumatology. 45(1):22.

Murakami S, Mealey BL, Mariotti A, Chapple ILC. 2018. Dental plaque-induced gingival conditions. J Clin Periodontol. 45 Suppl 20:S17-s27.

Murakami Y, Akahoshi T, Aoki N, Toyomoto M, Miyasaka N, Kohsaka H. 2009. Intervention of an inflammation amplifier, triggering receptor expressed on myeloid cells 1, for treatment of autoimmune arthritis. Arthritis Rheum. 60(6):1615-1623.

Nadkarni MA, Martin FE, Jacques NA, Hunter N. 2002. Determination of bacterial load by real-time pcr using a broad-range (universal) probe and primers set. Microbiology. 148(Pt 1):257-266.

Nanci A, Bosshardt DD. 2006. Structure of periodontal tissues in health and disease. Periodontology 2000. 40:11-28.

Needleman IG, Giedrys-Leeper E, Tucker RJ, Worthington HV. 2001. Guided tissue regeneration for periodontal infra-bony defects. Cochrane Database Syst Rev. (2):CD001724.

Negreiros-Lima GL, Lima KM, Moreira IZ, Jardim BLO, Vago JP, Galvão I, Teixeira LCR, Pinho V, Teixeira MM, Sugimoto MA et al. 2020. Cyclic amp regulates key features of macrophages via pka: Recruitment, reprogramming and efferocytosis. Cells. 9(1).

Nguyen A, Khoo WH, Moran I, Croucher PI, Phan TG. 2018. Single cell rna sequencing of rare immune cell populations. Front Immunol. 9:1553.

Noack M, Beringer A, Miossec P. 2019. Additive or synergistic interactions between il-17a or il-17f and tnf or il-1β depend on the cell type. Front Immunol. 10:1726.

Nociti FH, Jr., Cesco De Toledo R, Machado MA, Stefani CM, Line SR, Gonçalves RB. 2001. Clinical and microbiological evaluation of ligature-induced peri-implantitis and periodontitis in dogs. Clin Oral Implants Res. 12(4):295-300.

Novak ML, Koh TJ. 2013. Macrophage phenotypes during tissue repair. Journal of leukocyte biology. 93(6):875-881.

Ohyama H, Kato-Kogoe N, Kuhara A, Nishimura F, Nakasho K, Yamanegi K, Yamada N, Hata M, Yamane J, Terada N. 2009. The involvement of il-23 and the th17 pathway in periodontitis. J Dent Res. 88(7):633-638.

Oishi Y, Manabe I. 2018. Macrophages in inflammation, repair and regeneration. International Immunology. 30(11):511-528.

Ong G. 1998. Periodontal disease and tooth loss. International dental journal. 48(3 Suppl 1):233-238.

Onishi RM, Gaffen SL. 2010. Interleukin-17 and its target genes: Mechanisms of interleukin-17 function in disease. Immunology. 129(3):311-321.

Paquette DW, Ryan ME, Wilder RS. 2008. Locally delivered antimicrobials: Clinical evidence and relevance. J Dent Hyg. 82 Suppl 3:10-15.

Parameswaran N, Patial S. 2010. Tumor necrosis factor-α signaling in macrophages. Critical reviews in eukaryotic gene expression. 20(2):87-103.

Park JB, Matsuura M, Han KY, Norderyd O, Lin WL, Genco RJ, Cho MI. 1995. Periodontal regeneration in class iii furcation defects of beagle dogs using guided tissue regenerative therapy with platelet-derived growth factor. J Periodontol. 66(6):462-477.

Peterson JT. 2004. Matrix metalloproteinase inhibitor development and the remodeling of drug discovery. Heart Fail Rev. 9(1):63-79.
Pinto AR, Paolicelli R, Salimova E, Gospocic J, Slonimsky E, Bilbao-Cortes D, Godwin JW, Rosenthal NA. 2012. An abundant tissue macrophage population in the adult murine heart with a distinct alternatively-activated macrophage profile. PLOS ONE. 7(5):e36814.
Pitaru S, Tal H, Soldinger M, Noff M. 1989. Collagen membranes prevent apical migration of epithelium and support new connective tissue attachment during periodontal wound healing in dogs. J Periodontal Res. 24(4):247-253.
Pöllänen MT, Salonen JI, Uitto VJ. 2003. Structure and function of the tooth-epithelial interface in health and disease. Periodontology 2000. 31:12-31.
Poon IKH, Lucas CD, Rossi AG, Ravichandran KS. 2014. Apoptotic cell clearance: Basic biology and therapeutic potential. Nature Reviews Immunology. 14(3):166-180.
Preshaw PM, Alba AL, Herrera D, Jepsen S, Konstantinidis A, Makrilakis K, Taylor R. 2012. Periodontitis and diabetes: A two-way relationship. Diabetologia. 55(1):21-31.
Roca H, Varsos ZS, Sud S, Craig MJ, Ying C, Pienta KJ. 2009. Ccl2 and interleukin-6 promote survival of human cd11b+ peripheral blood mononuclear cells and induce m2-type macrophage polarization. The Journal of biological chemistry. 284(49):34342-34354.
Roussel L, Houle F, Chan C, Yao Y, Bérubé J, Olivenstein R, Martin JG, Huot J, Hamid Q, Ferri L et al. 2010. Il-17 promotes p38 mapk-dependent endothelial activation enhancing neutrophil recruitment to sites of inflammation. The Journal of Immunology. 184(8):4531.
Rovin S, Costich ER, Gordon HA. 1966. The influence of bacteria and irritation in the initiation of periodontal disease in germfree and conventional rats. J Periodontal Res. 1(3):193-204.
Sanz M, Bäumer A, Buduneli N, Dommisch H, Farina R, Kononen E, Linden G, Meyle J, Preshaw PM, Quirynen M et al. 2015. Effect of professional mechanical plaque removal on secondary prevention of periodontitis and the complications of gingival and periodontal preventive measures: Consensus report of group 4 of the 11th european workshop on periodontology on effective prevention of periodontal and peri-implant diseases. J Clin Periodontol. 42 Suppl 16:S214-220.
Satija R, Farrell JA, Gennert D, Schier AF, Regev A. 2015. Spatial reconstruction of single-cell gene expression data. Nature Biotechnology. 33:495.
Scheller J, Chalaris A, Schmidt-Arras D, Rose-John S. 2011. The pro- and anti-inflammatory properties of the cytokine interleukin-6. Biochimica et Biophysica Acta (BBA) - Molecular Cell Research. 1813(5):878-888.
Schenk M, Bouchon A, Seibold F, Mueller C. 2007. Trem-1--expressing intestinal macrophages crucially amplify chronic inflammation in experimental colitis and inflammatory bowel diseases. The Journal of clinical investigation. 117(10):3097-3106.
Schloss PD, Westcott SL, Ryabin T, Hall JR, Hartmann M, Hollister EB, Lesniewski RA, Oakley BB, Parks DH, Robinson CJ et al. 2009. Introducing mothur: Open-source, platform-independent, community-supported software for describing and comparing microbial communities. Appl Environ Microbiol. 75(23):7537-7541.
Segata N, Izard J, Waldron L, Gevers D, Miropolsky L, Garrett WS, Huttenhower C. 2011. Metagenomic biomarker discovery and explanation. Genome Biol. 12(6):R60.
Serhan CN, Chiang N, Van Dyke TE. 2008. Resolving inflammation: Dual anti-inflammatory and pro-resolution lipid mediators. Nature reviews Immunology. 8(5):349-361.
Serhan CN, Savill J. 2005. Resolution of inflammation: The beginning programs the end. Nature immunology. 6(12):1191-1197.

Shalek AK, Satija R, Shuga J, Trombetta JJ, Gennert D, Lu D, Chen P, Gertner RS, Gaublomme JT, Yosef N et al. 2014. Single-cell rna-seq reveals dynamic paracrine control of cellular variation. Nature. 510(7505):363-369.

Shen F, Gaffen SL. 2008. Structure-function relationships in the il-17 receptor: Implications for signal transduction and therapy. Cytokine. 41(2):92-104.

Shen Z, Kuang S, Zhang Y, Yang M, Qin W, Shi X, Lin Z. 2020. Chitosan hydrogel incorporated with dental pulp stem cell-derived exosomes alleviates periodontitis in mice via a macrophage-dependent mechanism. Bioactive Materials. 5(4):1113-1126.

Shibutani T, Murahashi Y, Tsukada E, Iwayama Y, Heersche JN. 1997. Experimentally induced periodontitis in beagle dogs causes rapid increases in osteoclastic resorption of alveolar bone. J Periodontol. 68(4):385-391.

Shrestha N, Bahnan W, Wiley DJ, Barber G, Fields KA, Schesser K. 2012. Eukaryotic initiation factor 2 (eif2) signaling regulates proinflammatory cytokine expression and bacterial invasion. The Journal of biological chemistry. 287(34):28738-28744.

Sierra-Filardi E, Nieto C, Domínguez-Soto A, Barroso R, Sánchez-Mateos P, Puig-Kroger A, López-Bravo M, Joven J, Ardavín C, Rodríguez-Fernández JL et al. 2014. Ccl2 shapes macrophage polarization by gm-csf and m-csf: Identification of ccl2/ccr2-dependent gene expression profile. Journal of immunology (Baltimore, Md : 1950). 192(8):3858-3867.

Sima C, Cheng Q, Rautava J, Levesque C, Sherman P, Glogauer M. 2016. Identification of quantitative trait loci influencing inflammation-mediated alveolar bone loss: Insights into polygenic inheritance of host-biofilm disequilibria in periodontitis. J Periodontal Res. 51(2):237-249.

Sorensen WP, Löe H, Ramfjord SP. 1980. Periodontal disease in the beagle dog. A cross sectional clinical study. J Periodontal Res. 15(4):380-389.

Sutton CE, Mielke LA, Mills KH. 2012. Il-17-producing γδ t cells and innate lymphoid cells. Eur J Immunol. 42(9):2221-2231.

Tacke F, Alvarez D, Kaplan TJ, Jakubzick C, Spanbroek R, Llodra J, Garin A, Liu J, Mack M, van Rooijen N et al. 2007. Monocyte subsets differentially employ ccr2, ccr5, and cx3cr1 to accumulate within atherosclerotic plaques. The Journal of clinical investigation. 117(1):185-194.

Tammaro A, Derive M, Gibot S, Leemans JC, Florquin S, Dessing MC. 2017. Trem-1 and its potential ligands in non-infectious diseases: From biology to clinical perspectives. Pharmacology & Therapeutics. 177:81-95.

Tanaka T, Terada M, Ariyoshi K, Morimoto K. 2010. Monocyte chemoattractant protein-1/cc chemokine ligand 2 enhances apoptotic cell removal by macrophages through rac1 activation. Biochemical and biophysical research communications. 399(4):677-682.

Tang F, Barbacioru C, Wang Y, Nordman E, Lee C, Xu N, Wang X, Bodeau J, Tuch BB, Siddiqui A et al. 2009. Mrna-seq whole-transcriptome analysis of a single cell. Nature Methods. 6(5):377-382.

Tanner AC, Kent R, Jr., Kanasi E, Lu SC, Paster BJ, Sonis ST, Murray LA, Van Dyke TE. 2007. Clinical characteristics and microbiota of progressing slight chronic periodontitis in adults. J Clin Periodontol. 34(11):917-930.

Taubman MA, Valverde P, Han X, Kawai T. 2005. Immune response: The key to bone resorption in periodontal disease. J Periodontol. 76(11 Suppl):2033-2041.

Teitelbaum SL. 2000. Bone resorption by osteoclasts. Science (New York, NY). 289(5484):1504-1508.

Teles RP, Teles FR. 2009. Antimicrobial agents used in the control of periodontal biofilms: Effective adjuncts to mechanical plaque control? Braz Oral Res. 23 Suppl 1:39-48.
ter Steeg PF, Van der Hoeven JS, de Jong MH, van Munster PJ, Jansen MJ. 1987. Enrichment of subgingival microflora on human serum leading to accumulation of bacteroides species, peptostreptococci and fusobacteria. Antonie Van Leeuwenhoek. 53(4):261-272.
Tonetti MS, Greenwell H, Kornman KS. 2018. Staging and grading of periodontitis: Framework and proposal of a new classification and case definition. J Periodontol. 89 Suppl 1:S159-s172.
Udagawa N, Takahashi N, Katagiri T, Tamura T, Wada S, Findlay DM, Martin TJ, Hirota H, Taga T, Kishimoto T et al. 1995. Interleukin (il)-6 induction of osteoclast differentiation depends on il-6 receptors expressed on osteoblastic cells but not on osteoclast progenitors. The Journal of experimental medicine. 182(5):1461-1468.
Van Dyke TE, Offenbacher S, Braswell L, Lessem J. 2002. Enhancing the value of scaling and root-planing: Arestin clinical trial results. J Int Acad Periodontol. 4(3):72-76.
Van Dyke TE, Sima C. 2020. Understanding resolution of inflammation in periodontal diseases: Is chronic inflammatory periodontitis a failure to resolve? Periodontology 2000. 82(1):205-213.
Ventola CL. 2015. The antibiotic resistance crisis: Part 1: Causes and threats. P T. 40(4):277-283.
Verna C, Zaffe D, Siciliani G. 1999. Histomorphometric study of bone reactions during orthodontic tooth movement in rats. Bone. 24(4):371-379.
Verreck FAW, de Boer T, Langenberg DML, Hoeve MA, Kramer M, Vaisberg E, Kastelein R, Kolk A, de Waal-Malefyt R, Ottenhoff THM. 2004. Human il-23-producing type 1 macrophages promote but il-10-producing type 2 macrophages subvert immunity to (myco)bacteria. Proceedings of the National Academy of Sciences of the United States of America. 101(13):4560.
Viniegra A, Goldberg H, Çil Ç, Fine N, Sheikh Z, Galli M, Freire M, Wang Y, Van Dyke TE, Glogauer M et al. 2018. Resolving macrophages counter osteolysis by anabolic actions on bone cells. J Dent Res. 97(10):1160-1169.
Walker CB, Gordon JM, Magnusson I, Clark WB. 1993. A role for antibiotics in the treatment of refractory periodontitis. J Periodontol. 64(8 Suppl):772-781.
Walters J, Lai PC. 2015. Should antibiotics be prescribed to treat chronic periodontitis? Dent Clin North Am. 59(4):919-933.
Wang C, Yu X, Cao Q, Wang Y, Zheng G, Tan TK, Zhao H, Zhao Y, Wang Y, Harris D. 2013. Characterization of murine macrophages from bone marrow, spleen and peritoneum. BMC Immunol. 14:6.
Watanabe H, Numata K, Ito T, Takagi K, Matsukawa A. 2004. Innate immune response in th1- and th2-dominant mouse strains. Shock. 22(5):460-466.
Wikesjö UM, Razi SS, Sigurdsson TJ, Tatakis DN, Lee MB, Ongpipattanakul B, Nguyen T, Hardwick R. 1998. Periodontal repair in dogs: Effect of recombinant human transforming growth factor-beta1 on guided tissue regeneration. J Clin Periodontol. 25(6):475-481.
Willi M, Belibasakis GN, Bostanci N. 2014. Expression and regulation of triggering receptor expressed on myeloid cells 1 in periodontal diseases. Clin Exp Immunol. 178(1):190-200.
Wong RL, Hiyari S, Yaghsezian A, Davar M, Lin YL, Galvan M, Tetradis S, Camargo PM, Pirih FQ. 2017. Comparing the healing potential of late-stage periodontitis and peri-implantitis. The Journal of oral implantology. 43(6):437-445.

Xiao E, Mattos M, Vieira GHA, Chen S, Correa JD, Wu Y, Albiero ML, Bittinger K, Graves DT. 2017. Diabetes enhances il-17 expression and alters the oral microbiome to increase its pathogenicity. Cell host & microbe. 22(1):120-128.e124.

Xu LX, Kukita T, Kukita A, Otsuka T, Niho Y, Iijima T. 1995. Interleukin-10 selectively inhibits osteoclastogenesis by inhibiting differentiation of osteoclast progenitors into preosteoclast-like cells in rat bone marrow culture system. Journal of cellular physiology. 165(3):624-629.

Yago T, Nanke Y, Ichikawa N, Kobashigawa T, Mogi M, Kamatani N, Kotake S. 2009. Il-17 induces osteoclastogenesis from human monocytes alone in the absence of osteoblasts, which is potently inhibited by anti-tnf-α antibody: A novel mechanism of osteoclastogenesis by il-17. Journal of Cellular Biochemistry. 108(4):947-955.

Yamaguchi T, Movila A, Kataoka S, Wisitrasameewong W, Ruiz Torruella M, Murakoshi M, Murakami S, Kawai T. 2016. Proinflammatory m1 macrophages inhibit rankl-induced osteoclastogenesis. Infect Immun. 84(10):2802-2812.

Yan X, Anzai A, Katsumata Y, Matsuhashi T, Ito K, Endo J, Yamamoto T, Takeshima A, Shinmura K, Shen W et al. 2013. Temporal dynamics of cardiac immune cell accumulation following acute myocardial infarction. Journal of Molecular and Cellular Cardiology. 62:24-35.

You Z, Ge D, Liu S, Zhang Q, Borowsky AD, Melamed J. 2012. Interleukin-17 induces expression of chemokines and cytokines in prostatic epithelial cells but does not stimulate cell growth in vitro. International journal of medical and biological frontiers. 18(8):629-644.

Yu JJ, Ruddy MJ, Wong GC, Sfintescu C, Baker PJ, Smith JB, Evans RT, Gaffen SL. 2007. An essential role for il-17 in preventing pathogen-initiated bone destruction: Recruitment of neutrophils to inflamed bone requires il-17 receptor–dependent signals. Blood. 109(9):3794-3802.

Yu T, Zhao L, Huang X, Ma C, Wang Y, Zhang J, Xuan D. 2016. Enhanced activity of the macrophage m1/m2 phenotypes and phenotypic switch to m1 in periodontal infection. J Periodontol. 87(9):1092-1102.

Zhang Q, Atsuta I, Liu S, Chen C, Shi S, Shi S, Le AD. 2013. Il-17-mediated m1/m2 macrophage alteration contributes to pathogenesis of bisphosphonate-related osteonecrosis of the jaws. Clin Cancer Res. 19(12):3176-3188.

Zhang X, Goncalves R, Mosser DM. 2008. The isolation and characterization of murine macrophages. Curr Protoc Immunol. Chapter 14:Unit-14.11.

Zheng GXY, Terry JM, Belgrader P, Ryvkin P, Bent ZW, Wilson R, Ziraldo SB, Wheeler TD, McDermott GP, Zhu J et al. 2017. Massively parallel digital transcriptional profiling of single cells. Nature Communications. 8:14049.

Zhuang Z, Yoshizawa-Smith S, Glowacki A, Maltos K, Pacheco C, Shehabeldin M, Mulkeen M, Myers N, Chong R, Verdelis K et al. 2018. Induction of m2 macrophages prevents bone loss in murine periodontitis models. J Dent Res.22034518805984.

Zhuang Z, Yoshizawa-Smith S, Glowacki A, Maltos K, Pacheco C, Shehabeldin M, Mulkeen M, Myers N, Chong R, Verdelis K et al. 2019. Induction of m2 macrophages prevents bone loss in murine periodontitis models. J Dent Res. 98(2):200-208.

Zysset D, Weber B, Rihs S, Brasseit J, Freigang S, Riether C, Banz Y, Cerwenka A, Simillion C, Marques-Vidal P et al. 2016. Trem-1 links dyslipidemia to inflammation and lipid deposition in atherosclerosis. Nature Communications. 7(1):13151.